

Performance characteristics of an air-cooled steam condenser incorporating a hybrid (dry/wet) dephlegmator

Johan Adam Heyns

Dissertation presented in partial fulfilment of the requirements for the degree Master of
Engineering at the University of Stellenbosch

Thesis supervisor: Prof D.G. Kröger

Department of Mechanical Engineering
University of Stellenbosch

December 2008

Declaration

I, the undersigned, hereby declare that the work contained in this thesis is my own original work and that I have not previously in its entirety or in part submitted it at any university for a degree.

Johan A. Heyns

Date: _____

Abstract

This study evaluates the performance characteristics of a power plant incorporating a steam turbine and a direct air-cooled dry/wet condenser operating at different ambient temperatures. The proposed cooling system uses existing A-frame air-cooled condenser (ACC) technology and through the introduction of a hybrid (dry/wet) dephlegmator achieves measurable enhancement in cooling performance when ambient temperatures are high. In order to determine the thermal-flow performance characteristics of the wet section of the dephlegmator, tests are conducted on an evaporative cooler. From the experimental results, correlations for the water film heat transfer coefficient, air-water mass transfer coefficient and the air-side pressure drop over a deluged tube bundle are developed. During periods of high ambient temperatures the hybrid (dry/wet) condenser operating in a wet mode can achieve the same increased turbine performance as an oversized air-cooled condenser or an air-cooled condenser with adiabatic cooling (spray cooling) of the inlet air at a considerably lower cost. For the same turbine power output the water consumed by an air-cooled condenser incorporating a hybrid (dry/wet) dephlegmator is at least 20% less than an air-cooled condenser with adiabatic cooling of the inlet air.

Acknowledgements

I would like to thank the following people for their valuable contributions:

Prof. D.G. Kröger for his guidance and support throughout the project;

Mr C. Zietsman and his team who helped with the construction of the test facility and for his continuous assistance.

I would also like to thank the Center for Renewable and Sustainable Energy as well as the California Energy Commission for their financial support.

Table of Contents

Declaration.....	ii
Abstract	iii
Acknowledgements.....	iv
Table of Contents.....	v
List of figures.....	vii
Nomenclature.....	ix
1 Executive summary	1
2 Introduction.....	3
2.1 Dry-cooling.....	3
2.2 Dry/wet cooling systems	6
2.3 Adiabatic cooling of inlet air.....	9
2.4 Proposed hybrid (dry/wet) cooling system.....	12
3 Performance analysis of hybrid (dry/wet) condenser.....	15
3.1 A-frame finned tube air-cooled condenser.....	16
3.2 Smooth galvanized steel tube bundle operated as an evaporative condenser	16
3.2.1 Development of the analysis of evaporative coolers and condensers.....	16
3.2.2 Analysis of the thermal performance characteristics of an evaporative condenser	19
3.3 Plain tube bundle operated as an air-cooled condenser	27
4 Experimental investigation of an evaporative heat exchanger	28
4.1 Apparatus.....	28
4.2 Determining the heat and mass transfer coefficients	30
4.3 Results and observations	32
4.4 Conclusion.....	40
5 Experimental investigation of the plain tube bundle operated dry	42
6 Performance characteristics of a steam turbine incorporating an air-cooled condenser with a hybrid (dry/wet) dephlegmator.....	44

6.1	Conclusion.....	52
7	Conclusions.....	53
8	References.....	54
Appendix A:	Properties of fluids	A.1
Appendix B:	Empirical correlations	B.1
Appendix C:	Adiabatic cooling	C.1
Appendix D:	Hybrid (dry/wet) condenser performance analysis	D.1

List of figures

Figure 2.1: Direct air-cooled steam condenser.....	4
Figure 2.2: Direct air-cooled condenser street.....	4
Figure 2.3: Indirect dry-cooling system.....	5
Figure 2.4: Schematic representation of the San Juan dry/wet cooling tower.....	7
Figure 2.5: Preheater/peak coolers inside the cooling towers.....	8
Figure 2.6: Exhaust steam back pressure for dry-, wet- and dry/wet cooling.....	9
Figure 2.7: Adiabatic cooling of inlet air.....	10
Figure 2.8: Hybrid dry/wet dephlegmator.....	12
Figure 2.9: Second stage of the hybrid (dry/wet) dephlegmator.....	13
Figure 3.1: Diagram of steam flow through condenser.....	15
Figure 3.2: Schematic representation of an evaporative condenser.....	21
Figure 3.3: Control volume for the evaporative condenser.....	21
Figure 4.1: Schematic layout of the apparatus.....	29
Figure 4.2: Tube bundle layout and tube dimensions.....	29
Figure 4.3: Variation in the deluge water temperature.....	32
Figure 4.4: Heat transfer coefficient as a function of the air flow rate.....	33
Figure 4.5: Heat transfer coefficient as a function of the deluge water flow rate.....	34
Figure 4.6: Heat transfer coefficient as a function of the deluge water temperature.....	34
Figure 4.7: Film heat transfer coefficient.....	35
Figure 4.8: Mass transfer coefficient as a function of the air mass velocity.....	36
Figure 4.9: Mass transfer coefficient as a function of the deluge water mass velocity.....	36
Figure 4.10: Mass transfer coefficient as a function of the deluge water temperature.....	37
Figure 4.11: Air-water interface mass transfer coefficient.....	37
Figure 4.12: Air-side pressure drop as a function of the air mass velocity.....	38
Figure 4.13: Air-side pressure drop as a function of the deluge water mass velocity.....	39
Figure 4.14: Air-side pressure drop as a function of the deluge water temperature.....	39
Figure 4.15: Air-side pressure drop.....	40
Figure 5.1: Air-side heat transfer coefficient for dry tubes in cross-flow.....	42
Figure 5.2: Air-side pressure drop of a dry tube bundle in cross-flow.....	43
Figure 6.1: Performance characteristics of turbo-generator-condenser system.....	44
Figure 6.2: Sizing air-cooled condensers.....	45

Figure 6.3: Multi-row or multi-street (3streets) array of A-frame air-cooled condensers incorporating hybrid (dry/wet) dephlegmators.....	46
Figure 6.4: Power output for different air-cooled condenser configurations	47
Figure 6.5: Water consumption of the hybrid dry/wet condenser and adiabatic cooling of the inlet air of the A-frame air-cooled condenser having 3 condenser streets	48
Figure 6.6: Power output of the air-cooled condenser incorporating hybrid (dry/wet) dephlegmator having 3 condenser streets.....	49
Figure 6.7: Turbine exhaust steam backpressure (3 condenser streets).....	49
Figure 6.8: Power output for moist inlet air (3 condenser streets)	50
Figure 6.9: Changing air flow through the hybrid dephlegmator (3 condenser streets)	51
Figure 6.10: Changing deluge water mass flow rate through the hybrid dephlegmator (3 streets)	51
Figure 6.11: Power for different condenser unit arrangements	52

Nomenclature

A	Area, m^2
c_p	Specific heat at constant pressure, $J/kg\ K$
d	Diameter, m
d_e	Equivalent or hydraulic diameter, m
e	Effectiveness
G	Mass velocity, kg/sm^2
g	Gravitational acceleration, m/s^2
H	Height, m
h	Heat transfer coefficient, W/m^2K
h_d	Mass transfer coefficient, kg/m^2s
i	Enthalpy, J/kg
i_{fg}	Latent heat, J/kg
K	Loss coefficient
k	Thermal conductivity, W/mK
L	Length, m
M	Molecular weight, $kg/mole$
m	Mass flow rate, kg/s
NTU	Number of transfer units
Ny	Characteristic heat transfer parameter, m^{-1}
n	Number
P	Pitch, m , Power, W
p	Pressure, N/m^2
p_{cr}	Critical pressure, N/m^2
Q	Heat transfer rate, W
q	Heat flux, W/m^2
R	Gas constant, $J/kg\ K$
Ry	Characteristic flow parameter, m^{-1}
T	Temperature, $^{\circ}C$ or K

t	Thickness, m
U	Overall heat transfer coefficient, $\text{W}/\text{m}^2\text{K}$
u	Internal energy, J/kg
V	Volume flow rate, m^3/s
v	Velocity, m/s
w	Humidity ratio, $\text{kg water vapor}/\text{kg dry air}$
X	Mole fraction
x	Co-ordinate or quality
y	Co-ordinate
z	Co-ordinate

Greek letters

Γ	Water flow rate per unit length, kg/sm
Δ	Differential
δ	Film thickness, m
θ	Angle, $^\circ$
μ	Dynamic viscosity, kg/ms
ν	Kinematic viscosity, m^2/s
ρ	Density, kg/m^3
σ	Area ratio

Dimensionless numbers

Le	Lewis number, $k/\rho c_p D$
Le_f	Lewis factor, $h/c_p h_D$
Nu	Nusselt number, $h d/k$
Pr	Prantl number, $\mu c_p/k$
Re	Reynolds number, $\rho v d/\mu$

Subscripts

a	Air, or based on air-side area
-----	--------------------------------

<i>abs</i>	Absolute
<i>ac</i>	Adiabatic cooling
<i>atm</i>	Atmosphere
<i>av</i>	Mixture of dry air and water vapor
<i>b</i>	Bundle
<i>c</i>	Concentration, convective heat transfer, casing, critical or condensate
<i>cf</i>	Counterflow
<i>cr</i>	Critical
<i>cv</i>	Control volume
<i>d</i>	Diameter
<i>db</i>	Dry-bulb
<i>de</i>	Drop or drift eliminator
<i>ds</i>	Steam duct
<i>e</i>	Effective, equivalent, or evaporative
<i>F</i>	Fan
<i>f</i>	Fluid or friction
<i>fr</i>	Frontal area
<i>gen</i>	Generated
<i>H</i>	Height
<i>h</i>	Header or hub
<i>he</i>	Heat exchanger
<i>i</i>	Inlet, or inside
<i>int</i>	Air-water interface
<i>iso</i>	Isothermal
<i>j</i>	Jet
<i>l</i>	Laminar, longitudinal, or liquid, or lateral
<i>m</i>	Mean, mass transfer, or mixture
<i>max</i>	Maximum
<i>min</i>	Minimum
<i>o</i>	Outlet, or outside
<i>p</i>	Constant pressure, process water
<i>r</i>	Row, radial co-ordinate, refrigerant or ratio
<i>rz</i>	Rain zone

<i>s</i>	Screen, steam, saturation, support, or street
<i>sp</i>	Spray
<i>T</i>	Constant temperature, or temperature
<i>t</i>	Total, tube, transversal, blade tip, or fin tip
<i>tr</i>	Tube rows, or tubes per row
<i>ts</i>	Tube cross-section
<i>tus</i>	Windtunnel upstream cross-section
<i>ud</i>	Upstream and downstream
<i>up</i>	Upstream
<i>v</i>	Vapor
<i>w</i>	Water, or wall, or walkway
<i>wb</i>	Wetbulb
<i>x</i>	Co-ordinate, or quality
<i>y</i>	Co-ordinate
<i>z</i>	Co-ordinate
∞	Infinity, or free stream

1 Executive summary

Currently most power plants incorporating a steam cycle either employ wet-cooling systems which consume a relatively large amount of water, or air-cooled systems which operate inefficiently at high ambient temperatures. In some cases dry/wet or wet/dry cooling systems are employed, but these are often more expensive than other options.

This project investigates to what extent the thermal performance of an A-frame direct air-cooled condenser can be enhanced by the introduction of a hybrid (dry/wet) dephlegmator, while the amount of water consumed is limited. The proposed hybrid (dry/wet) dephlegmator consists of two stages: The first an air-cooled condenser with finned tubes and the second a bundle of galvanized steel tubes arranged horizontally. The second stage can either be operated as a dry air-cooled condenser or the tubes can be deluged with water and operated as an evaporative condenser.

During periods of high ambient temperatures or peak demand, the second stage of the hybrid (dry/wet) dephlegmator is deluged with water and operated as an evaporative condenser. Due to discrepancies in the performance characteristics given in the literature for evaporative coolers and condensers, tests are conducted on an evaporative cooler. From the experimental results, correlations for the water film heat transfer coefficient, h_w , air-water mass transfer coefficient, h_d , and air-side pressure drop over the deluged tube bundle, Δp , are obtained. It is found that the correlations for the water film heat transfer coefficient and the air-water mass transfer coefficient compare well with the correlations given by Mizushima et al. (1967).

The turbo-generator power output for a steam turbine incorporating an air-cooled condenser with a hybrid (dry/wet) dephlegmator is evaluated for different operating conditions and compared to the power output of other condenser configurations. A measurable increase in the turbo-generator power output can be achieved during periods of higher ambient temperatures if a hybrid (dry/wet) dephlegmator is incorporated into an air-cooled condenser. The possible increase in the turbo-generator output is the same as for an oversized air-cooled condenser (33% increase in the air-cooled condenser size) or an air-cooled condenser with adiabatic or sprays cooling of the inlet air (100% wetbulb depression of the inlet air with a 50% relative humidity). For the same increase in turbo-generator power output, the amount of water consumed by the air-cooled condenser incorporating a hybrid (dry/wet) dephlegmator

is at least 20% lower than the amount of water consumed by an air-cooled condenser with adiabatic or spray cooling of the inlet air. The capital cost of air-cooled condenser incorporating a hybrid (dry/wet) dephlegmator will be considerably less than over-sizing the air-cooled condenser. The air-cooled condenser incorporating a hybrid (dry/wet) dephlegmator may provide a cost effective alternative at locations which are subjected to high water prices or where the available water resources are limited.

2 Introduction

Due to the decreasing availability and rising cost of cooling water, dry-cooling towers or direct air-cooled condensers (ACC's) are increasingly employed to reject heat to the environment in modern power plants incorporating steam turbines. Unfortunately, with an increase in the ambient temperature, the effectiveness of these cooling systems decrease resulting in a corresponding reduction in turbine efficiency. The reduction in turbine output during hot periods may result in a significant loss in income, especially in areas where the demand and cost for power during these periods is high. Enhancing the cooling performance during these periods may thus be justified. Dry/wet cooling systems, with their relatively low water consumption rate, provide the option of enhanced thermal performance during periods of high ambient temperatures, but their use is limited due to their relatively high capital cost.

This study investigates the thermal performance characteristics of a practical cost-effective direct hybrid (dry/wet) condenser. Using a set of turbo-generator-condenser performance characteristics, the power plant output for the hybrid (dry/wet) condenser is compared to the power output for other condenser configurations. In order to determine the performance characteristics of the wet section of the condenser, tests are conducted on an evaporative cooler.

2.1 Dry-cooling

As the availability of water required for wet-cooling systems becomes more limited, modern power plants are increasingly employing indirect dry-cooling towers or direct air-cooled steam condensers to condense steam turbine exhaust vapor. Direct air-cooled condenser units in power plants usually consist of finned tubes arranged in the form of a delta or A-frame to drain condensate effectively, reduce distribution steam duct lengths and minimize the required ground surface area. An example of an A-frame finned tube air-cooled steam condenser unit is shown schematically in Figure 2.1.

A-frame direct air-cooled steam condenser units are normally arranged in multi-row or multi-street arrays. Each street consists of three to five main condenser units with a dephlegmator or secondary reflux condenser connected in series as shown in Figure 2.2. The addition of the dephlegmator increases the steam flow in the main condenser units to such an extent that there is a net flow of steam out of every tube. This inhibits the accumulation of non-

condensable gases in the tubes that may lead to corrosion, freezing or a reduction in the heat transfer capability of the system.

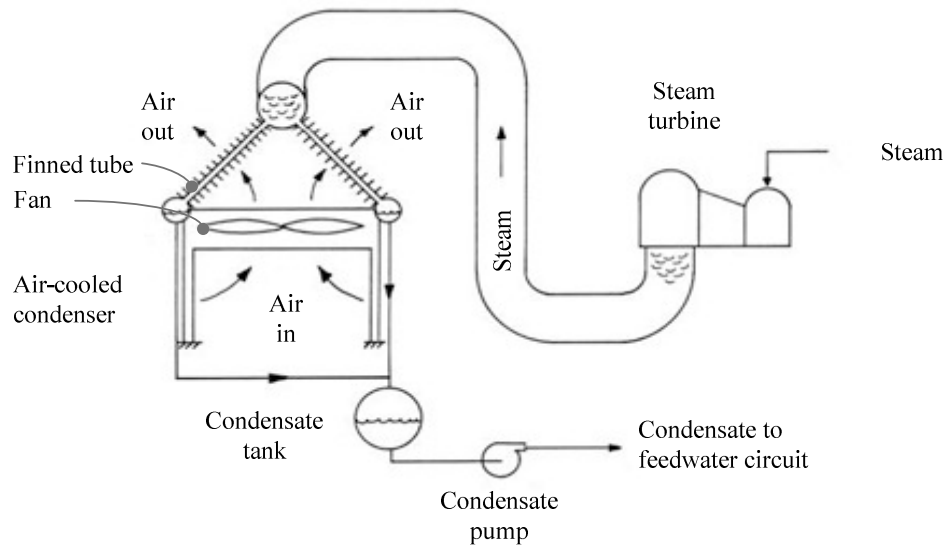


Figure 2.1: Direct air-cooled steam condenser

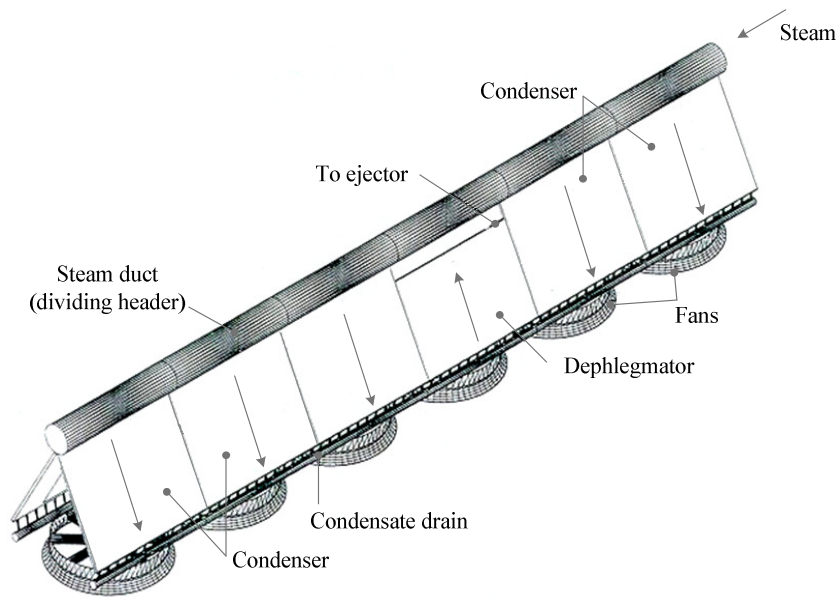


Figure 2.2: Direct air-cooled condenser street

An example of an indirect dry-cooling system, also sometimes referred to as the Heller system, is shown schematically in Figure 2.3. The waste heat in the Heller system is dissipated via either a surface or direct contact (spray) condenser.

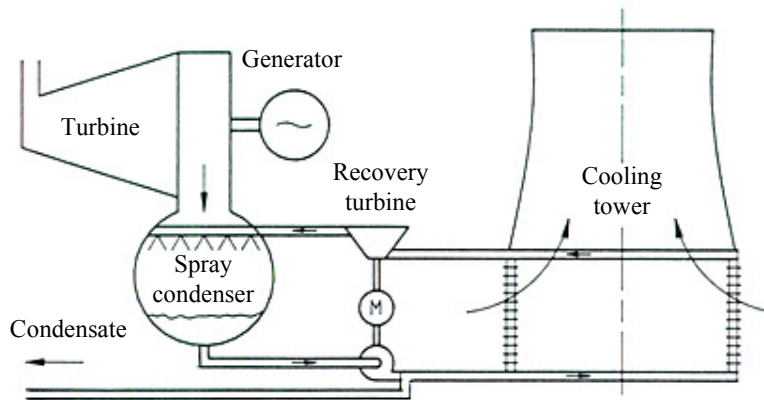


Figure 2.3: Indirect dry-cooling system

Unlike the thermal performance of wet-cooling systems, which are dependent on the wetbulb temperature of the ambient air, an air-cooled system's performance is directly related to the drybulb temperature. The ambient drybulb temperature is normally higher than the wetbulb temperature and experiences more drastic daily and seasonal changes. Although air-cooled systems provide a saving in cooling water, they experience performance penalties during periods of high ambient temperatures.

Maulbetsch and DiFilippo (2006) conducted a study on four different 500 MW gas-fired, combined-cycle power plants (170 MW produced by the steam turbine), located at different sites in California, and compared the cost of wet- and dry-cooling at each site. They found that although dry-cooling reduces the annual water consumption on average by 95% to 96%, the total plant cost is 5% to 15% higher if dry-cooling instead of wet-cooling is used. They also note that for dry-cooled systems, due to their performance penalties during periods of high ambient temperature, the reduction in the potential annual income may be 1% to 2% or amount to \$ 1.5 to \$ 3 million. The utilization of dry-cooling systems is therefore highly dependent on the availability and/or cost of water at a particular site.

2.2 Dry/wet cooling systems

Dry/wet or wet/dry cooling systems utilize characteristics of both dry- and wet-cooling towers. These systems' overall water consumption rates typically vary between 20 to 80 percent of those normally required for all-wet systems, but unlike air-cooled systems are not subjected to the dramatic loss in efficiency during periods of higher ambient temperatures (Maulbetsch, 2002). The performance characteristics of the dry/wet cooling systems are highly dependent on the chosen configuration. In the design of dry/wet cooling systems, it is desirable to achieve the highest possible thermodynamic efficiency while utilizing the smallest amount of cooling water in the most cost-effective manner.

The dry and wet sections, in the dry/wet systems, may be arranged in different combinations that will differ in capital cost and operating capabilities. Maulbetsch (2002) briefly summarized the different dry/wet system arrangements described by Lindahl and Jameson (1993) and Mitchell (1989). Some of the possible cooling tower arrangements include,

- Single-structure combined tower (hybrid) or separate dry and wet towers
- Series or parallel airflow paths through the dry and wet systems
- Series or parallel connected cooling water circuits

while possible condenser arrangements are,

- Common condenser
- Divided water box separating the cooling water flows from the wet and dry towers
- Separate condensers

A hybrid cooling system is a dry/wet or wet/dry cooling system that combines the dry and wet units in a single cooling tower. The induced draft cooling towers at the 500 MW(e) San Juan power plant in New Mexico, shown schematically in Figure 2.4, consists of five cells, of which each has sixteen air-cooled heat exchangers modules and two wet-cooled modules. The cooling water flows in series, from the dry to the wet section, while the air passes in parallel through the sections. At the design point of a drybulb and wetbulb temperature of respectively 35°C and 18.9°C, 63% of the heat is rejected as latent heat (evaporation of the cooling water). However during periods of lower ambient temperatures, the wet section can be bypassed for fully dry operation (Kröger 2004).

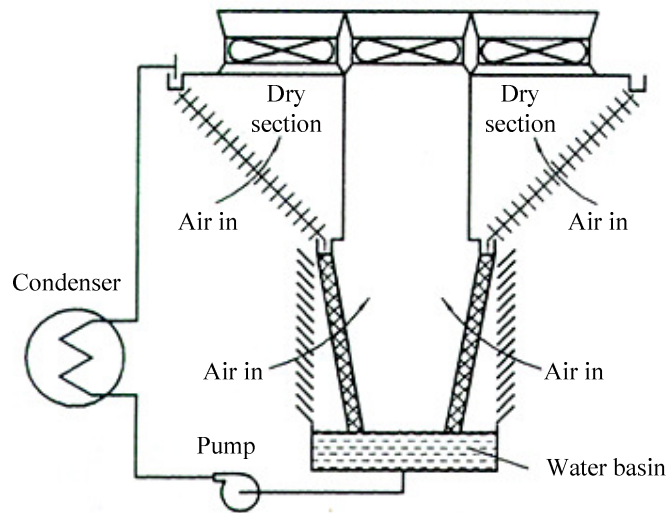


Figure 2.4: Schematic representation of the San Juan dry/wet cooling tower

The indirect Heller/EGI Advanced Dry/deluge (HEADd) combined cooling system introduces additional auxiliary and preheater/peak dry/wet cooling units to the conventional Heller system. The preheater/peak coolers, water-to-air heat exchangers, are installed inside the cooling towers as shown schematically in Figure 2.5. The preheater/peak coolers are connected in parallel to the main cooling deltas. With the start-up of the cooling tower during cold winter periods, these coolers help to preheat the cooling deltas before filling, while during the hottest peak periods they are deluged with water and operated in mechanical draft mode to improve the thermal performance of the tower. The preheater/peak coolers comprise approximately 5 percent of the total heat transfer surface area (Szabo 1991).

Cooling systems for plume abatement also include wet and dry cooling units in one tower. These systems are however essentially wet systems with just enough dry-cooling to reduce the humidity of the exiting air, so that no visible plume forms during cooler periods with higher humidity. The system's design is not aimed at reducing the amount of cooling water consumed.

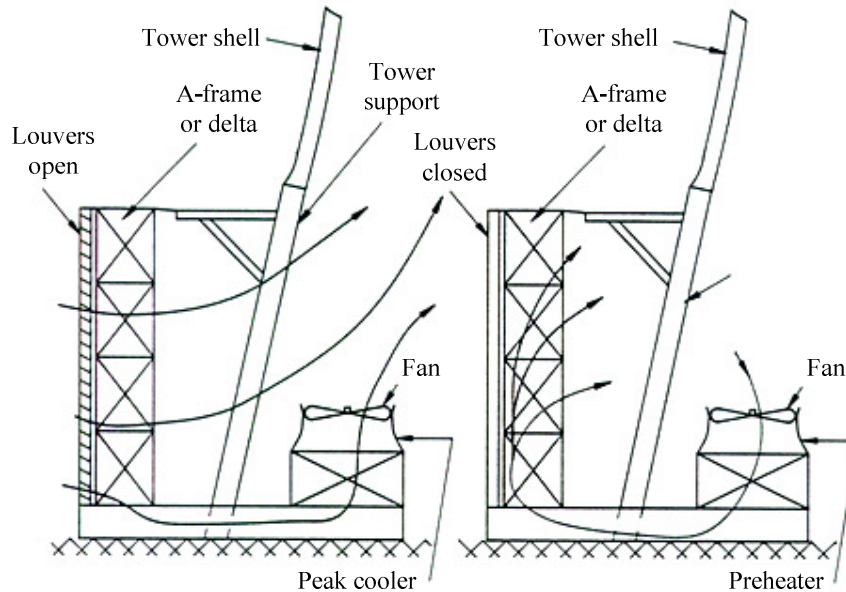


Figure 2.5: Preheater/peak coolers inside the cooling towers

De Backer and Wurtz (2003) investigated the use of mechanical draft wet-cooling towers connected in parallel to direct dry-cooling systems. Figure 2.6 shows that for a particular parallel dry/wet cooling system, during the warmest periods, the turbo-generator can operate at a 20 % lower steam back pressure than when an all-dry-cooling system is employed. The overall amount of water consumed by the particular dry/wet cooling system is only 4 % of the water an all-wet-cooling system will consume.

Boulay et al. (2005) conducted a study to determine whether it would be more economical to oversize direct air-cooled systems or use alternative dry/wet systems to achieve lower backpressures during summer time and generate additional revenue when energy prices peak. The cost and performance were compared at two sites: Northeastern USA (Harrisburg, PA) and a hotter and drier Southwestern location (Phoenix, AZ). The dry/wet systems offered better paybacks than over-sizing the air-cooled condensers, but due to their high capital cost, only had a marginal return at the Northeastern site and proved not to be economical for the Southwestern site.

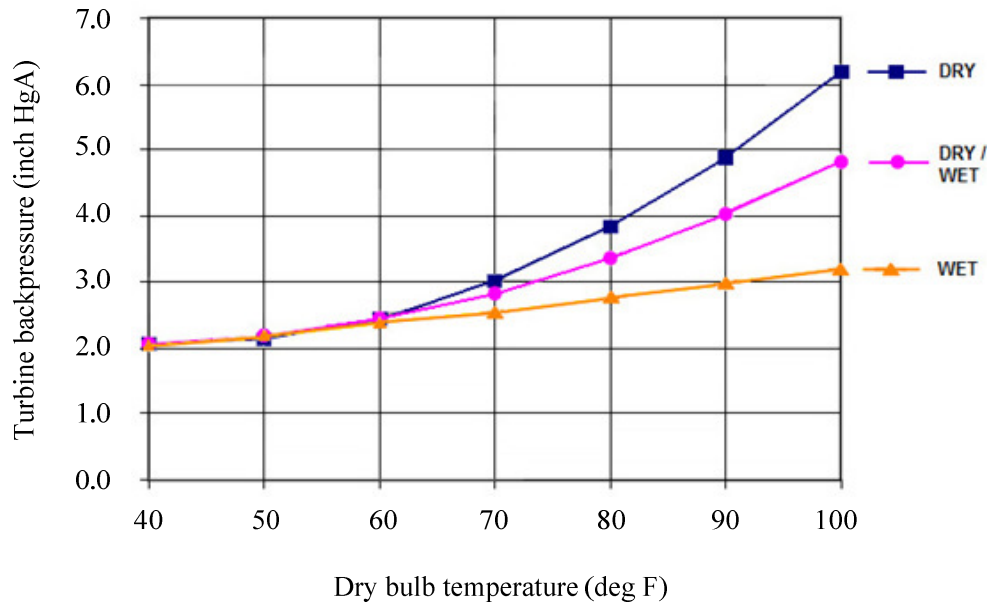


Figure 2.6: Exhaust steam back pressure for dry-, wet- and dry/wet cooling

Dry/wet systems provide relatively good thermal performance characteristics during warmer ambient conditions, while maintaining a low overall water consumption rate. The initial capital costs as well as the operating and maintenance costs of these systems are relatively high due to the fact that they consist of both dry and wet cooling towers. Utilization of the wet-cooling tower only during short periods of high ambient temperatures tends to reduce the lifecycle economical viability of dry/wet cooling systems.

To enhance the performance of dry-cooling systems, the air-side of the heat exchanger surface can be deluged with recirculating water. Deluge systems make use of both sensible and latent heat transfer. The latent heat transfer takes place through the evaporation of a small amount of deluge or cooling water into the air stream. By deluging the heat exchanger with cooling water and enabling evaporative cooling, the heat transfer rate may be improved significantly (Kröger, 2004). A problem associated with deluge cooling is the fouling and corrosion of the air-side of the tubes; this can however be limited in the case of plain tube bundles, so that its influence does not drastically inhibit the thermal performance.

2.3 Adiabatic cooling of inlet air

The performance of dry-cooled systems can also be enhanced by passing the entering air through a wet tower fill or by introducing a fine spray into the air upstream of the heat

exchanger, adiabatically cooling the air. Evaporation of the water cools the air to near its wetbulb temperature, resulting in a thermal performance improvement of the air-cooled heat exchanger.

Conradie and Kröger (1991) investigated and compared two methods of enhancing the thermal performance of an air-cooled condenser: Deluging the air-side surface of the air-cooled condenser with water, enabling both sensible and latent heat transfer, and the adiabatic spray cooling of air entering the air-cooled condenser. They showed that for both systems there are measurable increases in the thermal performance, but due to variations in the availability of water and system costs they could not provide a definite answer as to which system would provide the best option. The increase in the turbo-generator power output for a direct air-cooled condenser with the adiabatic cooling (spray cooling) of the inlet air is shown in Figure 2.7.

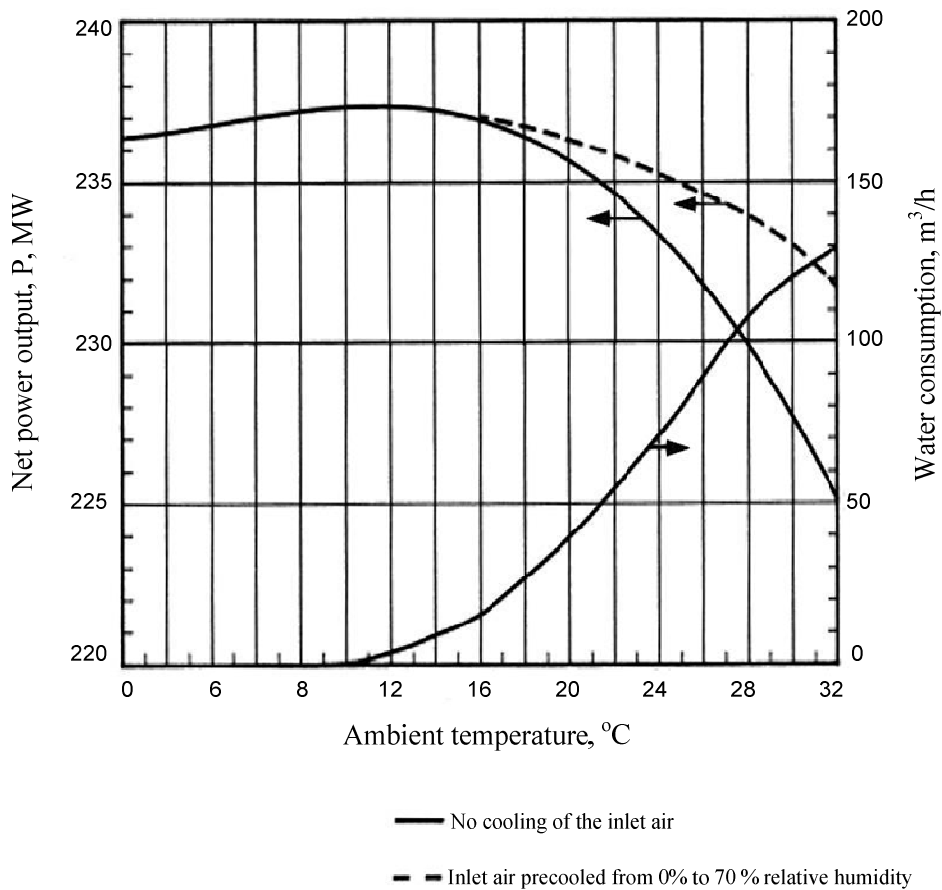


Figure 2.7: Adiabatic cooling of inlet air

Large spray droplets may inhibit complete evaporation and cause significant wetting of the heat transfer surface. Woest et al. (1991) studied corrosion behavior of galvanized fin tubes when sprayed with potable water and showed that it can result in severe corrosion of the tubes. Studies were then conducted to see whether it is possible to achieve complete evaporation of the spray droplets and prevent the wetting of the heat exchanger surface.

Wachtel (1974) reported that for droplets smaller than 20 μm complete evaporation can be achieved, while Duvenhage (1993) stated that droplets with a diameter of 50 μm have normally evaporated before they reach the heat exchanger. Branfield (2003) argued that the predictions of Wachtel (1974) and Duvenhage (1993) rely on variable parameters (such as the ambient conditions and the height of the heat exchanger above the inlet) and that wetting of the heat exchanger surface may occur even though the droplets are smaller than 20 μm in diameter.

Investigating adiabatic enhancement of air-cooled power plants in California, Maulbetsch and DiFilippo (2003) conducted tests on various low-pressure nozzles and the arrangement of the nozzles. They also investigated the effect of introducing a drift eliminator to reduce the amount of unevaporated droplets entering the finned tube bundle. Tests showed that during periods of high ambient temperatures it is possible to achieve between 60% and 100% of the prevailing wet-bulb depression and 75% of the turbine output losses can be recovered through the use of spray enhancement during the 1000 hottest hours of the year. Under these conditions the installation payback period will be between a year and two and a half years. However, for the nozzles tested only between 60% and 70% of the spray water is evaporated and even the introduction of the drift eliminator cannot ensure that the finned surfaces remain dry. The unevaporated water droplets accumulating on the structure lead to corrosion of the structure surfaces as well as undesirable rainback that causes surface and ground water contamination.

The high cost of generating a fine mist for spray cooling prompted Esterhuysen and Kröger (2005) to investigate whether the use of electrostatic forces (ionization) can prevent the wetting of the finned surfaces. Although the experiments showed that the droplet deposition is reduced as the induction voltage applied to the heat exchanger tubes is increased, some wetting still occurs. Uncertainty exists whether zero droplet deposition can be reached and concern over the safety (high voltage) of the system was raised.

2.4 Proposed hybrid (dry/wet) cooling system

The thermal performance characteristics of a cost effective direct dry/wet cooling system that makes use of existing A-frame air-cooled condenser technology is investigated. The system maintains good thermal performance during periods of high ambient temperatures, while only utilizing the limited water resources available.

As in an A-frame direct air-cooled system, the steam is fed via steam header to the primary condenser units; excess steam leaving the primary condenser units is condensed in the dephlegmator (secondary reflux condenser to remove non-condensable gases) as shown in Figure 2.2. It is proposed that the air-cooled dephlegmator be replaced by a hybrid (dry/wet) dephlegmator, consisting of two stages: It consists firstly of an air-cooled condenser with somewhat shortened inclined finned tubes, similar to those used in the A-frame configuration, and a second stage consisting of smooth galvanized steel tubes arranged horizontally. The configuration of the proposed hybrid dephlegmator is shown schematically in Figure 2.8. The second stage, as shown in Figure 2.9, can be operated either as an air-cooled condenser (dry) or the air-side surface of the tube bundle can be deluged with water, thus to be operated as an evaporatively cooled condenser.

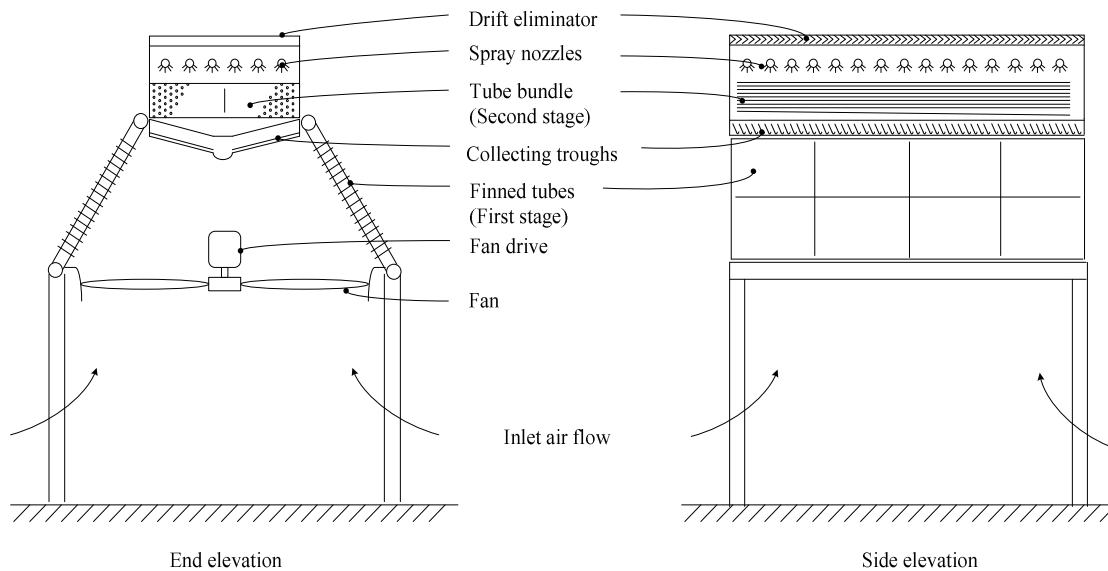


Figure 2.8: Hybrid dry/wet dephlegmator

The operation of the second stage depends on the ambient conditions. During periods of low ambient temperatures where air-cooling is sufficient, the second stage is operated in a dry mode. However, during hotter periods deluge water is sprayed over the galvanized steel tubes

and the second stage is operated as an evaporative condenser. The deluge water is collected under the tube bundle in troughs.

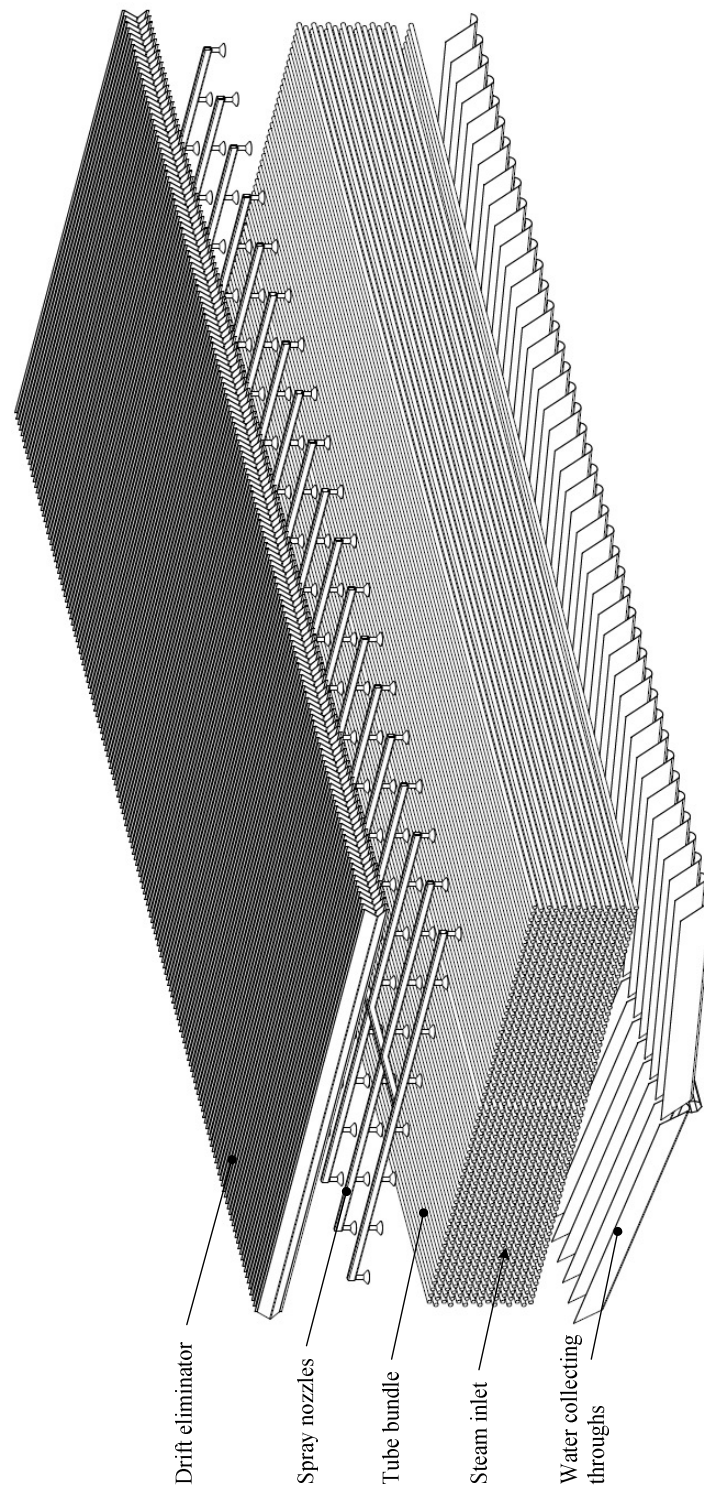


Figure 2.9: Second stage of the hybrid (dry/wet) dephlegmator

This system has the potential of enhanced thermal performance during periods of high ambient temperatures, while having a lower overall water consumption rate than a spray cooled system (adiabatic pre-cooling of inlet air) giving the same turbine performance enhancement. It is estimated that the capital cost of the hybrid (dry/wet) dephlegmator will be only slightly more than that of a standard A-frame air-cooled dephlegmator. Furthermore, the finned tubes of the unit remain dry, reducing the risk of corrosion and scaling while the galvanized wetted plain tube surface will be rinsed with clean water on a regular basis to minimize fouling.

3 Performance analysis of hybrid (dry/wet) condenser

The thermo-flow performance characteristics of the different sections of the three street air-cooled condenser incorporating a hybrid (dry/wet) dephlegmator (See Figure 6.3) are analyzed employing a one-dimensional approach. The different components are:

- The A-frame finned tube air-cooled primary condensers
- The first stage of the hybrid dephlegmator, which is an air-cooled reflux condenser with inclined finned tubes
- The second stage of the hybrid dephlegmator consists of a horizontal plain tube bundle. The mode of operation varies according to the performance requirements and the ambient conditions. The unit can either be operated dry as secondary air-cooled condenser or it can be deluged with water and operated as an evaporative condenser.

A schematic flowchart of the steam flow through a street of the condenser array is shown in Figure 3.1.

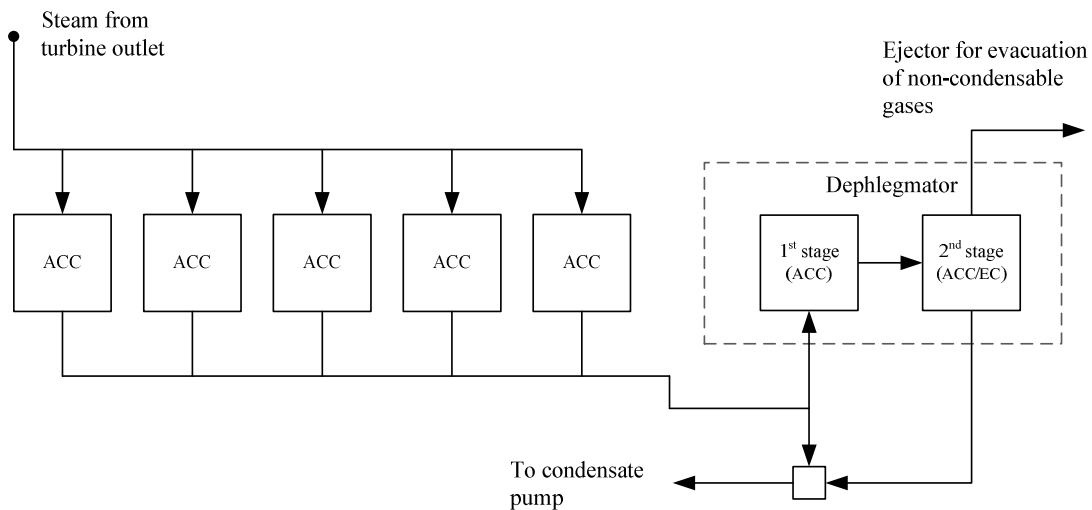


Figure 3.1: Diagram of steam flow through condenser

In the analysis of the systems performance characteristics the following assumptions are made:

- Saturated steam enters the air-cooled condenser units.
- All the steam is condensed and leaves the system as saturated water (condensate).

- The pressure drop inside the steam header, the condenser tubes and the rest of the cycle are neglected and the steam temperature is assumed to be constant throughout the system. For high inlet steam temperatures this assumption is reasonably accurate.
- The performance of each of the A-frame air-cooled condenser units is assumed to be identical.

3.1 A-frame finned tube air-cooled condenser

Kröger (2004) presents a one-dimensional numerical solution for the prediction of the thermo-flow performance characteristics of an A-frame finned tube air-cooled condenser. This model is used in the present analysis of the air-cooled condenser units and the inclined finned tube bundles in the first stage of hybrid (dry/wet) dephlegmator.

3.2 Smooth galvanized steel tube bundle operated as an evaporative condenser

When peak demand occurs during periods of high ambient temperatures the second stage of the dephlegmator, consisting of a bundle of smooth galvanized steel tubes arranged horizontally, is deluged with water and operated as an evaporative condenser.

3.2.1 Development of the analysis of evaporative coolers and condensers

In conventional evaporative condensers recirculated deluge water is sprayed over a horizontal tube bundle, while air is drawn over the bundle and steam in the tubes is condensed.

Some of the early pioneers studying evaporative condensers include: Goodman (1938), Thomsen (1946) and Gogolin and Mednikova (1948). Due to computational restrictions, they were forced to simplify the equations governing the analysis of evaporative coolers and condensers. Parker and Treybal (1961) later showed that in some cases these simplified models deviated by as much as 30 percent from experimental results. Early models assumed the deluge water temperature to be constant throughout the tube bundle.

The first practical design procedure for the evaluation of counterflow evaporative coolers was given by Parker and Treybal (1961). Their model makes use of the Lewis factor to find the relationship between the heat and mass transfer coefficient at the air-water interface and assumes that the Lewis factor is equal to unity. They further assumed that the amount of water evaporated is negligibly small and that the air saturation enthalpy is a linear function of the temperature. This makes it possible to integrate the differential equations simultaneously over the height of the tube bundle. In their work, Parker and Treybal (1961) noted the variation in the recirculating water temperature along the height of the bundle and its influence on the analysis.

Mizushina et al. (1967) experimentally investigated the characteristics of evaporative coolers and determined the applicable heat and mass transfer coefficients. A similar approach to that of Parker and Treybal (1961) is followed, but the differential equations are integrated numerically.

The performance enhancement of evaporative condensers using extended surfaces was studied by Kreid et al. (1978) and Leidenforst and Korenic (1982). They showed that in theory it is possible to obtain a substantial increase in the performance, but this is only achieved for maintained wetting of the fins which proves to be difficult in practice. Furthermore, finned tubes are subjected to more severe fouling and corrosion.

Bykov et al. (1984) investigated the influence of the regions above and below the tube bundle on the heat and mass transfer, as well as the variation in the deluge water temperature. They then classified the evaporative condenser into three sections: The spray zone (located between the sprayers and tube bundle), the tube bundle and the run-off zone (located between the tube bundle and the bottom sump). Bykov et al. (1984) concluded that there is only a slight temperature change in the spray zone and it may be safely neglected. The run-off zone does however have an effect on the heat rejection rate and cannot always be ignored. These results are dependent on the geometric layout of the unit.

Webb (1984) developed a unified theoretical treatment of evaporative systems: Cooling towers, evaporative coolers and evaporative condensers. His model considered the effect of the variation in temperature of the deluge water in an evaporative cooler, but states that for an evaporative condenser the film temperature remains essentially constant due to the fact that the variation in the refrigerant temperature is negligibly small.

Dreyer (1988) conducted an extensive study on evaporative coolers and condensers. He considered a detailed one-dimensional analytical model, similar to the one suggested by Poppe and Rögener (1984) that accurately describes the physics of the mass and heat transfer processes, as well as a simplified model, utilizing the assumptions made in a Merkel type analysis. Dreyer (1988) further investigated the heat and mass transfer correlations suggested by various authors in the literature and compared them graphically. He stated that the models of Parker and Treybal (1961) and Mizushina et al. (1967) are in good agreement if they use their own respective heat and mass transfer coefficients when determining the performance of an evaporative cooler or condenser, but recommends the use of the correlations of Mizushina et al. (1967) as they cover a wider range of conditions.

Zalewski and Gryglaszeski (1997) developed a mathematical model similar to the one described by Dreyer (1988), which is based on the analysis of Poppe and Rögener (1984). They suggested the use of correlations of Tovas et al. (1984) for calculating the heat transfer coefficient between the tube and the deluge water and adapted data given by Grimison (1937) for the heat transfer over dry tube banks to determine the convective heat transfer coefficient from the deluge water to the moist air. They used the equation suggested by Bosnjakovic and Blackshear (1965) to determine the Lewis factor and the relation between the heat and mass transfer at the interface of the deluge water and the moist air. In view of the difference between their theoretical prediction and their experimental results, they modified the mass transfer coefficient correlation by introducing a correction function.

Ettouney et al. (2001) performed an analysis on evaporative condensers based on the water-to-air mass flow rate ratio and the steam temperature. They compared the performance of an evaporative condenser with the performance of the same system when it is operated dry and showed that thermal performance of the evaporative condenser is up to 60% higher than an air-cooled unit. It was found that the experimental work on the heat transfer coefficient was consistent with previous work done and available data in the literature.

Hasan and Siren (2002) did a comparative study between plain and finned tube evaporative coolers, where they showed an increase in the heat rejected by the finned tube bundle of between 92 and 140 %. From the experimental results it was however found that the energy index of the two heat exchangers is almost the same, where the energy index is defined as the ratio of the volumetric thermal conductance over the air-side pressure drop per unit length. It was furthermore found that the wet fins have a lower efficiency than the dry fins.

Stabat and Marchio (2004) developed a model based on the effectiveness NTU-method for evaluating the performance characteristics of an evaporative cooler. They assume the water film temperature along the coil to be constant and that the rate at which the water film evaporates is negligibly small. Furthermore, they evaluated the performance characteristics of different evaporative cooler configurations and compared their results to the heat rejection predicted by the manufacturer Baltimore Aircoil Company. They showed that there is a good correlation (less than a 10 % error) between the heat rejected as predicted by their analysis and the manufacture's prediction.

Qureshi and Zubair (2005) developed a model to analyze and predict the impact of fouling on the performance of evaporative coolers and condensers. The methodology followed in analyzing the thermal performance of the evaporative condenser is similar to the one given by Dreyer (1988), but introduces a fouling model based on the material balance equation proposed by Kern and Seaton (1959). The model was compared to numerical examples given by Dreyer (1988) and was within 2.2 percent of the predicted heat transfer.

Ren and Yang (2005) developed an analytical model based on the effectiveness NTU-method to evaluate the performance characteristics of an evaporative cooler for different flow configurations. They compared the analytical solution to the models which employ a Poppe type analysis, which are solved numerically, and the simplified models, employing the assumptions of Merkel. They state that the analytical model combines the simplicity of the simplified models while maintaining the accuracy of the detailed models which require numerical integration.

Qureshi and Zubair (2006) investigated the evaporation losses of evaporative coolers. They suggest an empirical correlation for determining the evaporative water losses. In a comparison with work of Dreyer (1998), Mizushima (1967) and Finlay and Harris (1984) errors of less than 4% in the evaporative water losses were noted, which is better than the approximations given by Baltimore Aircoil Company.

3.2.2 Analysis of the thermal performance characteristics of an evaporative condenser

In an evaporative cooler as shown in Figure 3.2, water (process water) is cooled inside the tubes, while deluge water is sprayed over a bundle of staggered horizontal plain tubes. In a

process of non-adiabatic heat and mass transfer, the deluge water evaporates into the air passing through the bundle.

In the present analysis of an evaporative condenser as shown in Figure 3.2, the following initial assumptions are made:

- It is a steady state process.
- Since the temperature differences are small, heat transfer by radiation is neglected.
- If the tube surfaces are uniformly wetted, the air flow and thermal states are uniformly distributed at the inlet and uniformity is maintained throughout the bundle, the problem can be analyzed in one dimension.
- If it is assumed that the re-circulating deluge water circuit is insulated from the surroundings and that pump work can be neglected, the temperature of the deluge water at the inlet and outlet of the tube bundle is the same.
- At the air-water interface surface, the air temperature approaches the temperature of the deluge water and the humidity of the air at the interface corresponds to that of a saturated air-vapor mixture.

By employing these assumptions and following an approach similar to Dreyer (1988), Poppe and Rögener (1984) and Bourilott (1983), an analytical model of the evaporative condenser can be derived from basic principles. Consider an elementary control volume about a tube as shown in Figure 3.3. Evaporation of the downward flowing water occurs at the air-water interface. Due to the one-dimensional characteristic of the unit, the properties of the air and water at any horizontal cross-section are assumed to be constant.

The mass balance applicable to the control volume is

$$m_a(1+w) + m_w + m_s = m_a[1+(w+dw)] + (m_w + dm_w) + m_s \quad (3.1)$$

or

$$dm_w = -m_a dw \quad (3.2)$$

where m_a is the mass flow rate of the dry air.

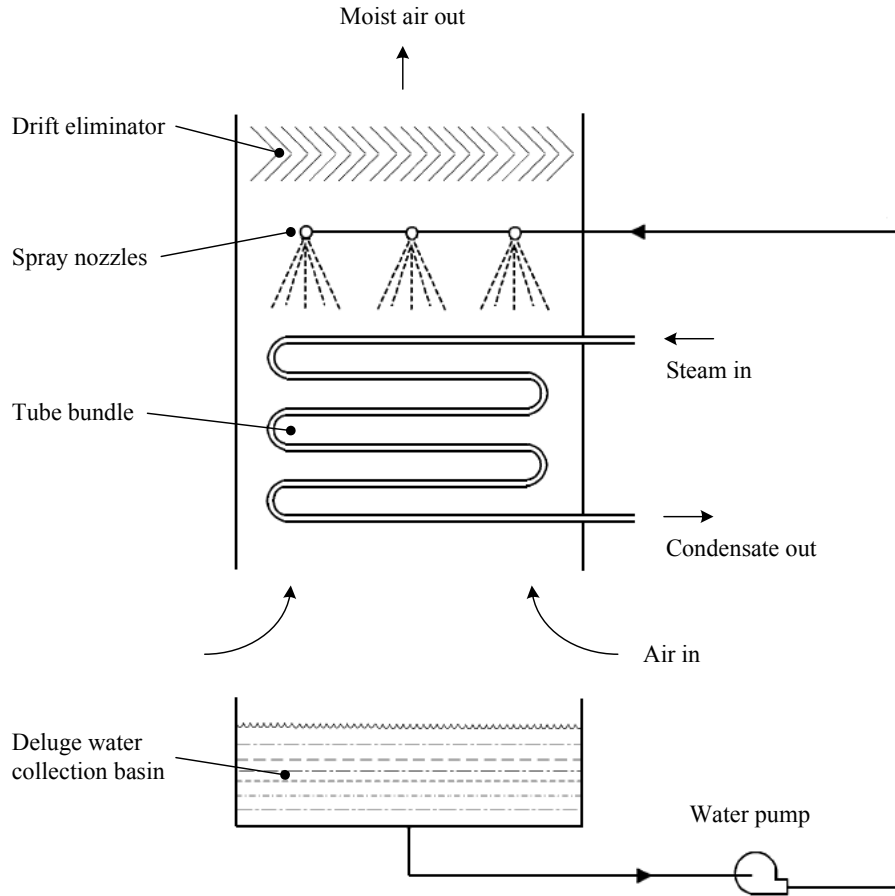


Figure 3.2: Schematic representation of an evaporative condenser

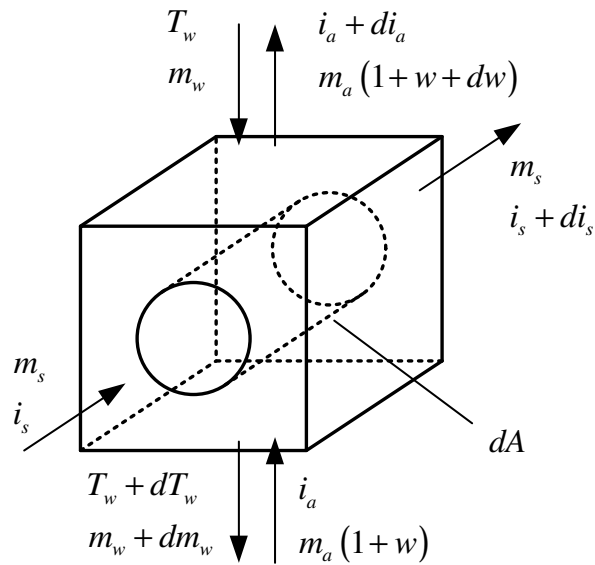


Figure 3.3: Control volume for the evaporative condenser

The energy balance over the control volume gives

$$m_a i_{ma} + m_w c_{pw} T_w + m_s i_s = \quad (3.3)$$

$$(m_w + dm_w) c_{pw} (T_w + dT_w) + m_a (i_{ma} + di_{ma}) + m_s (i_s + di_s)$$

where the deluge water temperature T_w is in °C.

Neglect the second order terms and simplify equation (3.3) to

$$dT_w = \frac{1}{m_w c_{pw}} (-m_a di_{ma} - c_{pw} T_w dm_w - m_s di_s) \quad (3.4)$$

where i_{ma} refers to the enthalpy of the air-vapor mixture per unit mass of dry air, which can be expressed as

$$i_{ma} = c_{pa} T_a + w(i_{fgwo} + c_{pv} T_a) \quad (3.5)$$

The latent heat, i_{fgwo} , is evaluated at 0°C and specific heats, c_{pv} and c_{pa} at $T_a/2^\circ \text{C}$.

If the moist air is un-saturated, the total enthalpy transfer at the air-water interface consists of an enthalpy transfer due to the difference in vapor concentration and the difference in temperature,

$$dQ = dQ_m + dQ_c \quad (3.6)$$

where the subscripts m and c refer to the enthalpies associated with the mass transfer and convective heat transfer.

The mass flow rate of the deluge water evaporating into the air stream is expressed as

$$dm_w = h_d (w_{sw} - w) dA \quad (3.7)$$

where w_{sw} is the saturated humidity ratio of the air evaluated at the bulk water film temperature.

The corresponding enthalpy transfer at the air-water interface due to the difference in the vapor concentration is then

$$dQ_m = i_v dm_w = i_v h_d (w_{sw} - w) dA \quad (3.8)$$

The enthalpy of the water vapor, i_v , calculated at the local bulk water film temperature, is given by

$$i_v = i_{fgwo} + c_{pv}T_w \quad (3.9)$$

where T_w is in °C and c_{pv} is evaluated at $T_w/2$ °C.

The convective transfer of sensible heat at the interface is given by

$$dQ_c = h(T_w - T_a)dA \quad (3.10)$$

Substituting equations (3.8) and (3.10) into equation (3.6), find the total enthalpy transfer at the air-water interface i.e.

$$dQ = i_v h_d (w_{sw} - w)dA + h(T_w - T_a)dA \quad (3.11)$$

The enthalpy of the saturated air at the air-water interface evaluated at the local bulk water film temperature is

$$i_{masw} = c_{pa}T_w + w_{sw} (i_{fgwo} + c_{pv}T_w) = c_{pa}T_w + w_{sw}i_v \quad (3.12)$$

which may be written as

$$i_{masw} = c_{pa}T_w + wi_v + (w_{sw} - w)i_v \quad (3.13)$$

Subtracting equation (3.5) from equation (3.13) and ignoring the small difference in the specific heats, the equation can be simplified as follows:

$$i_{masw} - i_{ma} \approx (c_{pa} + wc_{pv})(T_w - T_a) + (w_{sw} - w)i_v \quad (3.14)$$

or

$$T_w - T_a = [(i_{masw} - i_{ma}) - (w_{sw} - w)i_v] / c_{pam} \quad (3.15)$$

where $c_{pam} = c_{pa} + wc_{pv}$.

Substitute equation (3.15) into equation (3.11) and find

$$dQ = h_d \left[\frac{h}{c_{pma} h_d} (i_{masw} - i_{ma}) + \left(1 - \frac{h}{c_{pma} h_d} \right) i_v (w_{sw} - w) \right] dA \quad (3.16)$$

Noting that the enthalpy transfer must be equal to the enthalpy change of the moist air stream

$$\begin{aligned} di_a &= \frac{1}{m_a} dQ \\ &= \frac{h_d}{m_a} \left[\frac{h}{c_{pma} h_d} (i_{masw} - i_{ma}) + \left(1 - \frac{h}{c_{pma} h_d} \right) i_v (w_{sw} - w) \right] dA \end{aligned} \quad (3.17)$$

The heat transfer from the condensing steam to the deluge water is given by

$$dQ = U (T_s - T_w) dA \quad (3.18)$$

where U is the overall heat transfer coefficient between the steam inside the tubes and the deluge water on the outside.

$$U = \left[\frac{1}{h_w} + \frac{d_o \ln(d_o/d_i)}{2k_t} + \frac{d_o}{d_i h_c} \right] \quad (3.19)$$

The change in the enthalpy of the steam can now be written as

$$di_s = -\frac{dQ}{m_s} \quad (3.20)$$

Substituting equation (3.18) into equation (3.20) yields

$$di_s = \frac{U}{m_s} (T_s - T_w) dA \quad (3.21)$$

For the case where the moist air is not saturated, equations (3.2),(3.4),(3.7),(3.17) and (3.21) describe the processes that take place in the control volume of the evaporative condenser.

The model can be simplified by making use of the assumptions of a Merkel-type analysis: Firstly it is assumed that the amount of deluge water that evaporates is small compared to the mass flow rate of the deluge water and secondly the Lewis factor, which gives the relation between the heat and mass transfer, is equal to unity. The Lewis factor can be expressed as

$$Le_f = h / (c_{pma} h_d).$$

For the Merkel type analysis the governing equations (3.4),(3.17) and (3.21) become:

$$dT_w = -(m_a di_{ma} + m_s di_s) / m_w c_{pw} \quad (3.22)$$

$$di_a = \frac{h_d}{m_a} (i_{masw} - i_{ma}) dA \quad (3.23)$$

$$di_s = \frac{U}{m_s} (T_s - T_w) dA \quad (3.24)$$

If the evaporative condenser is evaluated using the iterative step-wise Merkel type analysis, it is found that the three governing equations must describe four unknown parameters. The Merkel type analysis is often used in evaluating the thermal performance characteristics of fills or packs, in wet-cooling towers. In the analysis of wet-cooling towers, the Merkel integral is numerically integrated over the deluge water temperature, T_w (using for example the four-point Chebyshev integration technique) (Kloppers and Kröger 2005). If the inlet and outlet deluge water temperature of evaporative heat exchanger is the same, then the solution of the numerical integral is trivial.

Kröger (2004) suggests the use of the simplified Merkel type analysis, where a constant mean deluge water temperature is assumed and only the inlet and outlet values of the fluid parameters are evaluated. It is possible to solve the simplified Merkel type analysis analytically if the assumption of Merkel is made that the outlet air is saturated.

The heat transfer rate of the evaporative condenser is given by the following equation:

$$Q = m_a (i_{ao} - i_{ai}) = m_s (x_i - x_o) i_{fg} \quad (3.25)$$

where x_i and x_o is respectively the steam quality at the inlet and the outlet and i_{fg} is the latent heat of evaporation of the steam.

In the case where saturated vapor enters the tube and is completely condensed to saturated liquid, the heat transfer rate can be expressed as

$$Q = m_s i_{fg} \quad (3.26)$$

The governing equations (3.23) and (3.24) for the simplified model are

$$m_a di_a = h_d (i_{masw} - i_{ma}) dA \quad (3.27)$$

$$m_a di_a = U (T_s - T_w) dA \quad (3.28)$$

Assuming a constant mean deluge water temperature through the condenser, integrate equation (3.28) between the inlet and outlet conditions and find

$$(i_{ao} - i_{ai}) = \frac{UA}{m_a} (T_s - T_{wm}) \quad (3.29)$$

Similarly for equation (3.27)

$$\ln \left[\frac{i_{maswm} - i_{ai}}{i_{maswm} - i_{ao}} \right] = \frac{h_d}{m_a} A_a \quad (3.30)$$

where A_a is the air-water interface area.

Equation (3.30) may then be expressed in terms of the outlet air enthalpy as

$$i_{ao} = i_{maswm} - (i_{maswm} - i_{ai}) e^{-NTU_a} \quad (3.31)$$

$$\text{where } NTU_a = \frac{h_d}{m_a} A_a .$$

Rearranging equation (3.29), the mean temperature of the deluge water can be expressed as

$$T_{wm} = T_s - (m_a/UA)(i_{ao} - i_{ai}) \quad (3.32)$$

For both the Poppe and the simplified Merkel analyses the water film heat transfer coefficients, h_w , and the air-water mass transfer coefficients, h_d , are obtained experimentally. To evaluate the heat and mass transfer coefficients, performance tests are conducted on an evaporative cooler. In the following chapter the experimental results of the water film heat transfer coefficient, air-water mass transfer coefficient and the air-side pressure drop over the deluged tube bundle are presented and discussed.

3.3 Plain tube bundle operated as an air-cooled condenser

During periods of lower ambient temperatures or lower demands the plain tube bundles of the hybrid dephlegmator are operated as a dry air-cooled condenser.

The heat rejected by the air-cooled condenser is

$$Q = m_a c_{pa} (T_{ao} - T_{ai}) = m_s (x_i - x_o) i_{fg} \quad (3.33)$$

The governing equation for the air-cooled condenser is

$$m_a c_{pa} dT_a = U_a (T_s - T_a) dA \quad (3.34)$$

where U_a is the overall heat transfer coefficient between the steam inside the tubes and the air on the outside

$$U_a = \left[\frac{1}{h_a} + \frac{d_o \ln(d_o/d_i)}{2k_t} + \frac{d_o}{d_i h_c} \right] \quad (3.35)$$

The heat transfer between the tube wall and the air flowing through the bundle, h_a , is discussed in Chapter 5.

4 Experimental investigation of an evaporative heat exchanger

The analysis of evaporative condensers is presented in section 3.2. It is found that there are measurable differences in the existing empirical correlations used for determining the film heat transfer coefficient, h_w , and the air-water mass transfer coefficient, h_d . Performance tests are conducted on an evaporative cooler consisting of 15 tube rows with 38.1 mm outer diameter galvanized steel tubes arranged in a 76.2 mm triangular pitch. From experimental results, correlations for the water film heat transfer coefficient, air-water mass transfer coefficient and the air-side pressure drop over the deluged tube bundle are developed.

For the simplified Merkel analysis the heat transfer coefficient at the tube-water interface, h_w , and air-water mass transfer coefficient, h_d , are obtained experimentally under different operating conditions employing the procedure given in section 4.2. Although the simplified Merkel analysis does not predict the amount of water lost by evaporation as accurately as the Poppe analysis, it will predict the heat rejection rate of an evaporative cooler correctly if the abovementioned experimentally obtained transfer coefficients are used in the analysis.

4.1 Apparatus

A schematic layout of the apparatus and the placement of the measurement equipment is shown in Figure 4.1.

The tube bundle consists of $n_r = 15$ rows of externally galvanized steel tubes. The tubes are $L = 0.65$ m long and are arranged in a triangular pattern at a transversal pitch of $P_t = 76.2$ mm as shown in Figure 4.2. The outside diameter of the tubes is $d_o = 38.1$ mm and the inside diameter is $d_i = 34.9$ mm. There are $n_{tr} = 8$ tubes per tube row.

To ensure uniform flow of the air through the tube bundle, inactive halftubes are installed at the sides of the tube bundle. In the spray frame a header distributes or divides the deluge water into several conduits or lateral branches. Each lateral branch consists of a two perforated stainless steel tubes, the one placed inside the other. With this configuration it is possible to establish a uniform pressure distribution in the lateral branches (perforated tubes) and achieve a uniform water distribution.

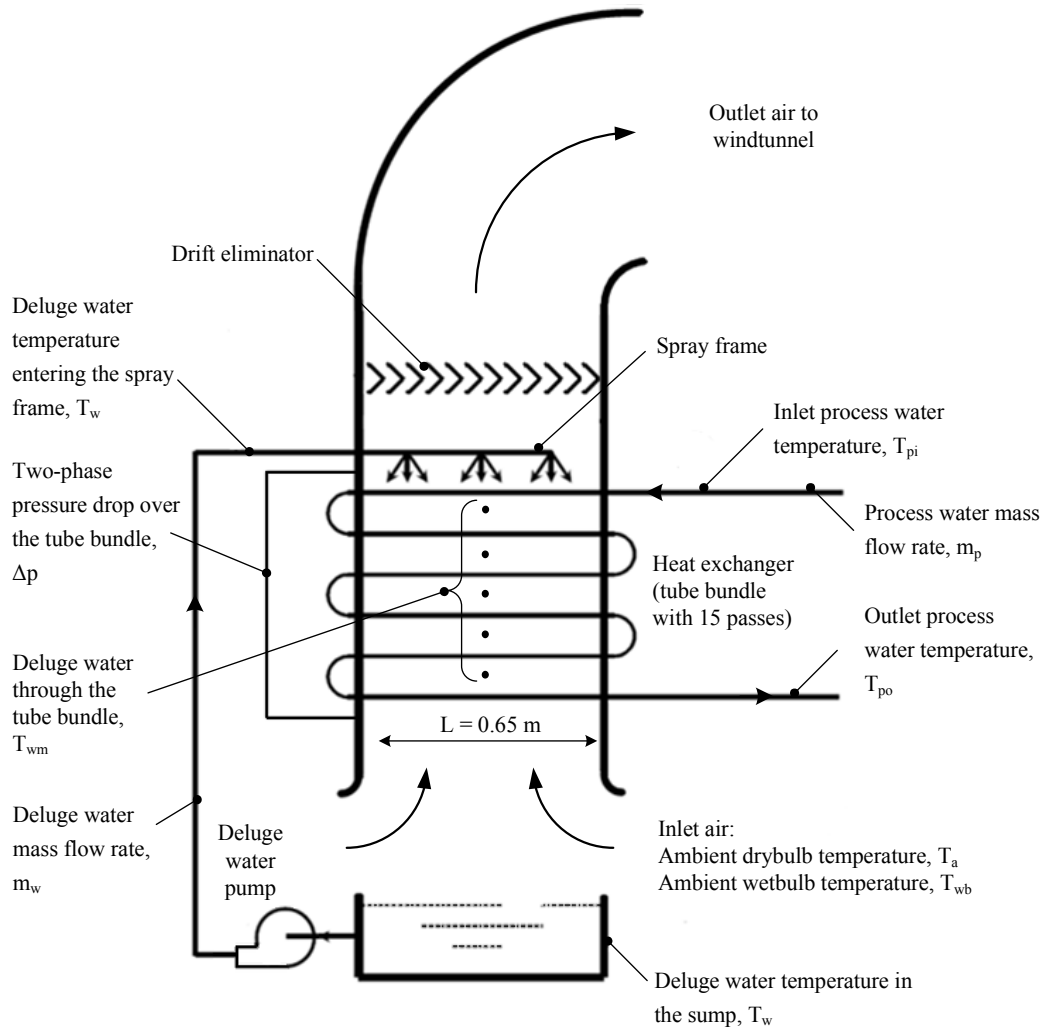


Figure 4.1: Schematic layout of the apparatus

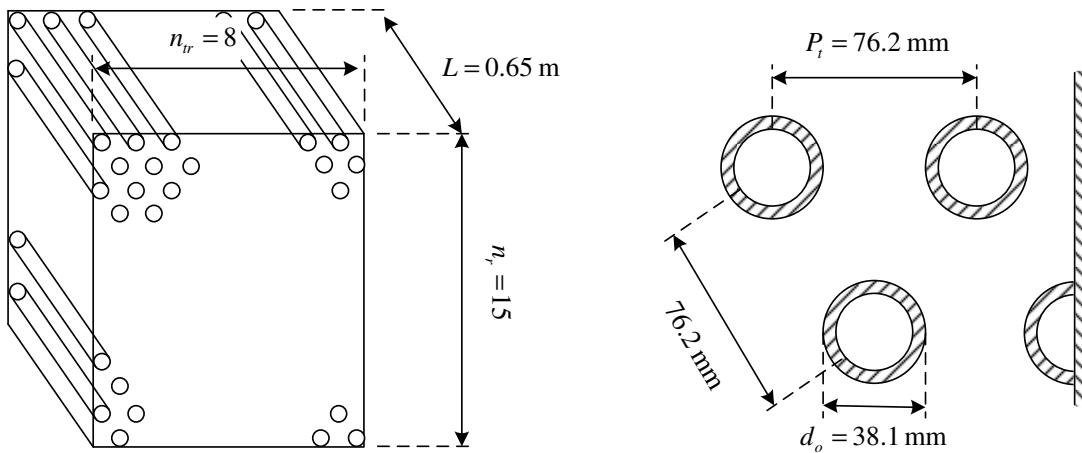


Figure 4.2: Tube bundle layout and tube dimensions

The mass flow rate of the deluge water is measured using a thin-plate orifice. The deluge water temperature is measured in the collecting basin and before it enters the spray frame. The deluge water temperatures through tube bundle are measured with thermocouples placed after each tube row; the mean deluge water temperature, T_{wm} , is taken as the average of these thermocouple readings.

The inlet temperature of the warm process water, T_{pi} , is measured as it enters the top inlet header. After flowing through the tubes the process water exits the bundle at the bottom outlet header, where its temperature, T_{po} , is measured. Process water mass flow rate, m_p , is obtained at the start of each set of tests by means of the displacement method. The process water is heated in a 72 kW, 156 l geysers.

The test section is connected to the inlet of an atmospheric open-loop induced draft windtunnel, drawing air over the tube bundle. By measuring the pressure drop over an elliptical flow nozzle located in the windtunnel the air mass flow rate can be determined. The pressure drop over the tube bundle is measured with the aid of a differential pressure transducer.

Drybulb and wetbulb temperatures of the ambient air, are measured at the inlet of the tube bundle, while the atmospheric pressure is read from a mercury column barometer.

After steady-state conditions are reached the measured data is integrated over a period of two minutes and logged. The water film heat transfer coefficient, air-water mass transfer coefficient and the air-side pressure drop over the deluged tube bundle is evaluated for different air mass flow rates, deluge water mass flow rates and deluge water temperatures.

4.2 Determining the heat and mass transfer coefficients

The governing equations for the simplified Merkel type analysis of an evaporative cooler can be derived by following a procedure similar to the one given for the analysis of the evaporative condenser in Section 3.2.

$$m_p c_{pp} dT_p = U (T_p - T_{wm}) dA \quad (4.1)$$

$$di_a = \frac{h_d}{m_a} (i_{aswm} - i_a) dA_a \quad (4.2)$$

The heat transfer rate of the evaporative cooler is given by the following equation:

$$Q = m_a (i_{ao} - i_{ai}) = m_p c_{pp} (T_{pi} - T_{po}) \quad (4.3)$$

Assuming a constant mean deluge water temperature, T_{wm} , through the cooler, integrate equation (4.1) between the inlet and outlet conditions and find

$$T_{po} = T_{wm} + (T_{pi} - T_{wm}) e^{-UA/m_p c_{pp}} \quad (4.4)$$

where

$$\frac{1}{UA} = \left[\frac{1}{h_p A_i} + \frac{d_o \ln(d_o/d_i)}{2k_i A_o} + \frac{1}{h_w A_o} \right] \quad (4.5)$$

All the values in equation (4.4) and equation (4.5) are measured or known and $h_w A_o$ can be determined. The average water film heat transfer coefficient, h_w , is based on the mean deluge water temperature, T_{wm} .

Integrate equation (4.2) to and find

$$i_{mao} = i_{awm} - (i_{awm} - i_{mai}) e^{-NTU_a} \quad (4.6)$$

where $NTU_a = h_d A_a / m_a$

The outlet air enthalpy is determined from equation (4.3). All the values in equation (4.6) are measured or known and h_{de} can be determined. Due to droplet and strand formation it is not possible to accurately determine the air-water interface area, A_a , and the tube outer area, A_o is then used as reference area. The effective average air-water mass transfer coefficient, h_d , based on the mean deluge water temperature, T_{wm} , and the tube outer area, A_o .

4.3 Results and observations

To ensure a good deluge water distribution Niitsu et al. (1969) recommends a water loading that should not be less than $\Gamma_m/d_o = 0.8 \text{ kg/m}^2\text{s}$ or $G_w = 1.6 \text{ kg/m}^2\text{s}$. From the present experimental study it is found that a deluge water mass velocity of $G_w = 1.7 \text{ kg/m}^2\text{s}$ is required to ensure uniform wetting of all the tubes in the bundle.

At air mass velocities higher than $G_a = 3.5 \text{ kg/m}^2\text{s}$ the deluge water is partially held up on the tubes. This water breaks away from the tube surface and flows sideways in the form of strands that straddle the tubes. There are no visible traces of entrained droplets downstream of the drift eliminator at this air mass velocity.

In Figure 4.3 an example of the change in the deluge water temperature through the tube bundle is shown. For almost all of the tests the deluge water temperature deviated by less than 3°C from the mean deluge water temperature.

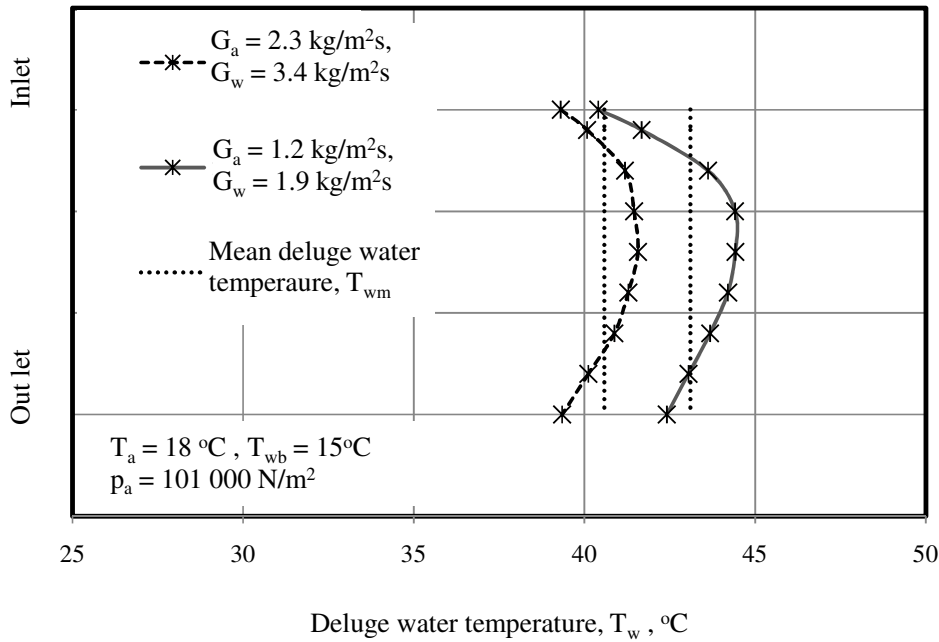


Figure 4.3: Variation in the deluge water temperature

The experimental tests investigated the influences of the air mass flow rate, deluge water flow rate and the deluge water temperature on the film heat transfer coefficient, the air-water mass transfer as well as the air-side pressure drop over the deluged tube bundle.

Mizushina et al. (1967), Niitsu et al. (1969) and Leidenforst and Korenic (1982) express the film heat transfer coefficient as function of only the deluge water mass flow rate. Parker and Treybal (1961) extended their correlation to include the effect of the deluge water temperature. The present experimental results show that the deluge water mass flow rate has the greatest influence on the film heat transfer coefficient, h_w , but this coefficient is also a function of the air mass flow rate and the deluge water temperature as given by equation (4.7). Parker and Treybal (1961) state that h_w increases linearly with the deluge water temperature. This is well approximated by $T_w^{0.3}$, as given in equation (4.7), over the range tested. The experimental results of the film heat transfer coefficient as a function of the air mass velocity, deluge water mass velocity and deluge water temperature is shown in Figure 4.4, Figure 4.5 and Figure 4.6.

$$h_w = 470 G_a^{0.1} G_w^{0.35} T_w^{0.3} \tag{4.7}$$

for $0.7 < G_a < 3.6 \text{ kg/m}^2\text{s}$, $1.8 < G_w < 4.7 \text{ kg/m}^2\text{s}$ and $35 < T_{wm} < 53 \text{ }^\circ\text{C}$.

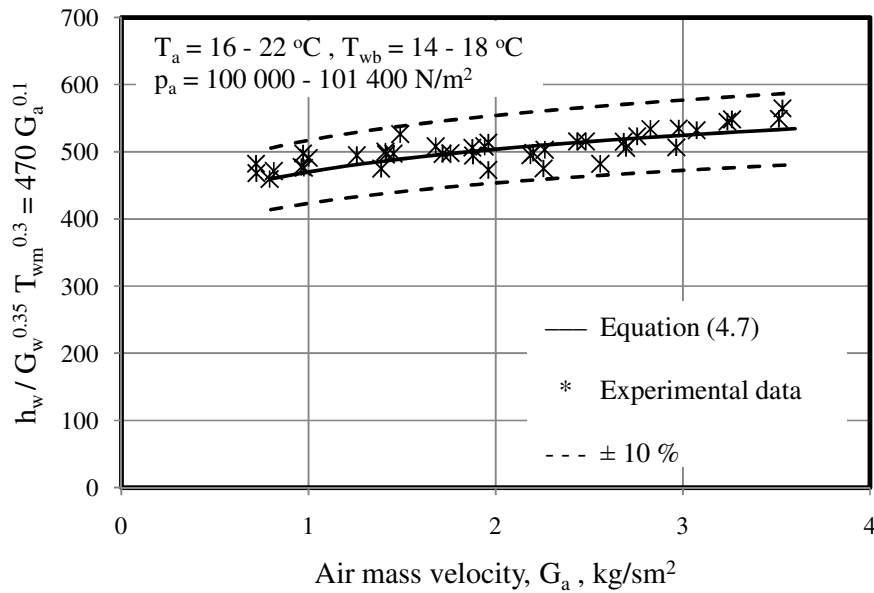


Figure 4.4: Heat transfer coefficient as a function of the air flow rate

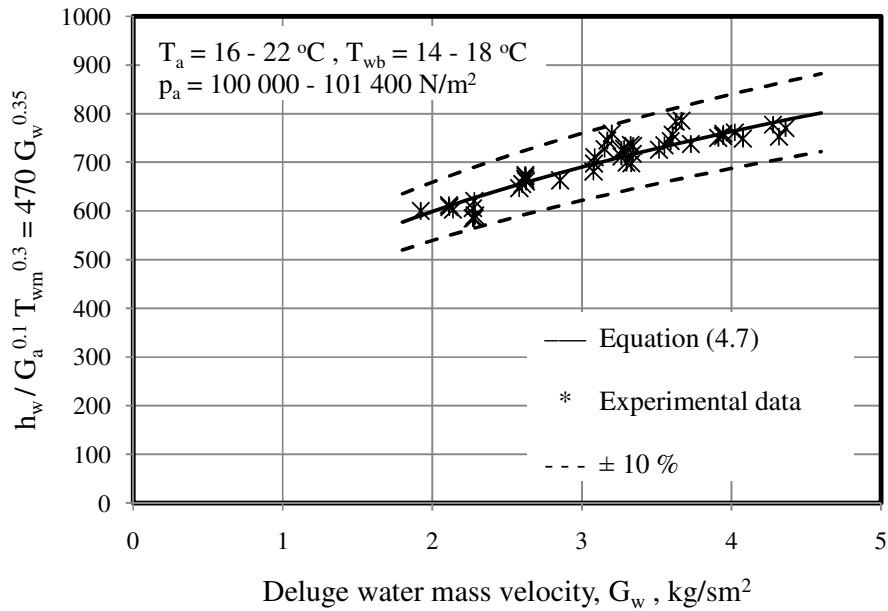


Figure 4.5: Heat transfer coefficient as a function of the deluge water flow rate

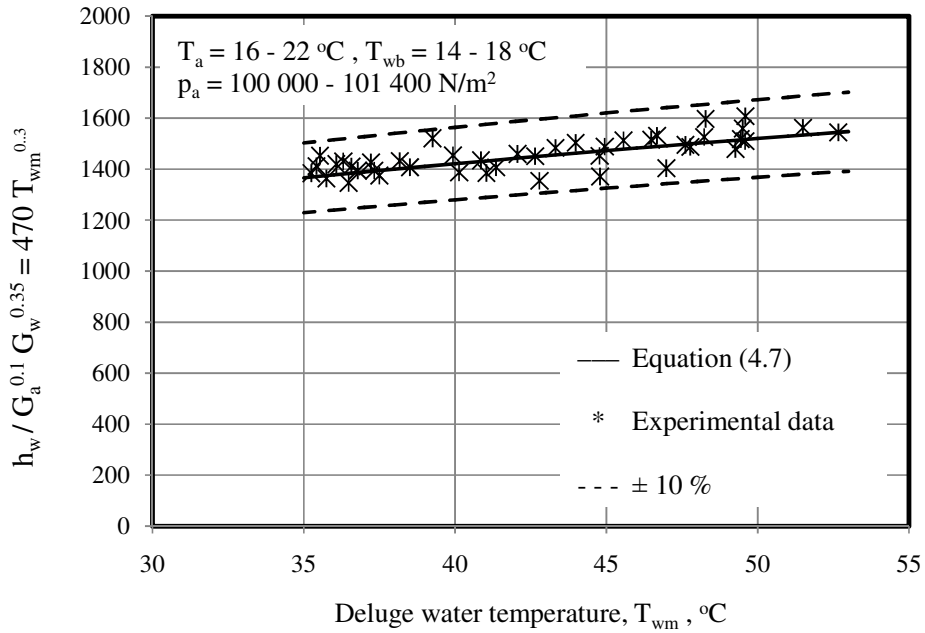


Figure 4.6: Heat transfer coefficient as a function of the deluge water temperature

In Figure 4.7, Equation (4.7) is compared to the correlation given by Mizushina et al. (1967). The correlation compares well at an air mass velocity of $G_a = 3.2 \text{ kg/m}^2\text{s}$ (as stated earlier the correlation given by Mizushina et al. (1967) is not dependent on the air mass velocity).

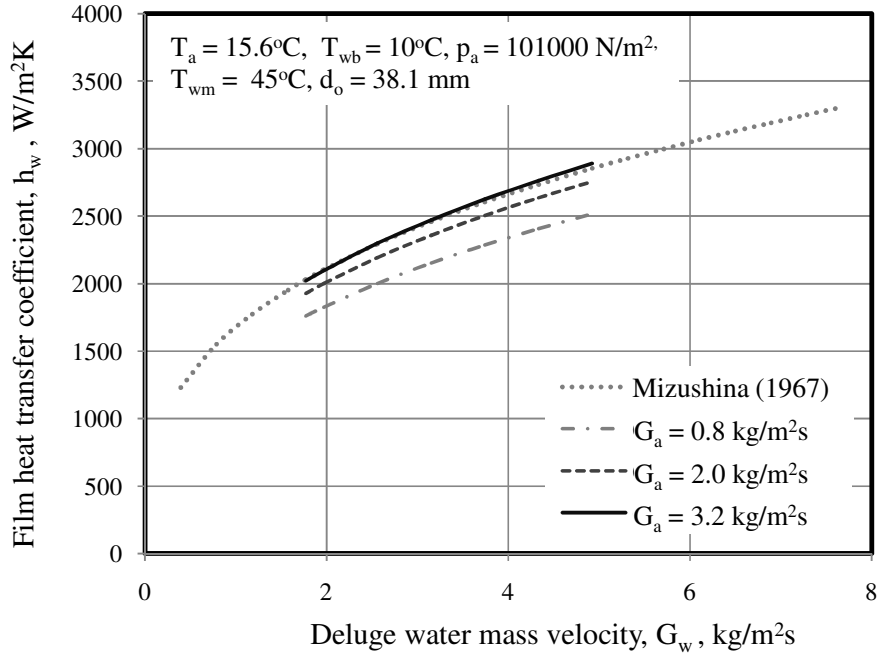


Figure 4.7: Film heat transfer coefficient

The correlations recommended by Parker and Treybal (1961) and Niitsu et al. (1969) for the air-water mass transfer coefficient, are only a function of the air mass velocity. The flow of the deluge water over the staggered tubes is similar to the flow of cooling water through fills and packs used in wet cooling towers. The mass transfer coefficient for fills or packs is typically given in terms of the air and the water flow rate. Mizushina et al. (1967) gives the mass transfer coefficient in terms of an air and deluge water Reynolds numbers. From the present experimental results it follows that the air-water mass transfer coefficient is a function of the air mass velocity and the deluge water mass velocity as given by equation (4.8). The experimental results of the air-mass transfer coefficient as a function of the air mass velocity, deluge water mass velocity and deluge water temperature are shown in Figure 4.8, Figure 4.9 and Figure 4.10

$$h_{de} = 0.038 G_a^{0.73} G_w^{0.2} \quad (4.8)$$

for $0.7 < G_a < 3.6 \text{ kg/m}^2s$ and $1.8 < G_w < 4.7 \text{ kg/m}^2s$.

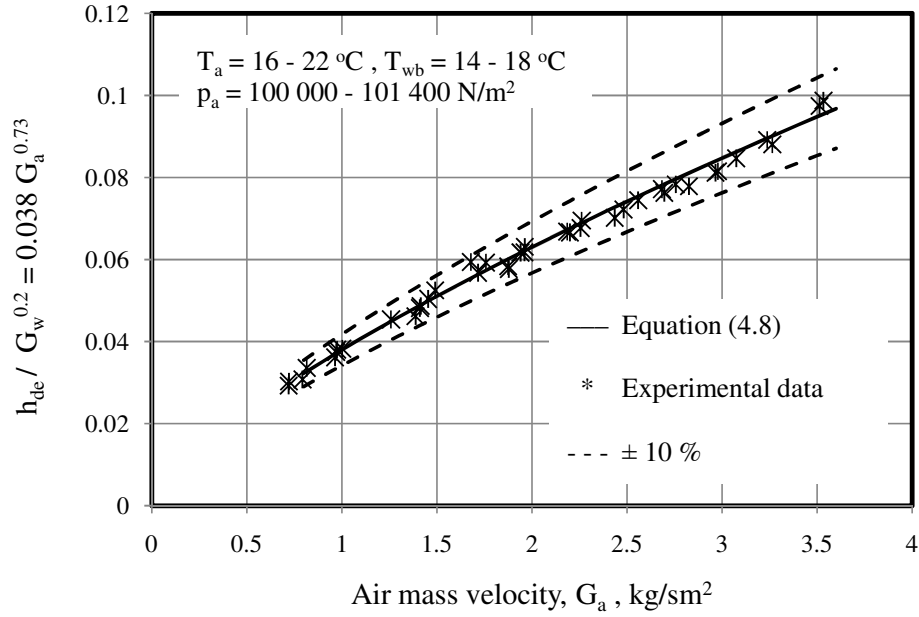


Figure 4.8: Mass transfer coefficient as a function of the air mass velocity

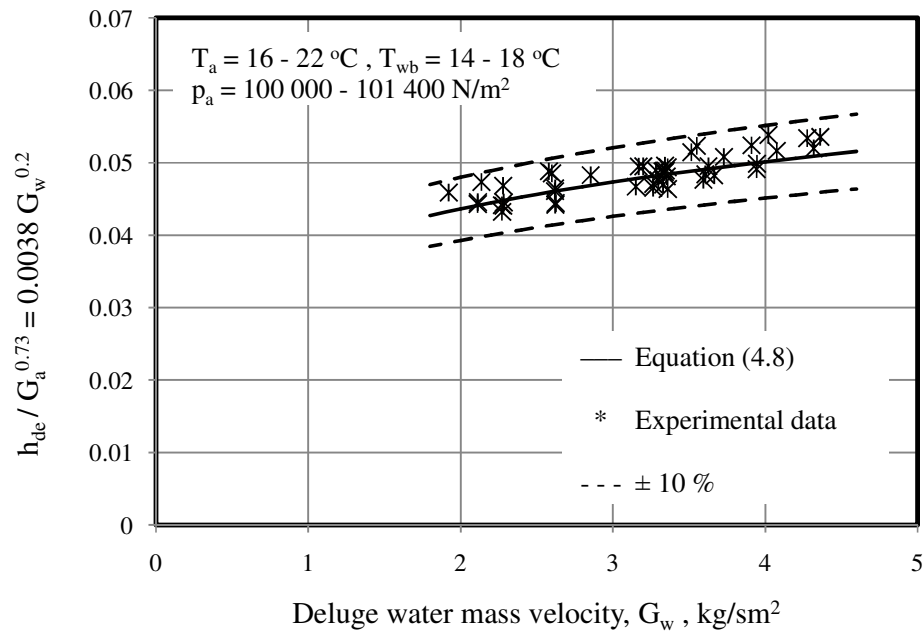


Figure 4.9: Mass transfer coefficient as a function of the deluge water mass velocity

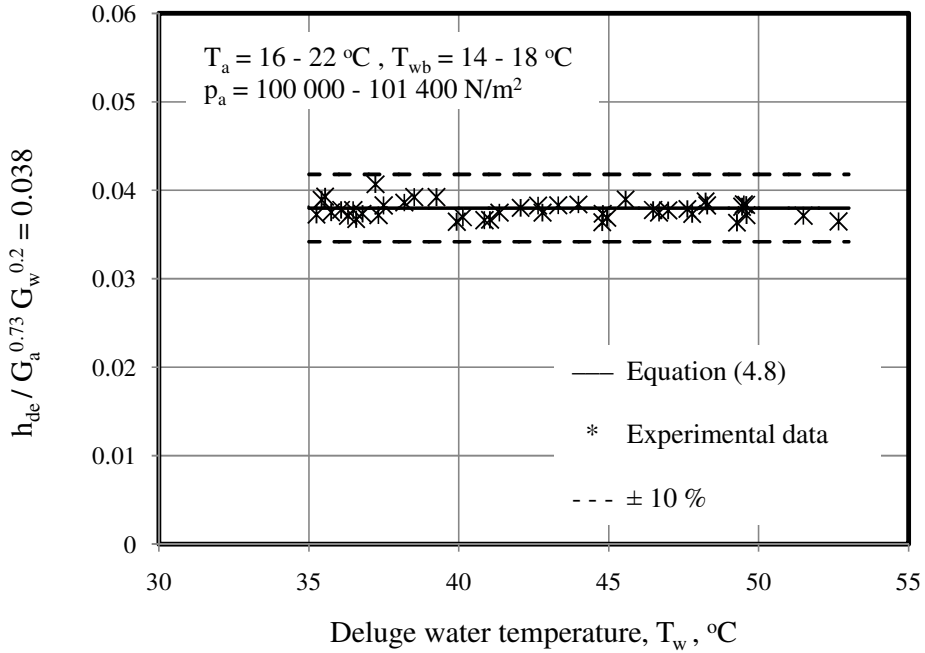


Figure 4.10: Mass transfer coefficient as a function of the deluge water temperature

In Figure 4.11, equation (4.8) is compared to the correlation of Mizushina et al. (1967).

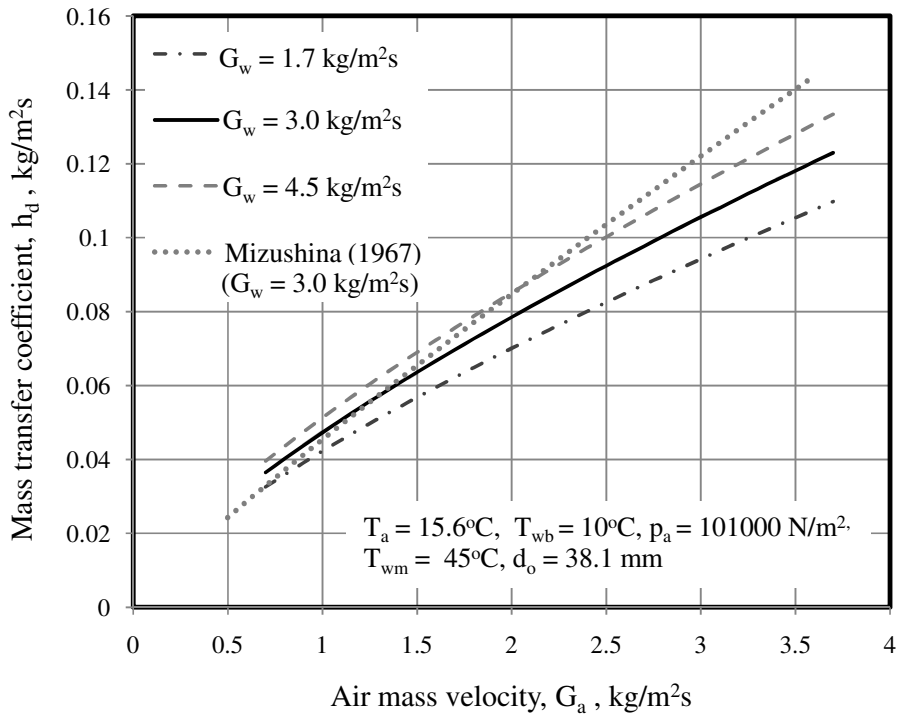


Figure 4.11: Air-water interface mass transfer coefficient

Relatively little published information is available for the predicting the pressure drop across deluged tube bundles. The correlation of Niitsu et al. (1969) for the air-side pressure drop over a deluged tube bundle with 16 mm diameter tubes is given in terms of the air flow rate as well as the deluge water flow rate. From the present experimental results it follows that the air-side pressure drop over the tube bundle is a function of the air mass velocity and the deluge water mass velocity as given by equation (4.9). The experimental results of the pressure drop over the tube bundle as a function of the air mass velocity, deluge water mass velocity and deluge water temperature are shown in Figure 4.12, Figure 4.13, and Figure 4.14.

$$\Delta p = 10.2 G_a^{1.8} G_w^{0.22} \tag{4.9}$$

for $0.7 < G_a < 3.6 \text{ kg/m}^2\text{s}$ and $1.8 < G_w < 4.7 \text{ kg/m}^2\text{s}$.

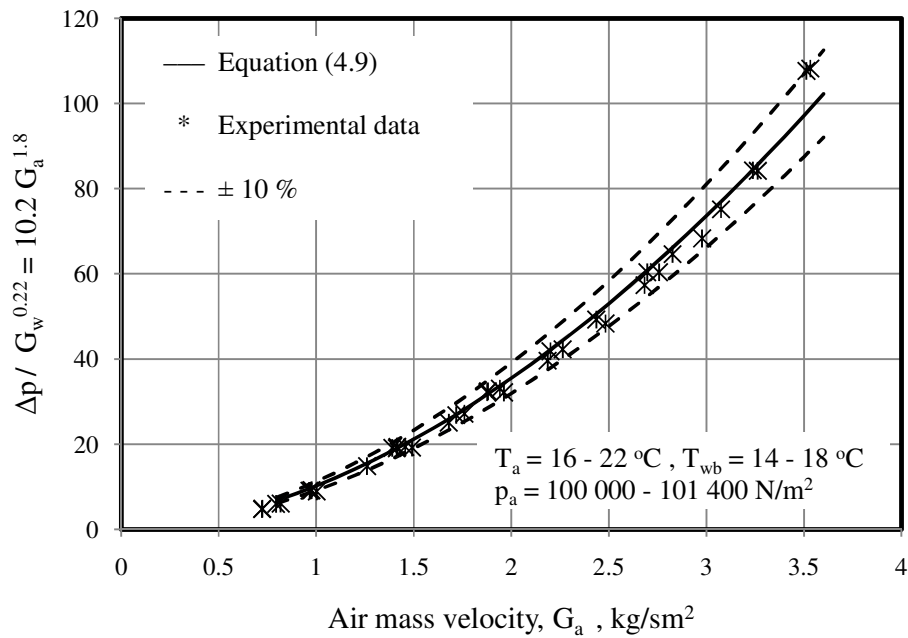


Figure 4.12: Air-side pressure drop as a function of the air mass velocity

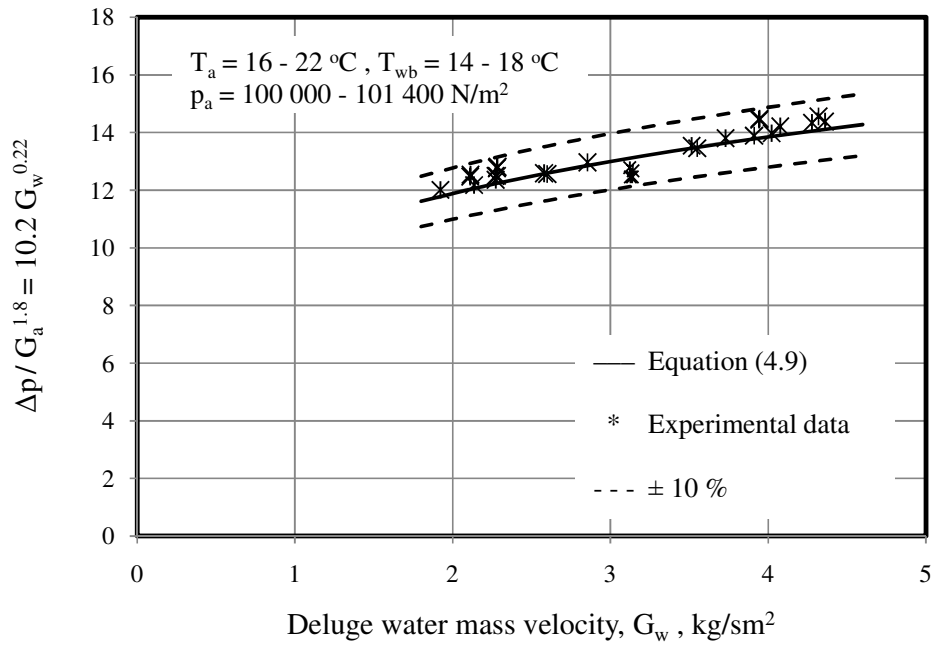


Figure 4.13: Air-side pressure drop as a function of the deluge water mass velocity

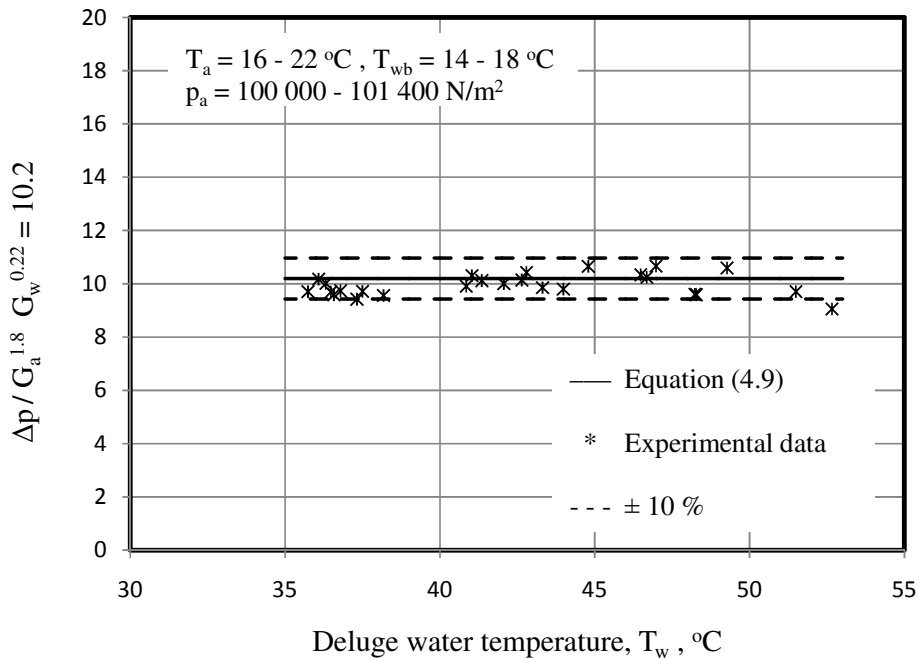


Figure 4.14: Air-side pressure drop as a function of the deluge water temperature

Equation (4.9) is plotted in Figure 4.15.

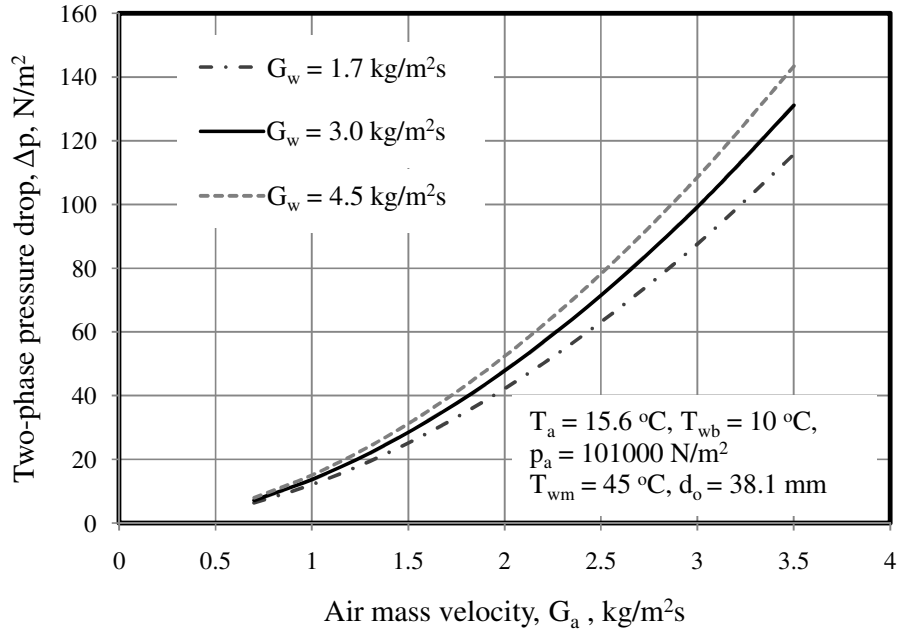


Figure 4.15: Air-side pressure drop

The correlations developed for the film heat transfer coefficient, air-water mass transfer coefficient and the air-side pressure drop are only valid for a bundle consisting of 15 tube rows with 38.1 mm diameter tubes.

For the simplified Merkel type analysis the assumption is made that the outlet air is saturated. The drybulb temperature is measured upstream of the elliptical nozzles in the windtunnel. Although there is some uncertainty in the measurements, it is found that the measured outlet air temperature for most tests is approximately 2°C higher than the predicted saturation temperature. The outlet air is thus unsaturated and the humidity ratio lower than predicted. The amount of water evaporated can be approximated by $m_{w(evap)} = m_a (w_{so} - w_i)$.

4.4 Conclusion

Performance tests were conducted on an evaporative cooler consisting of 15 tubes rows with 38.1 mm outer diameter galvanized steel tubes arranged in a 76.2 mm triangular pattern. Correlations for the water film heat transfer coefficient, the air-water mass transfer coefficient and the air-side pressure drop are developed from experimental results. The present experimental results show that the film heat transfer coefficient (Equation (4.7)) is a function of the air mass velocity, deluge water velocity as well as the deluge water

temperature, while the air-water mass transfer coefficient (Equation (4.8)) and the air-side pressure drop (Equation (4.9)) is a function of the air mass velocity and the deluge water mass velocity. The correlations for the water film heat transfer coefficient and the air-water mass transfer coefficient compare well with the correlations recommended by Mizushina et al. (1967).

5 Experimental investigation of the plain tube bundle operated dry

The thermo-flow characteristics of air-cooled tubes (horizontally arranged) in cross-flow are experimentally evaluated.

Grimson (1937) and Zukauskas and Ulinskas (1988) independently studied the air-side heat transfer of air-cooled tube bundles in cross-flow. Their correlations are compared to the present experimental results shown in Figure 5.1. The experimental results compare well with the correlations recommended by Grimson (1937) and Zukauskas and Ulinskas (1988). It is recommended that the correlation of Zukauskas and Ulinskas (1988) be used to determine the air-side heat transfer coefficient of the galvanized steel tube bundle of the hybrid (dry/wet) dephlegmator when operated as a dry air-cooled condenser.

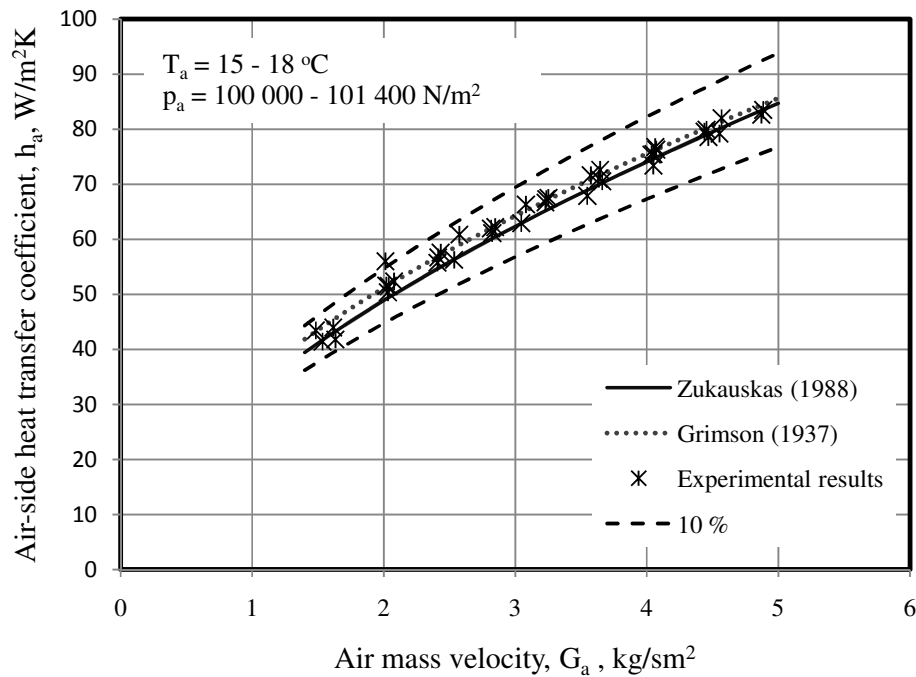


Figure 5.1: Air-side heat transfer coefficient for dry tubes in cross-flow

Jakob (1938) and Gaddis and Gnielinski (1985) studied the air-side pressure drop of air-cooled tube bundles in cross-flow. Their correlations for the air-side pressure drop over the tube bundle are compared to the present experimental results in Figure 5.2. Both correlations compares well with the present experimental results. It is recommended that the correlation of Gaddis and Gnielinski (1985) be used to calculate the pressure loss over the galvanized steel tubes of the second stage of the hybrid (dry/wet) dephlegmator when operated as a secondary air-cooled condenser

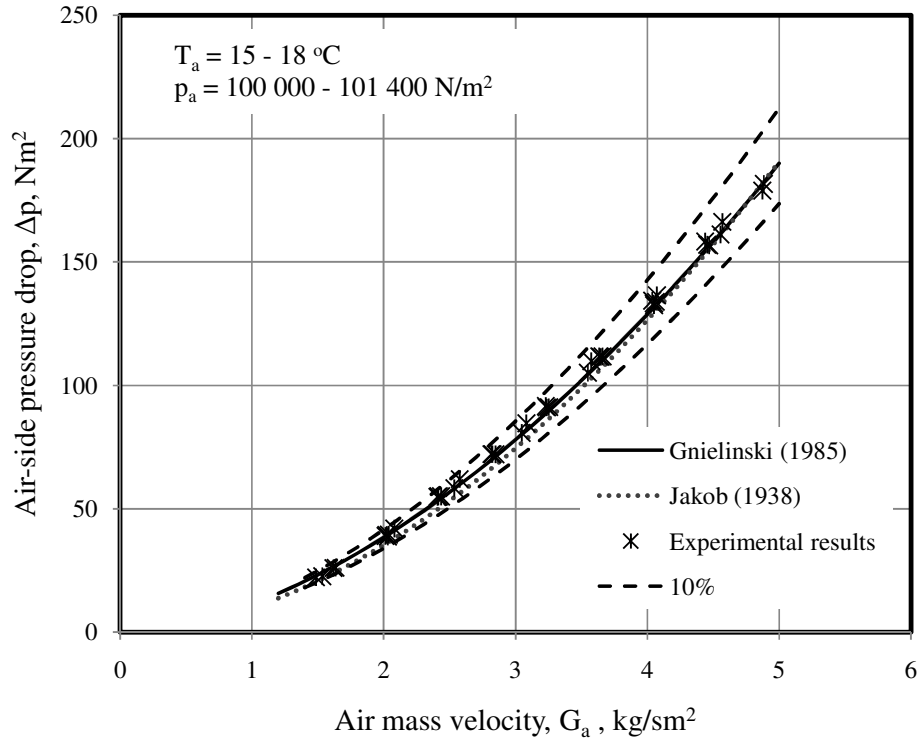


Figure 5.2: Air-side pressure drop of a dry tube bundle in cross-flow

6 Performance characteristics of a steam turbine incorporating an air-cooled condenser with a hybrid (dry/wet) dephlegmator

Consider a power plant in which the turbine exhaust steam is fed to three air-cooled condenser streets as shown in Figure 2.2. The turbo-generator power output can be expressed in terms of the steam temperature, T_v , i.e.

$$P_{gen} = 225.83 - 0.0043T_v + 0.01332T_v^2 - 0.000163T_v^3, \text{ MW}$$

while the corresponding heat to be rejected by the condenser is

$$Q = 336.4 + 0.18223T_v - 0.01601T_v^2 + 0.00018T_v^3, \text{ MW}$$

where T_v is in $^{\circ}\text{C}$. These curves are shown in Figure 6.1.

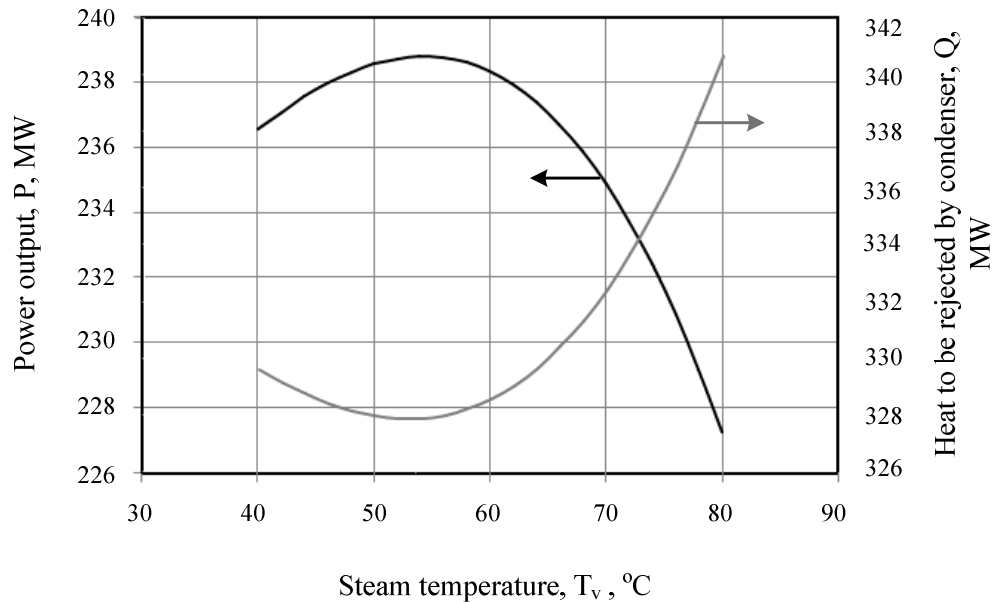


Figure 6.1: Performance characteristics of turbo-generator-condenser system

The turbo-generator power output for the steam turbine with three streets of A-frame air-cooled condensers is shown in Figure 6.2.

Based a study done by Boulay et al. (2005) on the oversizing of the air-cooled condensers, it was decided to investigate the performance characteristics of the steam turbine incorporating A-frame air-cooled condensers consisting of 4 and 5 condenser streets or rows. In Figure 6.2

the power output for these A-frame air-cooled condensers are shown as a function of the ambient temperature.

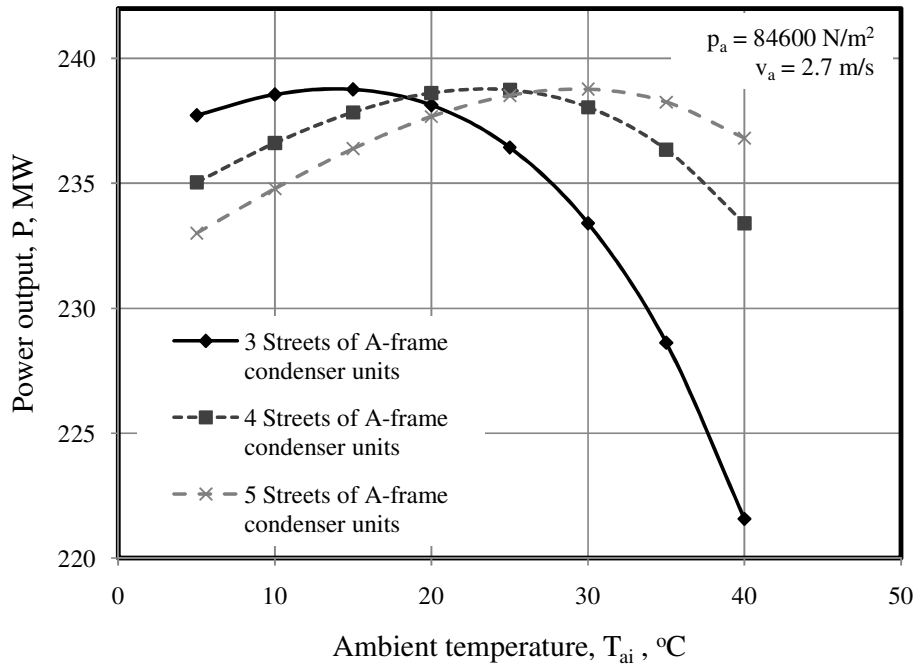


Figure 6.2: Sizing air-cooled condensers

At higher ambient temperatures, the turbo-generator power output with three streets can be improved with the addition of a further street. At an ambient temperature of 40°C, the increase in the power output for the particular turbine with this extra street is approximately 5%. The further increase in power output is only 1.7% if the number of condenser streets is increased to five. Boulay et al. (2005) stated that the increase in the initial capital cost of the air-cooled condenser is directly proportional to the condenser size.

In Section 2.3 the enhancement of an air-cooled condenser through the adiabatic cooling of the inlet air was discussed. The performance characteristics of the steam turbine incorporating three streets of A-frame air-cooled condensers with adiabatic cooling (spray cooling) of the inlet air is evaluated; the turbo-generator power output is shown in Figure 6.4. For the adiabatic cooling of the inlet air (50% relative humidity), it is assumed that a 100% wetbulb depression is achieved i.e. the drybulb temperature of the inlet air is lowered to the wetbulb temperature.

Consider the steam turbine incorporating three streets of A-frame air-cooled condensers with hybrid (dry/wet) dephlegmators (HDWC) as shown in Figure 6.3. The turbo-generator power output for the air-cooled condenser incorporating a hybrid (dry/wet) dephlegmator (operated in wet mode) is shown in Figure 6.4.

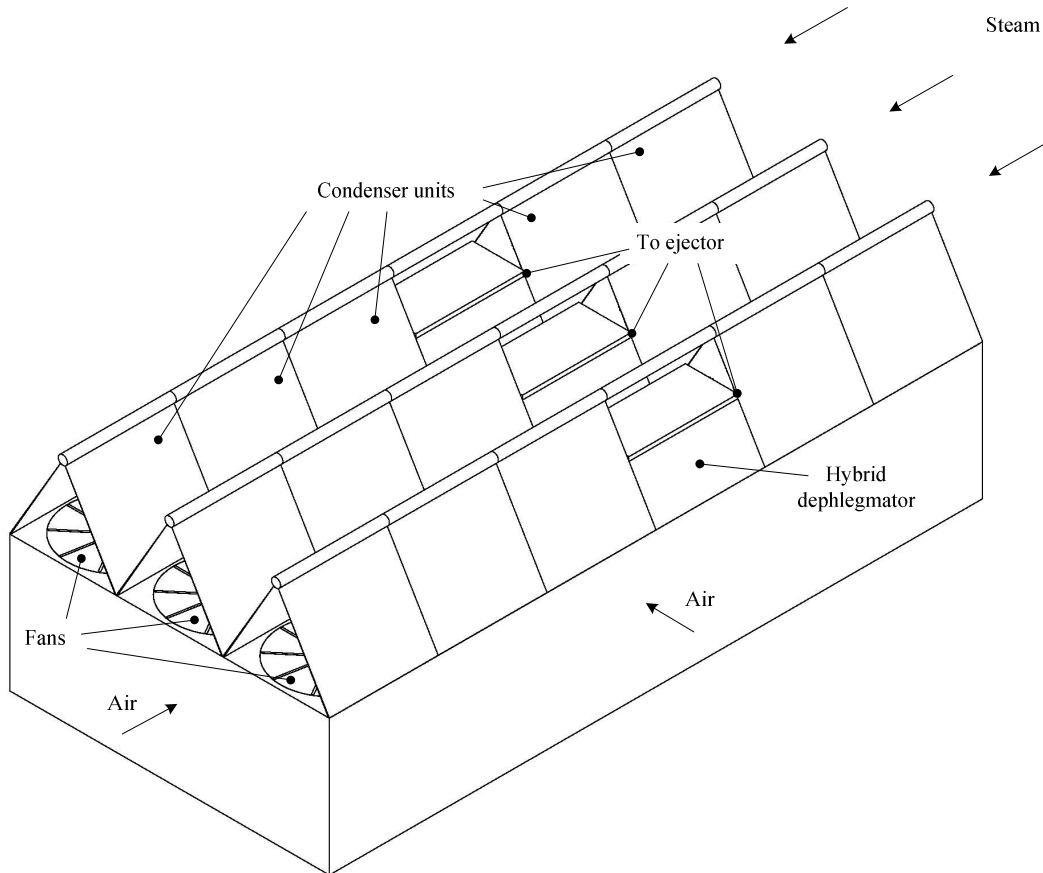


Figure 6.3: Multi-row or multi-street (3streets) array of A-frame air-cooled condensers incorporating hybrid (dry/wet) dephlegmators

The power output for three streets of air-cooled condensers incorporating a hybrid (dry/wet) dephlegmator operating in wet mode is almost the same as that for the dry air-cooled condenser with four streets. It is expected that the initial capital cost of the air-cooled condenser incorporating a hybrid (dry/wet) dephlegmator will however be considerably less than the cost of an additional street.

It is found that the power output is approximately the same for the air-cooled condenser with adiabatic cooling of the inlet air to that of the air-cooled condenser incorporating a hybrid (dry/wet) dephlegmator. In his studies Maulbetsch (2003) stated that wetbulb depression

varied between 60% and 100%. The heat rejected by the air-cooled condenser shown in Figure 6.4, where the inlet air is adiabatically cooled, will be lower when the wetbulb depression is not 100%.

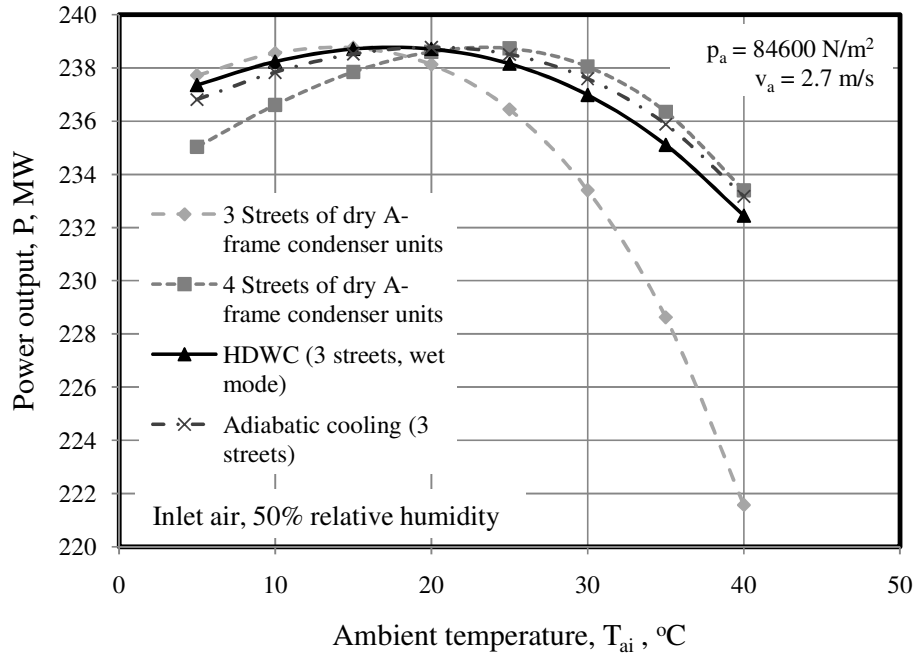


Figure 6.4: Power output for different air-cooled condenser configurations

The water consumption of the air-cooled condenser incorporating a hybrid (dry/wet) dephlegmator and the air-cooled condenser with adiabatic cooling of the inlet air is shown in Figure 6.5. For ideal adiabatic cooling of the inlet air, it is assumed that all the water is evaporated. At high ambient temperatures where these systems would be considered, the water consumption of the air-cooled condenser with adiabatic cooling of the inlet air is more than 20 % higher than that of the air-cooled condenser incorporating the hybrid dephlegmator. Maulbetsch (2003) states that in reality only between 60 to 70 % of the water evaporates and the rest is lost in the form of entrained droplets in the air flow, increasing the effective water consumption rate of the air-cooled condenser with adiabatic cooling of the inlet air.

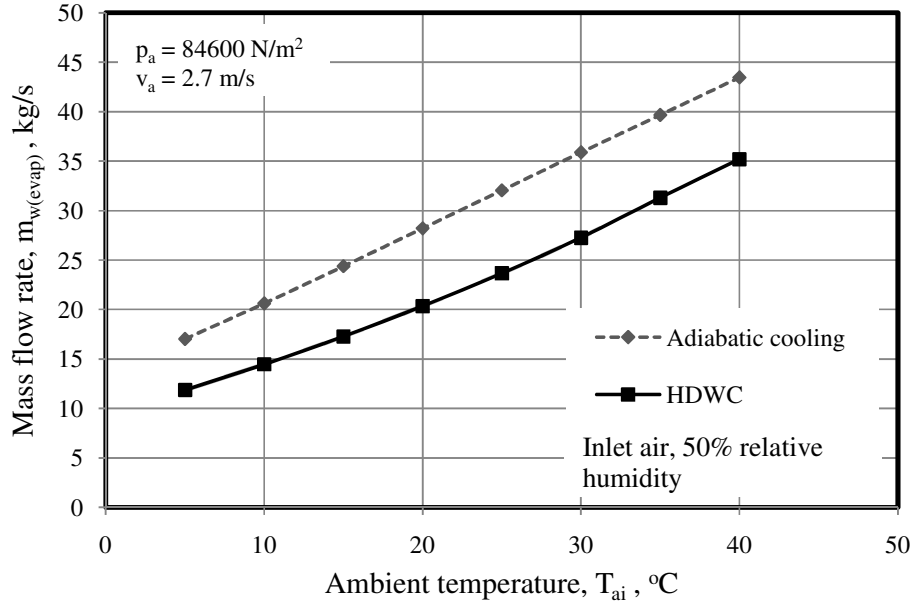


Figure 6.5: Water consumption of the hybrid dry/wet condenser and adiabatic cooling of the inlet air of the A-frame air-cooled condenser having 3 condenser streets

To reduce the water consumption, the second stage of the hybrid (dry/wet) dephlegmator need only be deluged with water during periods of high ambient temperatures or peak demand periods. Figure 6.6 shows the turbo-generator power output when the air-cooled condenser incorporating a hybrid (dry/wet) dephlegmator is operated as an all dry system and when the second stage is deluged with water. Although, the power output when the hybrid (dry/wet) dephlegmator is operated dry at higher ambient temperatures is slightly less than that of the conventional A-frame arrangement, there is no noticeable difference at the design temperature of $T_a = 15.6^\circ\text{C}$.

The turbine backpressure for the A-frame air-cooled condenser with three streets and the A-frame air-cooled condenser incorporating a hybrid (dry/wet) dephlegmator (3 streets) is given in Figure 6.7 as a function of the ambient temperature.

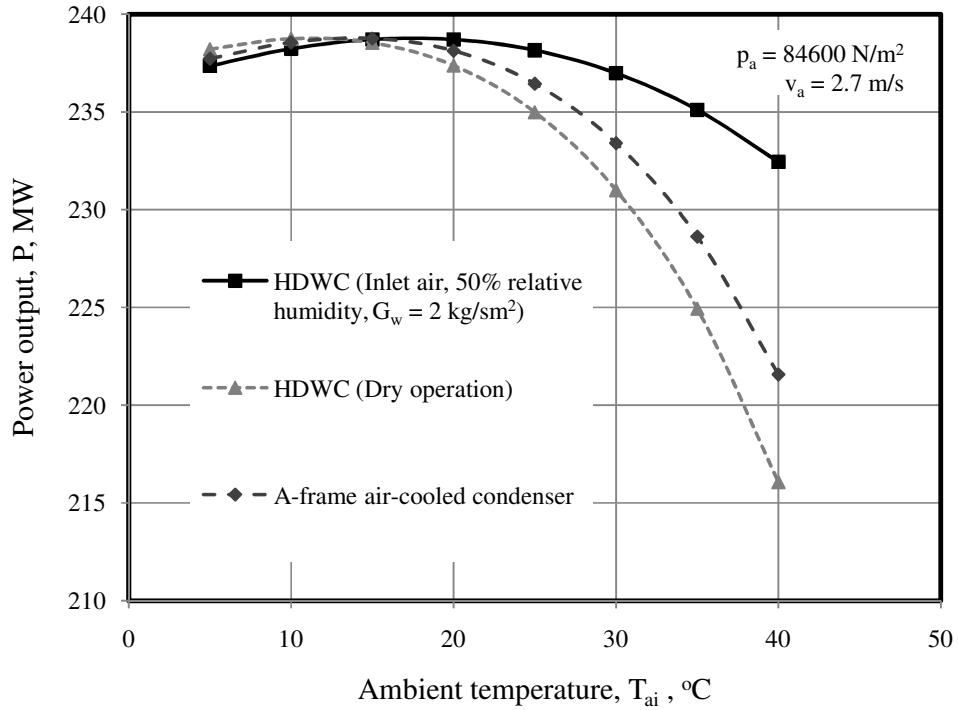


Figure 6.6: Power output of the air-cooled condenser incorporating hybrid (dry/wet) dephlegmator having 3 condenser streets

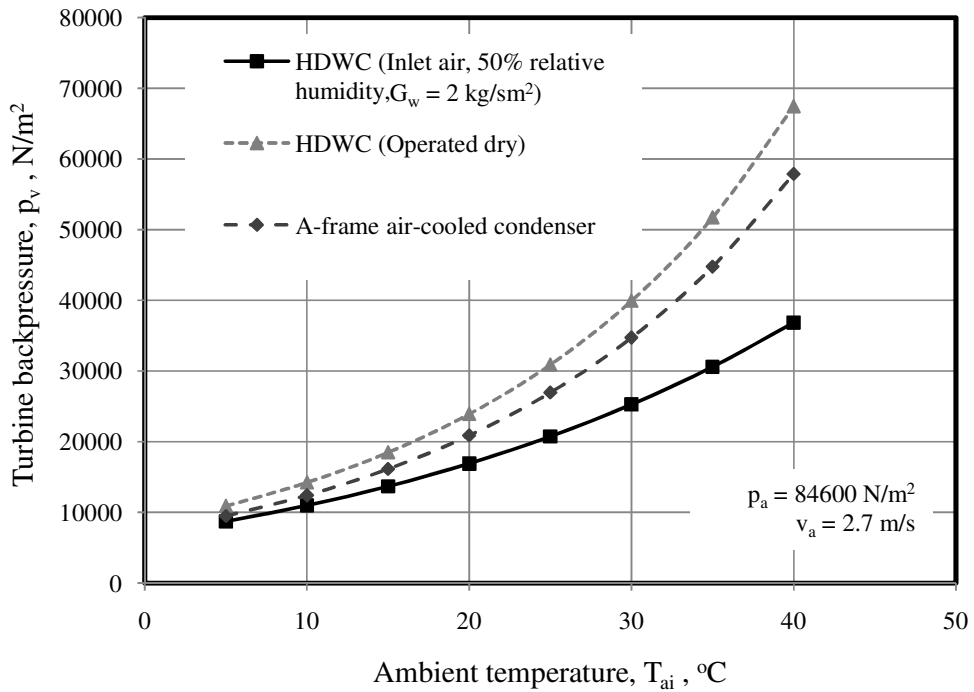


Figure 6.7: Turbine exhaust steam backpressure (3 condenser streets)

The power output of the turbo-generator with an air-cooled condenser incorporating a hybrid (dry/wet) dephlegmator for ambient air with a 0%, 50 % and 100% relative humidity is shown in Figure 6.8. At higher relative humidity of the inlet air, the decrease in the power output is relatively small for the hybrid (dry/wet) condenser.

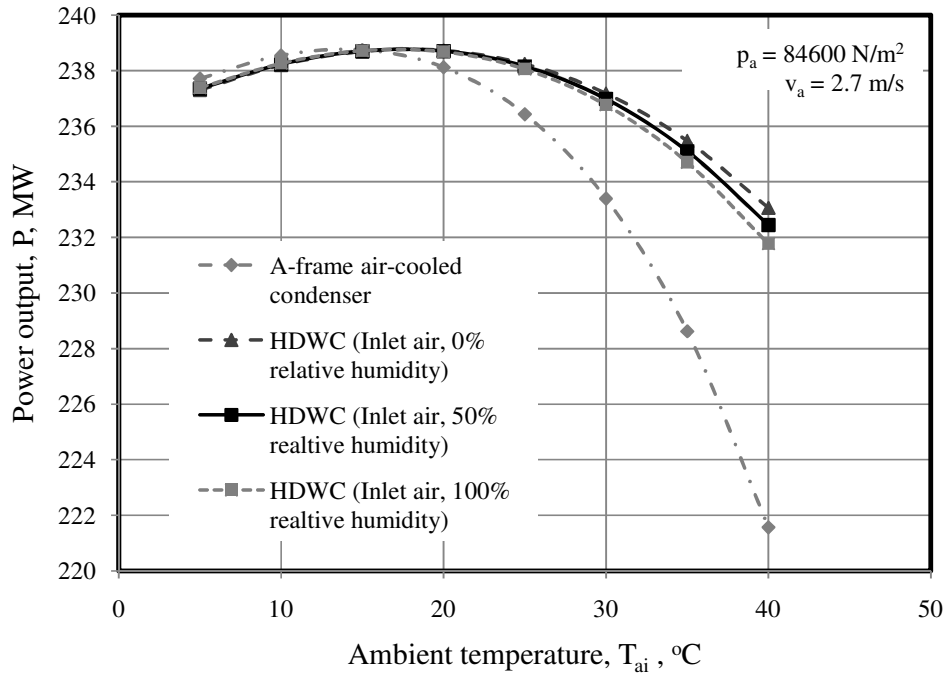


Figure 6.8: Power output for moist inlet air (3 condenser streets)

The turbo-generator power output for different air mass flow rates are shown in Figure 6.9. At an ambient temperature of 40°C, a 20 % change in the air mass velocity through the hybrid dephlegmator results in approximately a 0.5 % change in the power output of the turbo-generator.

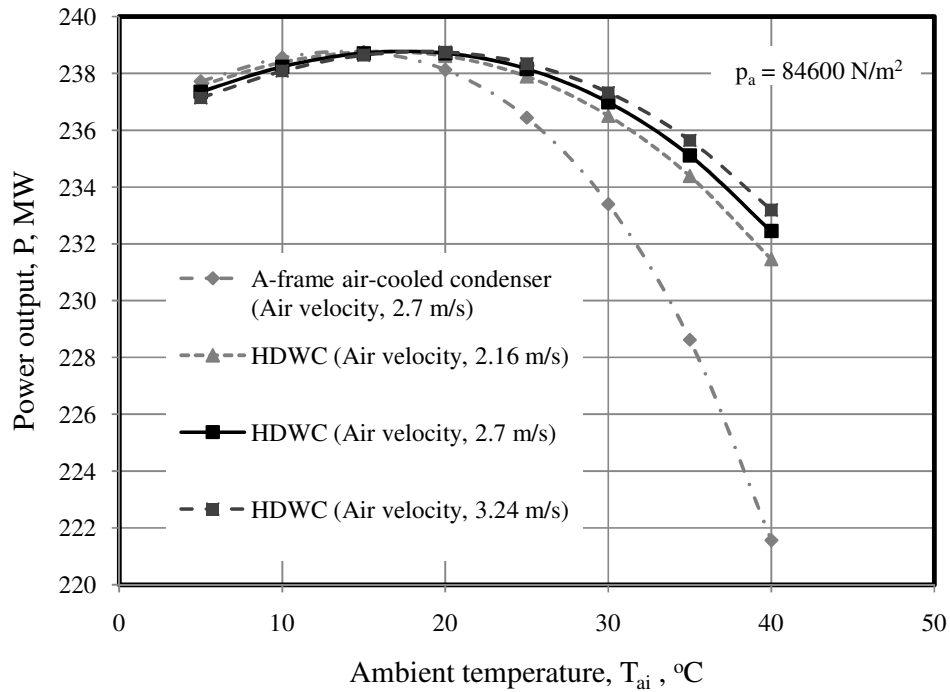


Figure 6.9: Changing air flow through the hybrid dephlegmator (3 condenser streets)

In Figure 6.10 the turbo-generator power output for different deluge water mass flow rates is shown.

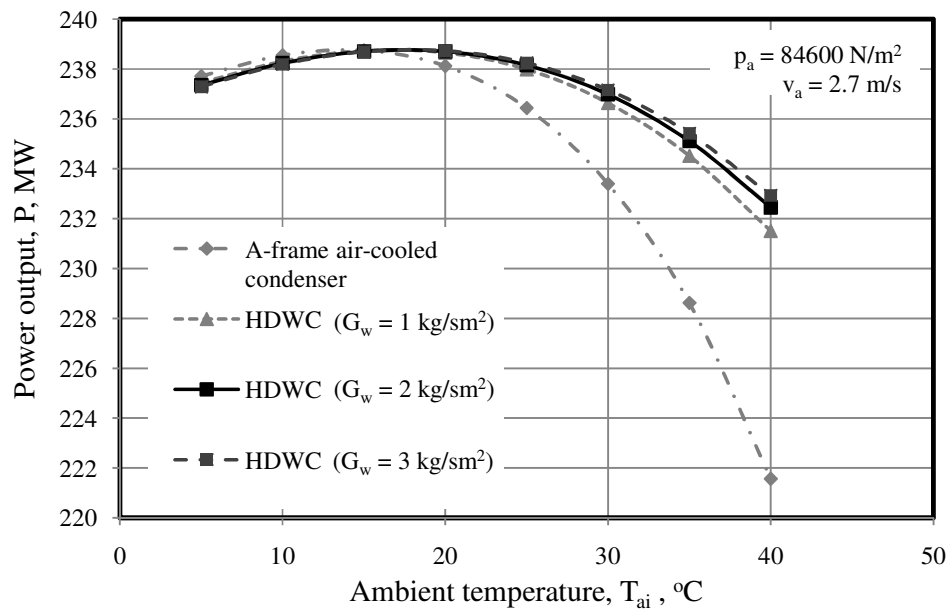


Figure 6.10: Changing deluge water mass flow rate through the hybrid dephlegmator (3 streets)

In the current condenser unit arrangement, there are five air-cooled condensers and one dephlegmator in each condenser street. The power output of the turbo-generator for an arrangement where every street has four air-cooled condensers and two hybrid (dry/wet) dephlegmators is shown in Figure 6.11. For this arrangement the power output at an ambient temperature of 40°C is only 2% more than the reference case.

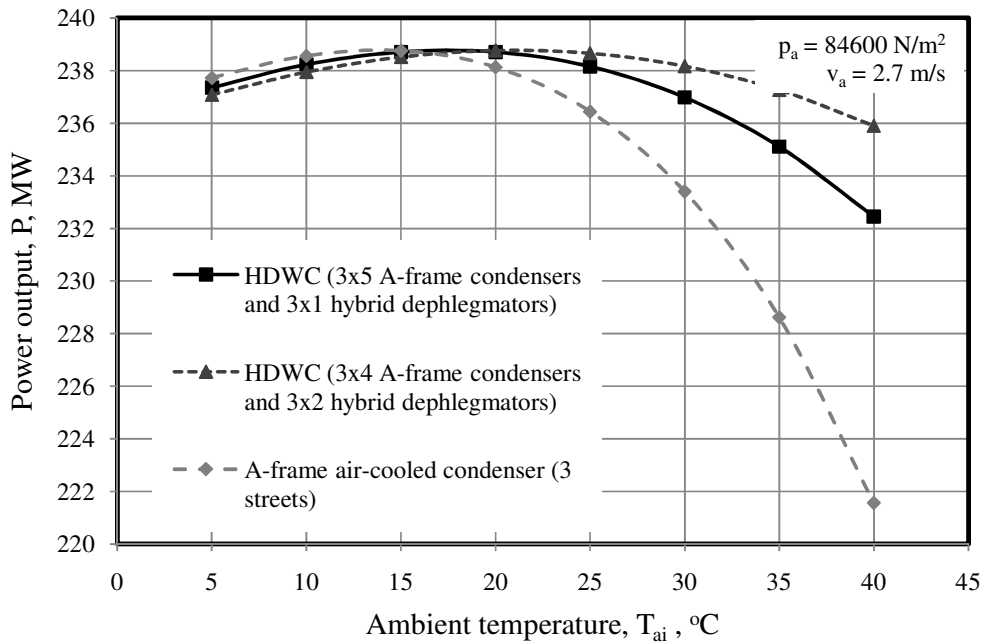


Figure 6.11: Power for different condenser unit arrangements

6.1 Conclusion

During periods of high ambient temperatures, a direct air-cooled condenser incorporating a hybrid (dry/wet) dephlegmator can provide the same increased turbo-generator performance as over-sized air-cooled condenser or an air-cooled condenser with adiabatic cooling of the inlet air. It is expected that the increase in the capital cost of the air-cooled condenser incorporating a hybrid (dry/wet) dephlegmator will be considerably less than the cost of oversizing the air-cooled condenser. For similar turbo-generator power outputs the water consumed by an air-cooled condenser incorporating a hybrid (dry/wet) dephlegmator is at least 20 % less than an air-cooled condenser with adiabatic cooling of the inlet air.

7 Conclusions

The performance characteristics of a steam turbine incorporating an A-frame air-cooled condenser with a hybrid (dry/wet) dephlegmator are evaluated.

Through the introduction of the hybrid (dry/wet) dephlegmator the cooling performance of the air-cooled condenser can be measurably enhanced. The hybrid (dry/wet) dephlegmator consists of two stages: The first an air-cooled condenser with finned tubes and the second a bundle of galvanized steel tubes arranged horizontally. The second stage can either be operated as a dry air-cooled condenser or the tubes can be deluged with water and operated as an evaporative condenser.

To evaluate the thermal-flow performance characteristics of the second stage of the hybrid (dry/wet) dephlegmator when operated in wet mode (deluged with water), an experimental study of an evaporative cooler is conducted. From the experimental results, correlations for the water film heat transfer coefficient and the air-water mass transfer coefficient are developed. These correlations compare well with the correlations given by Mizushina et al. (1967). From the experimental results, a correlation for the air-side pressure drop over the deluged tube bundle is also developed.

In evaluating a particular turbo-generator power output for different condenser configurations; it is found that the air-cooled condenser incorporating a hybrid (dry/wet) dephlegmator can provide the same turbo-generator performance increase as an over-sized air-cooled condenser (33% increase in the air-cooled condenser size) or an air-cooled condenser with adiabatic or spray cooling of the inlet air (100% wetbulb depression of the inlet air with a 50% relative humidity). For the same turbo-generator power output increase, the rate of water consumption of the air-cooled condenser with adiabatic cooling of the inlet air is at least 20 % higher than the air-cooled condenser incorporating a hybrid (dry/wet) dephlegmator. It is expected that the capital cost of the air-cooled condenser incorporating a hybrid (dry/wet) dephlegmator will only be slightly higher than the conventional air-cooled condenser with the same footprint.

Incorporating a hybrid (dry/wet) dephlegmator in an air-cooled condenser can increase the cooling performance measurably during periods of higher ambient temperatures and can provide a cost effective alternative in locations which are subjected to high water prices or where the available water resources are limited.

8 References

- Baltimore Aircoil Company, *Operating and maintenance instructions*, Bulletin M308/3-9
- Baltimore Aircoil Company, 1999, *Logiciel de Sélection Intégré*, ISP, Release 3/1.0
- Bosjnakovic, F., and P.L. Blackshear, 1965, *Technical thermodynamics*, Holt, Reinhart and Winston, New York, pp. 326-331
- Boulay, R.B., J.C. Miroslav and M. Massoudi, 2005, *Dry and Hybrid condenser cooling design to maximize operating income*, ASME Report, PWR2005-50225, Chicago, Illinois
- Bourillot, C., 1983, *Numerical model for calculating the performance of an evaporative cooling tower*, EPRI Report CS-3212-SR, California
- Branfield, G., 2003, *Precooling of fin-tube heat exchanger inlet air using fine water spray*, B.Eng thesis, University of Stellenbosch, Rep. of South Africa
- Bykov, A.V., V.A. Gogolin and N.V. Tovaras, 1984, *Investigation of heat, mass transfer and fluid flow characteristics in evaporative condensers*, International Journal of Refrigeration, Vol. 7, pp. 342-347
- Chato, J.C., 1962, *Laminar condensation inside horizontal and inclined tubes*, Journal of ASHRAE, pp. 52-60
- Conradie, T.A. and D.G. Kröger, 1991, *Enhanced performance of a dry dry-cooled power plant through air precooling*, Proceedings of the International Power Generation Conference, ASME, San Diego
- De Backer, L. and W.M. Wurtz, 2003, *Why every air-cooled steam condenser needs an cooling tower*, CTI Report, TP03-01
- Dreyer, A.A., 1988, *Analysis of Evaporative Coolers and Condensers*, MSc Thesis, University of Stellenbosch, Rep. of South Africa
- Duvenhage, K., 1993, *Warmteruiling met adiabatiese voorverkoeling*, MSc Thesis, University of Stellenbosch, Rep. of South Africa
- Esterhuysen, B.D. and D.G. Kroger, 2005, *The effect of ionisation of spray in cooling air on the wetting characteristics of finned tube heat exchanger*, Applied Thermal Engineering, Vol. 25, pp. 3129-313

Ettouney, H.M., H.T. El-Dessouky, W. Bouhamra and B. Al-Azmi, 2001, *Performance of evaporative condensers*, Heat Transfer Engineering, Vol. 22, pp. 41-55

Finlay, I.C, and D. Harris, 1984, *Evaporative cooling of tube banks*, International Journal of Refrigeration, Vol. 7 (4), pp. 214-224

Gaddis, E.S. and V. Gnielinski, 1985, *Pressure drop in cross flow across tube bundles*, International Chemical Engineering, Vol. 25, pp. 1-15

Gogolin, V.A., and N.M. Mednikova, 1948, *Evaporative condenser computations*, Kholodil'naya Tekhnika, Vol. 2

Goodman, W., 1938, *The evaporative condenser*, Heating, Piping and Air Conditioning, Vol. 10, pp. 165 – 168

Grimson, E.D., 1937, *Correlation and utilization of new data on flow resistance and heat transfer in cross flow of gasses over tube bank*, Trans. American Society of Mechanical Engineers, Vol. 59, pp. 583-94

Hasan, A., and K. Siren, 2002, *Performance investigation of Plain and finned tube evaporatively cooled heat exchangers*, Applied Thermal Engineering, Vol. 23, pp. 325-340

Jakob, M., 1938, *Heat transfer and flow resistance in cross flow of gasses over tube banks*, Trans. ASME, Vol. 60, pp. 384

Kern, D.Q. and R.E. Seaton, 1959, *A theoretical analysis of thermal surface fouling*, Br. Journal of Chemical Engineering, Vol 4 (5), pp. 258-262

Kloppers, J.C. and D.G. Kröger, 2005, *A critical investigation into the heat and mass transfer analysis of counterflow wet-cooling towers*, International Journal of Heat and Mass transfer, Vol. 48, pp. 765-777

Kreid, D.K., B.M. Johnson and D.W. Faletti, 1978, *Approximate analysis of the heat transfer from the surface of a wet finned heat exchanger*, ASME paper no. 78-HT-26

Kröger, D.G., 2004, *Air-cooled Heat exchangers and Cooling Towers: Thermal-Flow Performance Evaluation and Design*, PennWell Corporation, Tulsa, Oklahoma, USA

- Leidenforst, W., and B. Korenic , 1982, *Evaporative Cooling and Heat Transfer Augmentation Related to Reduced Condenser Temperatures*, Heat Transfer Engineering, Vol. 3, pp.38-59
- Lindahl, P. and R.W. Jameson, 1993, *Plume abatement and water conservation with wet/dry cooling towers*, CTI Journal, Vol. 14(2)
- Maulbetsch J.S., 2002, *Comparison of alternative cooling technologies for California Power Plants: Economic, Environmental and Other Tradeoffs*, EPRI, Palo Alto, CA, and California Energy Commission, Sacramento, CA, 500-02-079F
- Maulbetsch, J. and M. DiFilippo, 2003, *Spray enhancement of air cooled condensers*, EPRI, Palo Alto, CA, California Energy Commission, Sacramento, CA and Crockett Cogeneration, CA. 1005360
- Maulbetsch, J.S. and M.N. DiFilippo, 2006, *Cost and Value of Water Use at Combined-Cycle Power Plants, California Energy Commission, PIER Energy-Related Environmental Research, CEC-500-2006-034*
- Merkel, F., 1926, *Verdunstungskuling*, VDI-Zeitschrift, Vol. 70, pp. 123 – 128
- Mills, A.F., 1999, *Heat transfer*, Prentice Hall, ISBN 0-13-947624-5
- Mitchell, R.D., 1989, *Survey of Water-Conserving Heat Rejection systems*, EPRI report, Palo Alto, California, GS-6252
- Mizushina, T., R. Ito and H. Miyasita, 1967, *Experimental study of an evaporative cooler*, International Chemical Engineering, Vol. 7, pp. 727-732
- Mizushina, T., R. Ito and H. Miyasita, 1968, *Characteristics and methods of thermal design of evaporative coolers*, International Chemical Engineering, Vol. 8, pp. 532-538
- Niitsu, Y., K. Naito and T. Anzai, 1969, *Studies on characteristics and design procedure of evaporative coolers*, Journal of SHASE, Japan, Vol.43
- Parker, R.O., and R.E. Treybal, 1961, *Heat, mass transfer characteristics of evaporative coolers*, AIChE Chemical Engineering Progress Symposium Series, Vol. 57, pp.138-149
- Poppe, M., and H. Rögener, 1984, *Evaporative Cooling Systems*, VDI-Warmeatlas, Section Mh

- Qengel, Y.A., 2003, *Heat transfer, a practical approach*, McGraw-Hill Higher Education
- Qureshi, B.A, and S.M. Zubair, 2005, *A comprehensive design and rating study of evaporative coolers and condensers. Part I. Performance evaluation*, International Journal of Refrigeration, Vol. 29, pp. 645-658
- Qureshi, B.A. and S.M. Zubair, 2006, *Prediction of evaporation losses in evaporative fluid coolers*, Applied Thermal Engineering, Vol. 27, pp. 520-527
- Ren, C. and H. Yang, 2005, *An analytical model for the heat and mass transfer processes in an indirect evaporative cooling with parallel/counter flow configurations*, International Journal of Heat and Mass transfer, Vol. 49, pp. 617-6127
- Shah, M.M., 1979, *A General Correlation for Heat Transfer during Film Condensation inside Pipes*, International Journal of Heat and Mass Transfer, Vol. 22, pp 547-556
- Stabat, P. and D. Marchio, 2004, *Simplified model for indirect-contact evaporative cooling-tower behaviour*, Applied Energy, Vol. 78, pp. 433-451
- Szabo, Z., 1991, *Why use the 'Heller System'? Circuitry, characteristics and special features*, Paper presented at the Symposium on dry-cooling towers, Teheran
- Thomsen, E.G., 1946, *Heat transfer in evaporative condenser*, Refrigeration Engineering, Vol. 51, pp. 425-431
- Tovaras, N.V., A.V. Bykov and A.V. Gogolin, 1984, *Heat exchange at film water flow under operating conditions of evaporative condenser*, Holod The, Vol. 1, pp 25-29
- Wachtel, G.P., 1974, *Atomised water injection to improve dry cooling tower performance*, Franklin Institute Research Laboratories, Report no. COO-2241-1
- Webb, R.L, 1984, *A unified theoretical treatment for thermal analysis of cooling towers, evaporative condensers and fluid coolers*, ASHRAE Trans., Vol. 90, pp. 398-415
- Woest, M., I. Hearn and S.J. Lennon, 1991, *Investigation into the corrosion behaviour of galvanized finned tubing for cooling under enhanced wet/dry cooling conditions*, ESCOM, Scientific Investigations Report No. S91/030

Zalewski, W., and P.A. Gryglaszeski, 1997, *Mathematical model of heat and mass transfer processes in evaporative fluid coolers*, Chemical Engineering and Processing, Vol. 36, pp. 271-280

Zukauskas, A. and R. Ulinskas, 1988, *Heat transfer in tube banks in crossflow*, Hemisphere Publishing Corporation

Appendix A: Properties of fluids

The thermophysical properties summarized here is presented in Kröger (2004).

A.1. The thermophysical properties of dry air from 220K to 380K at standard atmospheric pressure (101325 N/m²)

Density:

$$\rho_a = p_a / (287.08 T), \text{ kg/m}^3 \quad (\text{A.1.1})$$

Specific heat:

$$c_{pa} = 1.045356 \times 10^3 - 3.161783 \times 10^{-1} T + 7.083814 \times 10^{-4} T^2 + 8.15038 \times 10^{-15} T^3, \text{ W/mK} \quad (\text{A.1.2})$$

Dynamic viscosity:

$$\mu_a = 2.287973 \times 10^{-6} + 6.259793 \times 10^{-8} T - 3.131956 \times 10^{-11} T^2 + 8.15038 \times 10^{-15} T^3, \text{ kg/sm} \quad (\text{A.1.3})$$

Thermal conductivity:

$$k_a = -4.937787 \times 10^{-4} + 1.018087 \times 10^{-4} T - 4.627937 \times 10^{-8} T^2 + 1.250603 \times 10^{-11} T^3, \text{ W/mK} \quad (\text{A.1.4})$$

A.2. The thermophysical properties of saturated water vapor from 273.15K to 380K.

Vapor pressure:

$$p_v = 10^z, \text{ N/m}^2$$

$$z = 10.79586(1 - 273.16/T) + 5.02808 \log_{10}(273.16/T) + 1.50474 \times 10^{-4} \left[1 - 10^{-8.29692\{(273.16/T)-1\}} \right] + 4.2873 \times 10^{-4} \left[10^{4.76955(1-273.16/T)} - 1 \right] + 2.786118312 \quad (\text{A.2.1})$$

Specific heat:

$$c_{pv} = 1.3605 \times 10^3 + 2.31334T - 2.46784 \times 10^{-10} T^5 + 5.91332 \times 10^{-13} T^6, \text{ J/kgK} \quad (\text{A.2.2})$$

Dynamic viscosity:

$$\mu_v = 2.562435 \times 10^{-6} + 1.816683 \times 10^{-8} T + 2.579066 \times 10^{-11} T^2 - 1.067299 \times 10^{-14} T^3, \text{ kg/ms} \quad (\text{A.2.3})$$

Thermal conductivity:

$$k_v = 1.3046 \times 10^{-2} - 3.756191 \times 10^{-5} T + 2.217964 \times 10^{-7} T^2 - 1.111562 \times 10^{-10} T^3, \text{ W/mK} \quad (\text{A.2.4})$$

Vapor density:

$$\rho_v = -4.062329056 + 0.10277044T - 9.76300388 \times 10^{-4} T^2 + 4.475240795 \times 10^{-6} T^3 - 1.004596894 \times 10^{-8} T^4 + 8.9154895 \times 10^{-12} T^5, \text{ kg/m}^3 \quad (\text{A.2.5})$$

Temperature:

$$T = 164.630366 + 1.832295 \times 10^{-3} p_v + 4.27215 \times 10^{-10} p_v^2 + 3.738954 \times 10^3 p_v^{-1} - 7.01204 \times 10^5 p_v^{-2} + 16.161488 \ln p_v - 1.437169 \times 10^{-4} p_v \ln p_v, \text{ K} \quad (\text{A.2.6})$$

A.3. The thermophysical properties of mixtures of air and water vapor,

Density:

$$\rho_{av} = (1+w) \left[1 - w / (w + 0.62198) \right] p_a / (287.08T), \text{ kg air-vapor/m}^3 \quad (\text{A.3.1})$$

Specific heat:

$$c_{pav} = (c_{pa} + w c_{pv}) / (1+w), \text{ J/K kg air-vapor} \quad (\text{A.3.2})$$

or the specific heat of the air-vapor mixture per unit mass of dry air

$$c_{pma} = (c_{pa} + w c_{pv}), \text{ J/K kg dry air} \quad (\text{A.3.3})$$

Dynamic viscosity:

$$\mu_{av} = \left(X_a \mu_a M_a^{0.5} + X_v \mu_v M_v^{0.5} \right) / \left(X_a M_a^{0.5} + X_v M_v^{0.5} \right), \text{ kg/ms} \quad (\text{A.3.4})$$

Where $M_a = 28.97 \text{ kg/mole}$, $M_v = 18.016 \text{ kg/mole}$, $X_a = 1/(1+1.608w)$ and $X_v = w/(w+0.622)$

Thermal conductivity:

$$k_{av} = \left(X_a k_a M_a^{0.33} + X_v k_v M_v^{0.33} \right) / \left(X_a M_a^{0.33} + X_v M_v^{0.33} \right), \text{ W/mK} \quad (\text{A.3.5})$$

Humidity ratio:

$$w = \left[\frac{2501.6 - 2.3263(T_{wb} - 273.15)}{2501.6 + 1.8577T_a - 4.184T_{wb}} \right] \left[\frac{0.62509 p_{vwb}}{p_a - 1.005 p_{vwb}} \right] - \left[\frac{1.00416(T_{ai} - T_{wb})}{2501.6 + 1.8577(T_a - 273.15) - 4.184(T_{wb} - 273.15)} \right] \text{ kg/kg dry air} \quad (\text{A.3.6})$$

Enthalpy:

$$i_{av} = \left[c_{pa} (T - 273.15) + w \{ i_{fgwo} + c_{pv} (T - 273.15) \} \right] / (1 + w) \text{ J/kg air-vapor} \quad (\text{A.3.7})$$

or the enthalpy of the air-vapor mixture per unit mass of dry air

$$i_{av} = c_{pa} (T - 273.15) + w \left[i_{fgwo} + c_{pv} (T - 273.15) \right] \text{ J/kg dry air} \quad (\text{A.3.8})$$

where the specific heats are evaluated at $(T + 273.15)/2$ and the latent heat i_{fgwo} , is evaluated at 273.15 K according to Equation (A.4.5.) i.e. $i_{fgwo} = 2.5016 \times 10^6 \text{ J/kg}$

A.4. The thermophysical properties of saturated water liquid from 273.15 K to 380 K ,

Density:

$$\rho_w = (1.49343 \times 10^{-3} - 3.7164 \times 10^{-6} T + 7.09782 \times 10^{-9} T^2) - 1.90321 \times 10^{-20} T^6, \text{ kg/m}^3 \quad (\text{A.4.1})$$

Specific heat:

$$c_{pw} = 8.15599 \times 10^3 - 2.80627 \times 10 T + 5.11283 \times 10^{-2} T^2 - 2.17582 \times 10^{-13} T^6, \text{ J/kgK} \quad (\text{A.4.2})$$

Dynamic viscosity:

$$\mu_w = 2.414 \times 10^{-5} \times 10^{247.8/(T-140)}, \text{ kg/ms} \quad (\text{A.4.3})$$

Thermal conductivity:

$$k_w = -6.14255 \times 10^{-1} + 6.9962 \times 10^{-3} T - 1.01075 \times 10^{-5} T^2 + 4.74737 \times 10^{-12} T^4, \text{ W/mK} \quad (\text{A.4.4})$$

Latent heat of vaporization:

$$i_{fgw} = 3.4831814 \times 10^6 - 5.8627703 \times 10^3 T + 12.139568 T^2 - 1.40290431 \times 10^{-2} T^3, \text{ J/kg} \quad (\text{A.4.5})$$

Critical pressure:

$$p_{wc} = 22.09 \times 10^6, \text{ N/m}^2 \quad (\text{A.4.6})$$

Appendix B: Empirical correlations

B.1. Correlations for the condensation heat transfer coefficient in a horizontal tube

For relative low inlet vapor velocities, $Re_v < 35000$, Chato (1962) recommends the following correlation for calculating the condensation heat transfer coefficient

$$h_c = 0.555 \left[\frac{9.8 \rho_c (\rho_c - \rho_{vs}) k_c^3 i'_{fg}}{\mu_c (T_v - T_{wall}) d_i} \right]^{0.25} \quad (\text{B.1.1})$$

with

$$i'_{fg} = i_{fg} + 0.68 c_{pc} (T_c - T_{wall}) \quad (\text{B.1.2})$$

The vapor Reynolds number at the tube bundle inlet can be expressed as

$$Re_v = m_s d_i / (n_b n_{hr} n_{tr} A_{ts} \mu_v)$$

where n_{hr} is the number of tube rows the inlet header feeds.

For higher vapor flow rates Shah (1979) recommends the following equation to determine the condensation heat transfer coefficient

$$Nu_c = \frac{h_c d_i}{k_c} = 0.023 Re_c^{0.8} Pr_c^{0.4} \left[0.55 + 2.09 (p_{crit} / p_v)^{0.38} \right] \quad (\text{B.1.3})$$

where

$$Re_c = \frac{m_s d_i}{n_b n_{hr} n_{tr} A_{ts} \mu_c}; \quad Pr_c = \frac{c_{pc} \mu_c}{k_c}$$

B.2. Correlations for the heat transfer coefficient in horizontal tubes

Gnielinski (1975) recommends the following correlation for the heat transfer coefficient of turbulent flow in a horizontal tube

$$Nu = \frac{(f_D/8)(Re-1000)Pr \left[1 + (d/L)^{0.67} \right]}{1 + 12.7(f_d/8)^{0.5} (Pr^{0.67} - 1)} \quad (\text{B.2.1})$$

where equation (B.2.1) is valid for, $2300 < Re < 10^6$, $0.5 < Pr < 10^4$ and $0 < d/L < 1$.

B.3. Correlations for the air-side heat transfer coefficient for an air-cooled tube bundle in cross-flow

Zukauskas and Ulinskas (1988) recommend the following equation for a tube bundle in cross-flow

$$Nu_D = 0.35 Re_D^{0.6} Pr_{am}^{0.38} \left(\frac{Pr_{am}}{Pr_{av}} \right)^{0.25} \left(\frac{P_t}{P_l} \right)^{0.2} \quad (\text{B.3.1})$$

with $h_a = Nu_D k_a / d_o$.

Grimson (1937) recommends the following equation for a tube bundle in cross-flow

$$Nu_D = 0.467 Re_D^{0.562} \quad (\text{B.3.2})$$

where

$$Re = \frac{v_{\max} d_o \rho}{\mu}$$

B.4. Correlations for the air-side pressure drop over dry tube bundles

Jakob (1938) gives the following equation to calculate the pressure drop over tube bundle in cross-flow

$$\Delta p = K n_r (\rho v_{\max}^2 / 2) \quad (\text{B.4.1})$$

where n_r is the number of restrictions and $K = \left(1 + 0.47 / (P_t / d_o - 1)^{1.06} \right) / (Re^{0.16})$.

Gaddis and Gnielinski (1985) recommend the following procedure for calculating the loss coefficient, K , for a bundle with triangular arranged tubes in cross-flow

$$K = K_l f_{z,l} + K_t f_{z,t} \left[1 - \exp \left(- \frac{Re + 200}{1000} \right) \right]$$

$$K_l = \frac{f_{a,l,v}}{\text{Re}}$$

$$f_{a,l,v} = \frac{280\pi \left[(b^{0.5} - 0.6)^2 + 0.75 \right]}{(4ab - \pi) c^{1.6}}$$

$$K_t = \frac{f_{a,t,v}}{\text{Re}^{0.25}}$$

$$f_{a,t,v} = 2.5 + \frac{1.2}{(a - 0.85)^{1.08}} + 0.4 \left(\frac{b}{a} - 1 \right)^3 - 0.01 \left(\frac{a}{b} - 1 \right)^3$$

where $a = P_i/d_o$, $b = P_i/d_o$ and $c = P_d/d_o$.

The Reynolds number is defined as

$$\text{Re} = \frac{v_{\max} d_o \rho}{\mu}$$

The laminar and turbulent viscosity correction factors are respectively correlated as follows

$$f_{z,l} = \left(\frac{\mu_w}{\mu} \right)^{0.57 / \left[\left((4ab/\pi) - 1 \right) \text{Re} \right]^{0.25}}$$

$$f_{z,t} = \left(\frac{\mu_w}{\mu} \right)^{0.14}$$

B.5. Correlations for the film heat transfer coefficient of evaporative coolers and condensers

Parker and Treybal (1961) recommend the following correlation for tubes with an outside diameter of 19 mm and an equilateral pitch

$$h_w = 704(1.3936 + 0.02214T_{wm})(\Gamma_m/d_o)^{0.333}, \text{ W/m}^2\text{K} \quad (\text{B.5.1})$$

where T_{wm} is in °C. The correlation is valid for, $15 < T_{wm} < 70$ °C and $1.4 \leq \Gamma_m/d_o \leq 3$ kg/m²s and the maximum air Reynolds number ($m_{avm}d_o/A_c\mu_{avm}$) of 5000.

Mizushina et al (1967)

$$h_w = 2102.9(\Gamma_m/d_o)^{0.333}, \text{ W/m}^2\text{K} \quad (\text{B.5.2})$$

and is valid for $2 < (\Gamma_m/d_o) < 5.5$ kg/m²s and an air-side Reynolds number of between 1500 and 8000. The tubes used for the tests varied between 12.7 mm and 40 mm in diameter and were arranged in a $2 \times d_o$ equilateral pitch.

Niitsu et al. (1969), staggered banks of plain tubes, 16 mm outer diameter

$$h_w = 990(\Gamma_m/d_o)^{0.46}, \text{ W/m}^2\text{K} \quad (\text{B.5.3})$$

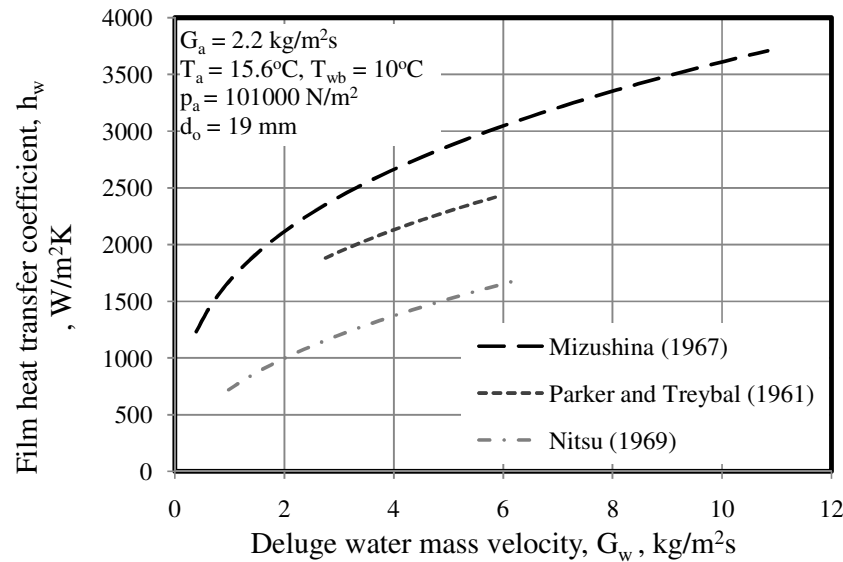


Figure B. 1: Film heat transfer coefficient

Dreyer (1988) gives a more extensive list of film heat transfer coefficients.

B.6. Correlations for the air-water mass transfer coefficient of evaporative coolers and condensers

Parker and Treybal (1961) recommend the following correlation for tubes with an outside diameter of 19 mm and an equilateral pitch

$$h_d = 0.04935 \left[(1+w)(m_a/A_c) \right]^{0.905}, \text{ kg/sm}^2 \quad (\text{B.6.1})$$

where A_c is the minimum cross-sectional air flow area between the tubes. The air-vapor mass velocity was in the range of $0.68 < (m_a/A_c) < 5 \text{ kg/sm}^2$.

Mizushina et al. (1967) tested tube bundles with 12–40 mm outer diameter arranged in $2d_o$ triangular pitch.

$$h_d = 5.5439 \times 10^{-8} \text{Re}_{avm}^{0.9} \text{Re}_{wm}^{0.15} d_o^{-1.6}, \text{ kg/sm}^2 \quad (\text{B.6.2})$$

The equation is valid for $1.2 \times 10^3 < \text{Re}_{avm} = m_{avm} d_o / (A_c \mu_{avm}) < 1.4 \times 10^4$ and $50 < \text{Re}_{wm} = m_{wm} d_o / (A_c \mu_{wm}) < 240$.

Niitsu et al. (1969) gives the following correlation for a tube bundle with plain tubes

$$h_d = 0.076 (m_{avm}/A_c)^{0.8}, \text{ kg/sm}^2 \quad (\text{B.6.3})$$

for $1.5 < (m_{avm}/A_c) < 5$

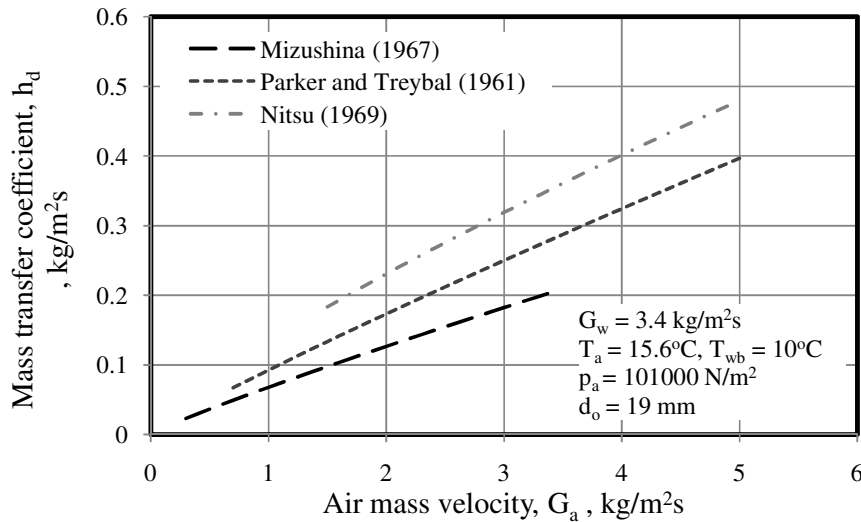


Figure B. 2: Air-water mass transfer coefficient

Dreyer (1988) gives a more extensive list of air-water mass transfer coefficients.

B.7. Correlations for the air-side pressure drop over evaporative coolers and condensers

Nitsu et al. (1969) recommend the following correlation for the air-side pressure drop over a wetted plain tube bundle.

$$\Delta p = 4.9n_r P_l (m_{avm}/A_c)^{1.85} (\Gamma_m/d_o)^{0.285}, \text{ N/m}^2 \quad \text{(B.7.1)}$$

where, $2 \leq (m_{avm}/A_c) \leq 6$ and $1.3 \leq \Gamma_m/d_o \leq 3.5 \text{ kg/m}^2\text{s}$

Appendix C: Adiabatic cooling

As the water is introduced into the inlet air stream of an air-cooled condenser as a very fine spray or mist, the evaporation of the water into the air stream (latent heat transfer) lowers the dry bulb temperature. If the temperature of spray water is the same as the wet bulb temperature of the air, the air is cooled down following essentially the line of constant wet bulb temperature. Figure C.1 shows the adiabatic cooling from the original state at 1 to the final state at 2, with $T_{wb2} = T_{wb1}$.

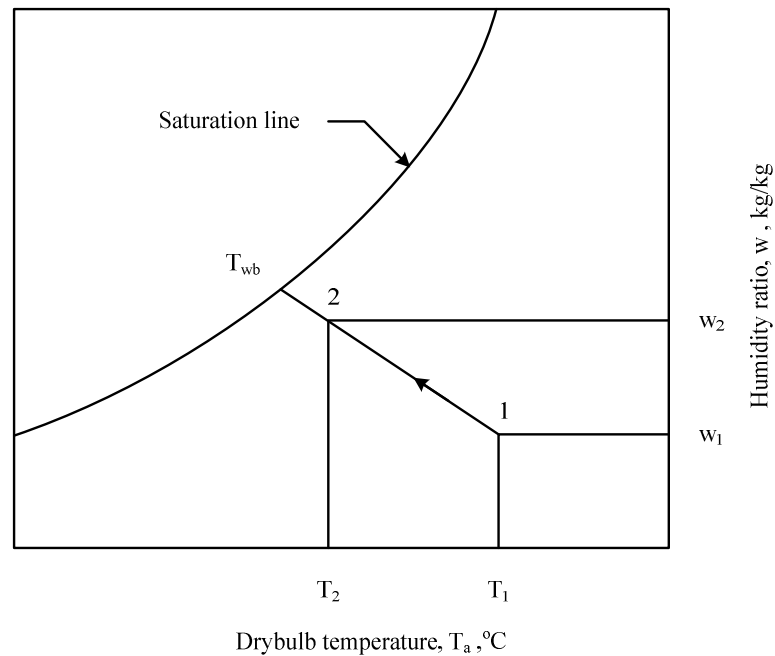


Figure C.1: Adiabatic cooling on psychrometric chart

The wetbulb depression can be expressed as

$$\text{Wetbulb depression} = \frac{T_{a(1)} - T_{a(2)}}{T_{a(1)} - T_{wb(1)}}$$

The amount of water evaporated can be approximated by

$$m_{w(\text{evap})} = m_a (w_{a(2)} - w_{a(1)})$$

Appendix D: Hybrid (dry/wet) condenser performance analysis

A numerical example is presented to illustrate the mathematical methodology followed in evaluating the performance characteristics of an arbitrary air-cooled steam condenser incorporating a hybrid (dry/wet) dephlegmator, shown schematically in Figure 6.3.

A schematic flowchart of the steam flowing through one of the three streets or rows in the array is shown in Figure 3.1. Each row consists of five A-frame air-cooled condenser units (ACC) and a hybrid (dry/wet) dephlegmator. The hybrid (dry/wet) dephlegmator consists of two stages; the first is an air-cooled condenser with somewhat shortened finned-tubes and the second is a bundle of galvanized steel tubes arranged horizontally.

In the analysis of the systems performance characteristics the following assumptions are made:

- Saturated steam enters the air-cooled condenser units.
- All the steam is condensed and leaves the system as saturated water.
- The pressure losses inside the steam header, the condenser tubes and the rest of the cycle are neglected and the steam temperature remains constant throughout the system. For high inlet steam temperatures this assumption is reasonably accurate.
- The performance of each of the five air-cooled condensers units is taken to be identical.

The operating conditions

Ambient conditions:

Atmospheric pressure $p_{a1} = 84600 \text{ N/m}^2$

Air temperature at ground level $T_{a1} = 15.6^\circ\text{C}$

Wetbulb temperature $T_{wb} = 10^\circ\text{C}$

(Ambient conditions correspond to 50% relative humidity and from equation (A.3.5) the humidity ratio is calculated to be $w = 0.0069 \text{ kg/kg dry air}$)

Steam conditions:

Saturated steam supply temperature $T_v = 60^\circ\text{C}$

Steam quality at the main condenser inlet $x = 1$

The following performance analyses are essentially as presented in Kröger (2004).

1. A-frame air-cooled condenser

The geometric parameters of the A-frame air-cooled condenser unit shown in Figure 2.1 are:

Steam inlet:

Diameter of the steam header	$d_s = 1.25 \text{ m}$
Total mean steam ducting loss coefficient based on the steam velocity at the inlet to the first tube row	$K_{sd} = 2.5$

Finned tube bundle specifications:

The condenser consists of two rows of staggered plate finned flattened tubes, each row having different performance characteristics such that approximately the same amount of steam condenses in each row.

Hydraulic diameter of the tube	$d_e = 0.02975 \text{ m}$
Inside area of the tube per unit length	$A_{ti} = 0.21341 \text{ m}$
Inside cross-sectional tube flow area	$A_{ts} = 0.00159 \text{ m}^2$
Length of finned tube	$L_t = 9.5 \text{ m}$
Inside height of the tube	$H_t = 0.097 \text{ m}$
Inside width of the tube	$W_t = 0.017 \text{ m}$
Number of tube rows	$n_r = 2$
Number of tubes per bundle (first row)	$n_{tb(1)} = 57$
Number of tubes per bundle (second row)	$n_{tb(2)} = 58$
Number of steam passes	$n_{vp} = 1$
Number of bundles	$n_b = 8$
Effective frontal area of one bundle (second row)	$A_{fr} = 27.55 \text{ m}^2$
Apex angle of the A-frame	$2\theta = 60^\circ$
Ratio of minimum to free stream flow area through finned tube bundle	$\sigma = 0.48$
Ratio of minimum to free stream flow area at the inlet to the finned tube bundle	$\sigma_{21} = 0.875$

Steam-side tube inlet loss coefficient

$$K_c = 0.6$$

The experimentally determined characteristic air-side heat transfer parameter for normal flow through the first row of tubes is given by the following empirical relation.

$$Ny_{(1)} = 366.007945Ry_{(1)}^{0.433256}$$

For the second row,

$$Ny_{(2)} = 360.588007Ry_{(2)}^{0.470373}$$

The heat transfer coefficient for inclined plate finned tubes may actually be slightly higher than under conditions of normal flow during testing. The more conservative normal flow correlations will however be retained for this example to make provision for distortions in the entering flow pattern. Any potential small enhancement in the heat transfer due to the turbulence in the wake of the fan may be assumed to be cancelled by some maldistribution of the air flow through the heat exchanger.

The air-side loss coefficient across the entire bundle under normal isothermal flow conditions is given as

$$K_{he} = 4177.08481Ry^{-0.4392686}$$

Fan installation specifications:

An 8-bladed, 9.145 m diameter axial fan with a blade angle of 16° is employed in this system

Fan diameter	$d_F = 9.145$ m
Fan casing diameter	$d_c = 9.170$ m
Fan hub diameter	$d_h = 1.4$ m
Rotational speed	$N = 125$ rpm
Efficiency of the fan drive system	$\eta_{Fd} = 0.9$
Inlet screen distance from the fan blade (upstream)	$x_{si} = 1.3$ m
Support beam distance from the fan blade (upstream)	$x_{bi} = 1.34$ m
Support beam distance from the fan blade (downstream)	$x_{bo} = 0.53$ m
Walkway distance from the fan blade (downstream)	$x_{so} = 1.0$ m
Ratio of the inlet screen to the fan casing area	$\sigma_{si} = 0.125$
Ratio of the support beam to the fan casing area (upstream)	$\sigma_{bi} = 0.15$

Ratio of the support beam to the fan casing area (downstream)	$\sigma_{bo} = 0.05$
Ratio of the walkway area to the fan casing area	$\sigma_{so} = 0.1$
Height of the fan above the ground level	$H_3 = 25 \text{ m}$
Height of the windwalls	$H_w = 8.27 \text{ m}$
Width of the walkway between the heat exchanger bundle and the windwall	$L_w = 0.2 \text{ m}$
Heat exchanger inlet support loss coefficient (based on the frontal area of the heat exchanger)	$K_{ts} = 1.5$

The fan performance characteristics at a reference density of 1.2 kg/m^3 can be approximated by the following correlations

Fan static pressure:

$$\Delta p_{Fs} = 320.0451719 - 0.2975215484V + 6.351486 \times 10^{-4}V^2 - 8.14 \times 10^{-7}V^3, \text{ N/m}^2$$

Fan power:

$$P_f = 186645.2333 - 59.413863388V + 0.476168398V^2 - 5.08308 \times 10^{-4}V^3, \text{ W}$$

The effects of flow separation at the inlet to the fan platform and the recirculation of hot plume air can be neglected

The thermal-flow performance characteristics of an A-frame air-cooled condenser unit:

In the present thermal-flow performance analysis of the air-cooled condenser unit, it is assumed that the air is essentially dry, $w = 0.0 \text{ kg vapor/kg dry air}$. Kröger (2004) showed that for an air-cooled condenser the error introduced by this assumption is negligibly small.

The relevant energy and draft equations are satisfied for the following values:

Air mass flow rate	$m_a = 604.326 \text{ kg/s}$
The inlet air temperature to the first tube row	$T_{ai(1)} = 15.614 \text{ }^\circ\text{C}$
The mean outlet air temperature after the first tube row	$T_{ao(1)} = 33.6313 \text{ }^\circ\text{C}$
The mean outlet air temperature after the second tube row	$T_{ao(2)} = 48.371 \text{ }^\circ\text{C}$

According to the perfect gas law, the density of the air immediately upstream of the heat exchanger bundles is

$$\rho_{a5} \approx p_{a1} / (RT_{ai(1)}) = (84600) / (287.08 \times (15.614 + 273.15)) = 1.020526711 \text{ kg/m}^3$$

Neglecting pressure changes through the heat exchanger, the air density after the bundles is similarly found to be

$$\rho_{a6} \approx p_{a1} / (RT_{ao(2)}) = (84600) / (287.08 \times (48.371 + 273.15)) = 0.916554051 \text{ kg/m}^3$$

The mean air temperature through the first row of the finned tubes is

$$T_{a(1)} = (T_{ai(1)} + T_{ao(1)}) / 2 = (15.614 + 33.6313) / 2 = 24.623 \text{ }^\circ\text{C} \text{ (297.773 K)}$$

The corresponding properties of dry air may be determined according to the equations given in appendix A.1

Density	$\rho_{a(1)} = 0.989651094 \text{ kg/m}^3$
Specific heat	$c_{pa(1)} = 1006.875332 \text{ J/kgK}$
Dynamic viscosity	$\mu_{a(1)} = 1.836608 \times 10^{-5} \text{ kg/ms}$
Thermal conductivity	$k_{a(1)} = 0.02604876774 \text{ W/mk}$
Prandtl number	$Pr_{a(1)} = 0.709912791$

The mean air temperature through the second row of tubes is

$$T_{a(2)} = (T_{ao(1)} + T_{ao(2)}) / 2 = (33.6313 + 48.371) / 2 = 41.00115 \text{ }^\circ\text{C} \text{ (314.15115 K)}$$

The corresponding properties of dry air may be determined according to the equations given in appendix A.1

Density	$\rho_{a(2)} = 0.93805601293 \text{ kg/m}^3$
Specific heat	$c_{pa(2)} = 1007.5518574 \text{ J/kgK}$
Dynamic viscosity	$\mu_{a(2)} = 1.911492 \times 10^{-5} \text{ kg/ms}$
Thermal conductivity	$k_{a(2)} = 0.02604876774 \text{ W/mk}$
Prandtl number	$Pr_{a(1)} = 0.705229678$

The rate of heat transfer to the air flowing through the first tube row is given by

$$\begin{aligned} Q_{a(1)} &= m_a c_{pa(1)} (T_{ao(1)} - T_{ai(1)}) = 604.326 \times 1006.875332 \times (33.6313 - 15.614) \\ &= 10963183.67 \text{ W} \end{aligned}$$

Similarly, through the second tube row

$$\begin{aligned} Q_{a(2)} &= m_a c_{pa(2)} (T_{ao(2)} - T_{ao(1)}) = 604.326 \times 1007.527568 \times (48.371 - 33.6313) \\ &= 8974636.386 \text{ W} \end{aligned}$$

The total heat transfer rate is then

$$Q_a = Q_{a(1)} + Q_{a(2)} = 10963183.67 + 8974636.386 = 19937820.06 \text{ W}$$

The air-side characteristic flow parameter for the first tube row, $Ry_{(1)}$, taking into consideration the reduced effective frontal area due to the smaller number of tubes (bundle side walls are assumed to be shaped to avoid any by-pass of air), is

$$\begin{aligned} Ry_{(1)} &= m_a / \left[\mu_{a(1)} A_{fr} n_b n_{tb(1)} / n_{tb(2)} \right] = 604.326 / \left[1.836608 \times 10^{-5} \times 27.55 \times 8 \times 57 / 58 \right] \\ &= 151913.495 \text{ m}^{-1} \end{aligned}$$

According to the given specifications, the heat transfer parameter is

$$Ny_{(1)} = 366.007945 Ry_{(1)}^{0.433256} = 366.007945 (151913.495)^{0.433256} = 64335.13599 \text{ m}^{-1}$$

and the effective heat transfer coefficient is

$$\begin{aligned} h_{ae(1)} A_{a(1)} &= k_{a(1)} Pr_{a(1)}^{0.333} n_b A_{fr} Ny_{(1)} n_{tb(1)} / n_{tb(2)} \\ &= 0.02604876774 \times 0.709912791^{0.333} \times 8 \times 27.55 \times 64335.136 \times 57 / 58 \\ &= 323850.9029 \text{ W/K} \end{aligned}$$

As it is assumed that the pressure losses in the steam header and ducts are negligible small, the temperature of the steam in the system remains constant. According to Appendix A.4, the corresponding thermophysical properties of the condensate in the first tube row are then

Density	$\rho_{c(1)} = 983.21684632 \text{ kg/m}^3$
Specific heat	$c_{pc(1)} = 4184.093614 \text{ J/KgK}$
Dynamic viscosity	$\mu_{c(1)} = 4.6310 \times 10^{-4} \text{ kg/ms}$

Thermal conductivity $k_{c(1)} = 0.65318917 \text{ W/mk}$

Latent heat of vaporation $i_{fg(1)} = 2.35861972 \times 10^6 \text{ J/kg}$

The mass flow rate of the steam condensed in the first tube row is

$$m_{c(1)} = Q_{a(1)} / i_{fg(1)} = 10963183.67 / 2.35861972 \times 10^6 = 4.64813534 \text{ kg/s}$$

Due to the relatively high steam velocity at the inlet of the tube, the shear stresses acting on the condensate film will have a strong influence on its development. However gravity control becomes more important further from the inlet and over the greater part of the tube the approximate condensation heat transfer coefficient is given by

$$h_c = 0.9245 \left[\frac{L_t k_{c(1)}^3 \rho_{c(1)}^2 g \cos(90^\circ - \theta) i_{fg(1)}}{\mu_{c(1)} m_{at(1)} c_{pa(1)} (T_{vm} - T_{ai}) \left[1 - \exp\left\{ -U_{c(1)} H_t L_t / (m_{at(1)} c_{pa(1)}) \right\} \right]} \right]^{0.333}$$

In the first tube row the inside tube area exposed to the condensing steam is

$$A_{c(1)} = n_{tb(1)} n_b A_i L_t = 57 \times 8 \times 0.21341 \times 9.5 = 924.49212 \text{ m}^2$$

By neglecting the thermal resistance of the condensate film, the approximate overall heat transfer coefficient based on the condensing surface area can be expressed as

$$U_{c(1)} H_t L_t = h_{ae(1)} A_{a(1)} / (2 n_{tb(1)} n_b) = 323850.9029 / (2 \times 57 \times 8) = 355.0996742 \text{ W/K}$$

The corresponding air mass flow rate flowing over one side of a finned tube is

$$m_{at(1)} = m_a / (2 n_{tb(1)} n_b) = 604.326 / (2 \times 57 \times 8) = 0.662638 \text{ kg/s}$$

The mean condensation heat transfer coefficient is then

$$\begin{aligned} h_{c(1)} &= 0.9245 \left[\frac{9.5 \times 0.65318917^3 \times 983.216846^2 \times 9.81 \times \cos(90^\circ - 30^\circ) \times 2.3586197 \times 10^6}{4.6310 \times 10^{-4} \times 0.662638 \times 1006.875332 \times (60 - 15.614)} \right]^{0.333} \\ &\times \left[1 - \exp\left\{ -355.0996742 / (0.662638 \times 1006.875332) \right\} \right]^{-0.333} \\ &= 15887.7 \text{ W/m}^2\text{K} \end{aligned}$$

The overall heat transfer coefficient for the first tube row is given by

$$UA_{(1)} = \left[\frac{1}{(h_{ae}A_a)_{(1)}} + \frac{1}{(h_{c(1)}A_{c(1)})} \right]^{-1} = \left[\frac{1}{323850.9029} + \frac{1}{15887.7 \times 924.4921} \right]^{-1}$$

$$= 316864.4869 \text{ W/K}$$

It is noted that the thermal resistance of the condensate film is small compared to the overall resistance..

The effectiveness for the first row of the condenser tubes may be expressed as

$$e_{(1)} = 1 - \exp \left[-UA_{(1)} / (m_a c_{pa(1)}) \right] = 1 - \exp \left[-316864.4869 / (604.326 \times 1006.875332) \right]$$

$$= 0.405923258$$

and the heat transfer rate for row one is then

$$Q_{a(1)} = m_a c_{pa(1)} (T_{vm(1)} - T_{ai(1)}) e_{(1)} = 604.326 \times 1006.875332 \times (60 - 15.614) \times 0.405923258$$

$$= 10963189.6 \text{ W}$$

This compares well with the value previously calculated for $Q_{a(1)}$.

A similar procedure is followed to determine conditions in the second tube row. As the steam pressure is the same in the two tube rows, the steam temperature and corresponding thermophysical properties are the same in the second tube row as in the first tube row.

The air-side characteristic flow parameter for the second tube row is

$$Ry_{(2)} = m_a / (\mu_{a(2)} A_{fr} n_b) = 604.326 / (1.911492 \times 10^{-5} \times 27.55 \times 8) = 143445.5911 \text{ m}^{-1}$$

The corresponding heat transfer parameter is according to the given specifications

$$Ny_{(2)} = 360.588007 Ry_{(2)}^{0.470373} = 360.588007 (143445.5911)^{0.470373} = 96064.34779 \text{ m}^{-1}$$

and the corresponding effective heat transfer coefficient is

$$h_{ae(2)} A_{a(2)} = k_{a(2)} Pr_{a(2)}^{0.333} n_b A_{fr} Ny_{(2)} = 0.027309922 \times 0.70522968^{0.333} \times 8 \times 27.55 \times 96064.3478$$

$$= 514740.5375 \text{ W/K}$$

It should be noted that the steam pressure drop in the different tube rows is usually not identical; with the result that backflow of steam may occur. A dephlegmator is installed after

the main condenser units to increase the net steam flow rate through the units to overcome the problem of the accumulation of noncondensables gases in the tubes.

$$T_{vm} = T_v = 60^\circ\text{C}$$

The thermophysical properties of the condensate are evaluated at T_v

Density	$\rho_{c(2)} = 983.21684632 \text{ kg/m}^3$
Specific heat	$c_{pc(2)} = 4184.093614 \text{ J/KgK}$
Dynamic viscosity	$\mu_{c(2)} = 4.6310 \times 10^{-4} \text{ kg/ms}$
Thermal conductivity	$k_{c(2)} = 0.65318917 \text{ W/mk}$
Latent heat of evaporation	$i_{fg(2)} = 2.35861972 \times 10^6 \text{ J/kg}$

The mass flow rate of the steam condensed in the second tube row is

$$m_{c(2)} = Q_{a(2)} / i_{fg(2)} = 8974636.386 / 2.35861972 \times 10^6 = 3.80503745 \text{ kg/s}$$

The effective condensation heat transfer area on the inside of the tubes is

$$A_{c(2)} = A_{c(1)} n_{tb(2)} / n_{tb(1)} = 924.49212 \times 58 / 57 = 940.71128 \text{ m}^2$$

and the approximate overall heat transfer coefficient based on this area is

$$U_{c(2)} H_i L_t = h_{ae(2)} A_{a(2)} / (2n_{tb(2)} n_b) = 514740.5375 / (2 \times 58 \times 8) = 554.67730 \text{ W/K}$$

The corresponding air mass flow rate flowing on the one side of a finned tube is

$$m_{at(2)} = m_a / (2n_{tb(2)} n_b) = 604.326 / (2 \times 58 \times 8) = 0.651213362 \text{ kg/s}$$

The condensation heat transfer coefficient is

$$\begin{aligned}
h_{c(2)} &= 0.9245 \left[\frac{L_t k_{c(2)}^3 \rho_{c(2)}^2 g \cos(90^\circ - \theta) i_{fg(2)}}{\mu_{c(2)} m_{at(2)} c_{pa(2)} (T_{vm} - T_{ao(1)}) \left[1 - \exp\left\{-U_{c(2)} H_t L_t / (m_{at(2)} c_{pa(2)})\right\}\right]} \right]^{-0.333} \\
&= 0.9245 \left[\frac{9.5 \times 0.653189^3 \times 983.216846^2 \times 9.81 \times \cos(90^\circ - 30^\circ) \times 2.3586197 \times 10^6}{4.6310 \times 10^{-4} \times 0.651213362 \times 1007.5518574 \times (60 - 33.6313)} \right]^{-0.333} \\
&\times \left[1 - \exp\left\{-554.67730 / (0.651213362 \times 1007.5518574)\right\} \right]^{-0.333} \\
&= 0.9245 \left[\frac{2.960984205 \times 10^{13}}{8.0122244822} \right]^{-0.333} (0.57060393)^{-0.333} \\
&= 17064.18327 \text{ W/m}^2 \text{K}
\end{aligned}$$

The actual overall heat transfer coefficient for the second tube row is

$$\begin{aligned}
UA_{(2)} &= \left[\frac{1}{(h_{ae} A_a)_{(2)}} + \frac{1}{(h_{c(1)} A_c)_{(2)}} \right]^{-1} = \left[\frac{1}{514740.5375} + \frac{1}{17064.18327 \times 940.71128} \right]^{-1} \\
&= 498747.6324 \text{ W/K}
\end{aligned}$$

The effectiveness for the second row of the condenser tubes may be expressed as

$$\begin{aligned}
e_{(2)} &= 1 - \exp\left[-UA_{(2)} / (m_a c_{pa(2)})\right] = 1 - \exp\left[-498747.6324 / (604.326 \times 1007.5518574)\right] \\
&= 0.55917613
\end{aligned}$$

and the heat transfer rate is given by

$$\begin{aligned}
Q_{a(2)} &= m_a c_{pa(2)} (T_{vm(2)} - T_{ao(1)}) e_{(2)} = 604.326 \times 1007.5518574 \times (60 - 33.6313) \times 0.55917613 \\
&= 8977926.186 \text{ W}
\end{aligned}$$

This value of $Q_{a(2)}$ compares well to the value previously calculated for the heat transfer rate of the second tube row.

Evaluation of the draft equation:

To evaluate the draft equation, the fan operating point has to be determined. The approximate air temperature at the fan suction side is

$$T_{a3} = T_{a1} - 0.00975 H_3 = 15.6 - 0.00975 \times 25 = 15.35625 \text{ }^\circ\text{C}$$

and the corresponding air density is

$$\rho_{a3} = p_{a1} / RT_{a3} = 84600 / (287.08 \times (15.35625 + 273.15)) = 1.02143844 \text{ kg/m}^3$$

The specific heat of the air is $c_{pa3} = 1006.474 \text{ J/kgK}$ and the volume flow rate through the fan is

$$V = m_a / \rho_{a3} = 604.326 / 1.021438844 = 591.6421134 \text{ m}^3 / \text{s}$$

This volume flow rate is more than the $573.148 \text{ m}^3/\text{s}$ at the point of maximum fan efficiency and the fan will thus operate effectively.

According to the empirical third order correlation specified for the fan static pressure in terms of the volume flow rate at the reference air density of 1.2 kg/m^3 , find

$$\begin{aligned} \Delta p_{Fs(1.2)} &= 320.0451719 - 0.2975215484V + 6.351486 \times 10^{-4} V^2 - 8.14 \times 10^{-7} V^3 \\ &= 320.0451719 - 0.2975215484(591.6421134) \\ &\quad + 6.351486 \times 10^{-4} (591.6421134)^2 - 8.14 \times 10^{-7} (591.6421134)^3 \\ &= 197.7682684 \text{ N/m}^2 \end{aligned}$$

The static pressure across this fan operating at a density of 1.0214 kg/m^3 is

$$\Delta p_{Fs} = \Delta p_{Fs(1.2)} \left(\rho_{a3} / \rho_{ref(1.2)} \right) = 197.7682684 \times (1.02143844 / 1.2) = 168.3400929 \text{ N/m}^2$$

The corresponding fan coefficient is

$$\begin{aligned} K_{Fs} &= 2 \Delta p_{Fs} \rho_{a3} (A_c / m_a)^2 = 2 \times 168.3400929 \times 1.02143844 \times [\pi \times 9.17^2 / (4 \times 604.326)]^2 \\ &= 4.107185354 \end{aligned}$$

The required fan shaft power at an air density of $\rho_{a3} = 1.0214 \text{ kg/m}^3$, follows from the density corrected specified fan power curve

$$\begin{aligned} P_F &= \left(\rho_{a3} / \rho_{ref} \right) (186645.2333 - 59.413863388V + 0.476168398V^2 - 5.08308 \times 10^{-4} V^3) \\ &= (1.02143844 / 1.2) [186645.2333 - 59.413863388(591.6421134) \\ &\quad + 0.476168398(591.6421134)^2 - 5.08308 \times 10^{-4} (591.6421134)^3] \\ &= 181221.708 \text{ W} \end{aligned}$$

The mean height of the heat exchanger inlet is

$$H_5 = H_3 + 0.5L_t \cos \theta = 25 + 0.5 \times 9.5 \times \cos 30 = 29.11362067 \text{ m}$$

Find the approximate temperature of the air before it enters the heat exchanger.

$$\begin{aligned} T_{a5} &= T_{ai(1)} = T_{a1} + P_F / (m_a c_{pa}) - 0.00975 H_5 \\ &= 15.6 + 181221.708 / (604.326 \times 1006.474) - 0.00975 \times 25 \\ &= 15.65419519 \text{ }^\circ\text{C} \end{aligned}$$

The electrical power input to the fan is determined as follows:

$$P_e = P_F / \eta_{Fd} = 181221.708 / 0.9 = 201357.4533 \text{ W}$$

The loss coefficient due to the fan safety screen, the support beams at both the fan suction and discharge sides and the walkway above the fan are determined by employing the bulk method, which relates the pressure loss coefficient to the total resistance area exposed to the flow, and to the distance between the fan rotor and the resistance.

By employing the area ratios and dimensionless distances the loss coefficients can be directly obtained from the curves given in Kroger (2004).

For the fan safety screen, $x_{si}/d_c = 0.142$ and $A_{si}/A_c = \sigma_{si} = 0.125$, $K_{si} = 0.1317$ and for the fan safety screen support beams, $x_{bi}/d_c = 0.146$ and $A_{bi}/A_c = \sigma_{bi} = 0.15$, $K_{bi} = 0.16523$.

Thus the total loss coefficient due to the flow obstacles at the fan suction or upstream side is

$$K_{up} = 0.1317 + 0.16523 = 0.29693$$

Similarly, the loss coefficients due to the flow obstacles at the fan discharge or downstream side is found to be

$$K_{do} = K_{so} + K_{bo} = 0.2324 + 0.1584 = 0.3908$$

The sum of the upstream and downstream losses is

$$K_{up} + K_{do} = 0.29693 + 0.3908 = 0.68773$$

The heat exchanger air-side loss coefficient under normal isothermal flow conditions is

$$K_{he} = 4177.08481Ry^{-0.4392686}$$

The characteristic flow number, Ry , is evaluated by using the mean dynamic viscosity μ_{a56} .

At the mean air temperature through the heat exchanger,

$T_{a56} = 0.5(T_{ai(1)} + T_{ao(2)}) = 31.9925$ °C, find the dynamic viscosity of the air stream,

$\mu_{a56} = 1.870461 \times 10^{-5}$ kg/ms. The corresponding characteristic flow number, based on the minimum frontal area is

$$\begin{aligned} Ry &= m_a / (n_b A_{fr} \mu_{a56} n_{tb(1)} / n_{tb(2)}) = 604.326 / (8 \times 27.55 \times 1.870461 \times 10^{-5} \times 57/58) \\ &= 149164.0511 \text{ m}^{-1} \end{aligned}$$

Thus

$$K_{he} = 4177.08481(149164.0511)^{-0.4392686} = 22.29693031 \text{ m}^{-1}$$

The contraction coefficient is

$$\begin{aligned} \sigma_{ci} &= 0.6144517 + 0.04566493\sigma_{21} - 0.336651\sigma_{21}^2 + 0.4082743\sigma_{21}^3 \\ &\quad + 2.672041\sigma_{21}^4 - 5.963169\sigma_{21}^5 + 3.558944\sigma_{21}^6 \\ &= 0.6144517 + 0.04566493(0.875) - 0.336651(0.875)^2 + 0.4082743(0.875)^3 \\ &\quad + 2.672041(0.875)^4 - 5.963169(0.875)^5 + 3.558944(0.875)^6 \\ &= 0.77515 \end{aligned}$$

The entrance contraction loss coefficient is

$$K_c = \left[\frac{1}{\sigma_{21}} \left(\frac{1}{\sigma_{ci}} - 1 \right) \right]^2 = \left[\frac{1}{0.875} \left(\frac{1}{0.77515} - 1 \right) \right]^2 = 0.1099$$

The effective mean inlet flow angle is

$$\theta_m = 0.0019\theta^2 + 0.9133\theta - 3.1558 = 0.0019(30)^2 + 0.9133(30) - 3.1558 = 25.95315^\circ$$

The downstream loss coefficient, K_d , consists of the turning and the jetting losses as well as the kinetic energy loss to the atmosphere, find the jetting loss

$$\begin{aligned}
K_{dj} &= \left[\left\{ -2.89188 \left(\frac{L_w}{L_t} \right) + 2.93291 \left(\frac{L_w}{L_t} \right)^2 \right\} \left(\frac{L_t}{L_s} \right) \left(\frac{L_b}{L_s} \right) \left(\frac{28}{\theta} \right)^{0.4} \right. \\
&\quad \left. + \left\{ \exp \left(2.36987 + 5.8601 \times 10^{-2} \theta - 3.3797 \times 10^{-3} \theta^2 \right) \left(\frac{L_s}{L_b} \right) \right\}^{0.5} \left(\frac{L_t}{L_r} \right) \right]^2 \\
&= \left[\left\{ -2.89188 \left(\frac{0.2}{9.5} \right) + 2.93291 \left(\frac{0.2}{9.5} \right)^2 \right\} \times \{ \sin 30^\circ - 1.25 / (2 \times 9.5) + 0.2 / 9.5 \}^{-1} \right. \\
&\quad \times \left[1 - 0.5 \times 1.25 / \{ 9.5 (\sin 30 + 0.2 / 9.5) \} \right]^{-1} \times (28 / 30)^{0.4} \\
&\quad + \left\{ \exp \left(2.36987 + 5.8601 \times 10^{-2} \times 30 - 3.3797 \times 10^{-3} \times 30^2 \right) \right. \\
&\quad \left. \times \left(1 - 0.5 \times 1.25 / (9.5 (\sin 30 + 0.2 / 9.5)) \right) \right\}^{0.5} \times \left\{ 1 + 0.2 / (9.5 \times \sin 30) \right\}^{-1} \left. \right]^2 \\
&= 1.955121
\end{aligned}$$

and the outlet loss coefficient is

$$\begin{aligned}
K_o &= \left[\left\{ -2.89188 \left(\frac{L_w}{L_t} \right) + 2.93291 \left(\frac{L_w}{L_t} \right)^2 \right\} \left(\frac{L_s}{L_b} \right)^3 \right. \\
&\quad \left. + 1.9874 - 3.02783 \left(\frac{d_s}{2L_b} \right) + 2.0187 \left(\frac{d_s}{2L_b} \right)^2 \right] \left(\frac{L_t}{L_s} \right)^2 \\
&= \left[\left\{ -2.89188 \left(\frac{0.2}{9.5} \right) + 2.93291 \left(\frac{0.2}{9.5} \right)^2 \right\} \times \left[1 - 0.5 \times 1.25 / \{ 9.5 (\sin 30 + 2 / 9.5) \} \right]^3 \right. \\
&\quad \left. + 1.9874 - 3.02783 \left\{ 0.5 \times 1.25 / 9.5 (\sin 30 + 0.2 / 9.5) \right\}^2 \right] \\
&\quad \times \{ \sin 30 - 1.25 / (2 \times 9.5) + 2 \times 9.5 \}^{-2} \\
&= 7.70772
\end{aligned}$$

Thus

$$K_d = 1.955121 + 7.70772 = 9.662841$$

Substituting these values into the following equation and find total loss coefficient of the A-frame array

$$\begin{aligned}
K_{\theta_t} &= K_{he} + \frac{2}{\sigma_{\min}^2} \left(\frac{\rho_{ai(1)} - \rho_{ao(2)}}{\rho_{ai(1)} + \rho_{ao(2)}} \right) + \frac{2\rho_{ao(2)}}{(\rho_{ai(1)} + \rho_{ao(2)})} \left(\frac{1}{\sin \theta_m} - 1 \right) \left[\left(\frac{1}{\sin \theta_m} - 1 \right) + 2K_{ci}^{0.5} \right] \\
&+ (K_{dj} + K_o) 2\rho_{ai(1)} / (\rho_{ai(1)} + \rho_{ao(2)}) \\
&= 22.29693031 + \frac{2}{(0.48)^2} \left(\frac{1.020526711 - 0.916554051}{1.020526711 + 0.916554051} \right) + \\
&\frac{2 \times 0.916554051}{(1.02052671 + 0.91655405)} \left(\frac{1}{\sin(25.95315^\circ)} - 1 \right) \left[\left(\frac{1}{\sin(25.95315^\circ)} - 1 \right) + 2 \times 0.1099^{0.5} \right] \\
&+ (9.662841) \times 2 \times 1.020526711 / (1.020526711 + 0.916554051) \\
&= 22.29693031 + 0.465928147 + 2.368861508 + 10.18149324 \\
&= 35.31321321
\end{aligned}$$

The harmonic mean density through the bundle is

$$\rho_{am} = 2 / (1/\rho_{ai(1)} + 1/\rho_{ao(2)}) = 2 / (1/1.020526711 + 1/0.916554051) = 0.965750018 \text{ kg/m}^3$$

Furthermore

$$A_c = \pi d_c^2 / 4 = \pi \times 9.17^2 / 4 = 66.04326762 \text{ m}^2$$

and

$$A_e = \pi (d_c^2 - d_e^2) / 4 = \pi (9.17^2 - 1.4^2) / 4 = 64.50388722 \text{ m}^2$$

The value of the left hand side of the draft equation is

$$\begin{aligned}
&P_{a1} \left[\left\{ 1 - 0.00975 (H_7 - H_6) / T_{a6} \right\}^{3.5} - \left\{ 1 - 0.00975 (H_7 - H_6) / T_{a1} \right\}^{3.5} \right] \\
&= 84600 \left[\left\{ 1 - 0.00975 (0.5 \times \cos 30^\circ \times 9.5) / (48.317 + 273.15) \right\}^{3.5} \right. \\
&\quad \left. - \left\{ 1 - 0.00975 (0.5 \times \cos 30^\circ \times 9.5) / (15.6 + 273.15) \right\}^{3.5} \right] \\
&= 84600 [0.999563391 - 0.999513929] \\
&= 4.184460751 \text{ N/m}^2
\end{aligned}$$

and the corresponding value of the right hand side of the draft equation is

$$\begin{aligned}
& K_{is} (m_a/A_2)^2 / (2\rho_{a1}) + K_{up} (m_a/A_e)^2 / (2\rho_{a3}) + K_{do} (m_a/A_e)^2 / (2\rho_{a3}) \\
& - K_{Fs} (m_a/A_c)^2 / (2\rho_{a3}) + K_{\theta t} (m_a/A_{fr})^2 / (2\rho_{am}) \\
& = \frac{1.5}{(2 \times 1.02057619)} \left(\frac{604.326}{(8 \times 27.55)} \right)^2 + \frac{0.68773}{(2 \times 1.02143844)} \left(\frac{604.326}{64.50388722} \right)^2 \\
& - \frac{4.107185354}{(2 \times 1.02143844)} \left(\frac{604.326}{66.04326762} \right)^2 + \frac{35.31321321}{(2 \times 0.965750018)} \left(\frac{604.326}{(8 \times 27.55)} \right)^2 \\
& = 5.525037241 + 29.54925663 - 168.3405175 + 137.455428 \\
& = 4.18920434
\end{aligned}$$

The agreement between the two sides of the draft equation is good and the draft equation is therefore satisfied.

As it is assumed that the performance characteristics of all the condenser units is the same, the combined heat transfer rate of the condenser units is then

$$Q_{pc} = n_s n_c Q_a = 3 \times 5 \times 19937820 = 299067300 \text{ W} \approx 300 \text{ MW}$$

where n_c is the number of condenser units per street or row and n_s is the number of streets.

The corresponding total mass flow rate of the steam that is condensed in the condenser units is

$$m_{c(pc)} = n_s n_c (m_{c(1)} + m_{c(2)}) = 3 \times 5 \times (4.64813 + 3.80513) = 126.7989 \text{ kg/s}$$

2. Hybrid (dry/wet) dephlegmator

The hybrid (dry/wet) dephlegmator consists of two stages: First, an air-cooled condenser with somewhat shortened finned tubes, similar to those used in the A-frame configuration, and a second stage with galvanized steel tubes arranged horizontally. The hybrid dephlegmator is shown schematically in Figure 2.8. The second stage can be operated dry as an dry air-cooled condenser or the air-side surface of the tube bundle can be deluged with water and operated as an evaporatively cooled condenser.

The following assumptions are made in the analysis of the hybrid dephlegmator

- As a first approximation it is assumed that the mass velocity of the air passing through the finned tube bundles and the plain tube bundles of the first and second stage of the hybrid dephlegmator respectively is the same as the air mass velocity through the finned tube bundles A-frame air-cooled condenser. In Section 3 it is shown that the air-side flow resistance of the first and second stage of the hybrid (dry/wet) dephlegmator is approximately the same.
- The effect of the fan work and inlet height of the heat exchanger on the air inlet temperature is neglected and it is assumed that the temperature of the air entering the bundles is the same as the ambient ground temperature.

2.a. First stage of hybrid (dry/wet) dephlegmator

The geometric parameters of the finned tube first stage of the hybrid dephlegmator are:

Finned tube bundle specifications:

The first stage of the dephlegmator consists of two rows of staggered plate finned tubes; each row having performance characteristics such that the amount of steam condensed in each is approximately the same (similar to condenser).

Hydraulic diameter of the tube	$d_e = 0.02975 \text{ m}$
Inside area of the tube per unit length	$A_{ti} = 0.21341 \text{ m}$
Inside cross-sectional tube flow area	$A_{ts} = 0.00159 \text{ m}^2$
Length of finned tube	$L_t = 4.5 \text{ m}$
Inside height of the tube	$H_t = 0.097 \text{ m}$
Inside width of the tube	$W_t = 0.017 \text{ m}$
Number of tube rows	$n_r = 2$
Number of tubes per bundle (first row)	$n_{tb(1)} = 57$
Number of tubes per bundle (second row)	$n_{tb(2)} = 58$
Number of steam passes	$n_{vp} = 1$
Number of bundles	$n_b = 8$
Effective frontal area of one bundle (second row)	$A_{fr} = 13.05 \text{ m}^2$
Apex angle of the A-frame	$2\theta = 60^\circ$

The experimentally determined characteristic air-side heat transfer parameter for normal flow through the first row of tubes is given by the following empirical relation.

$$Ny_{(1)} = 366.007945Ry_{(1)}^{0.433256}$$

For the second row,

$$Ny_{(2)} = 360.588007Ry_{(2)}^{0.470373}$$

The heat transfer coefficient for inclined plate finned tubes may be slightly higher than under conditions of normal flow during testing. The more conservative normal flow correlations are however retained to make provision for distortions in the entering flow pattern. Any potential small enhancement in the heat transfer due to the turbulence in the wake of the fan may be assumed to be cancelled by some maldistribution of the air flow through the heat exchanger.

Analysis of the first stage of the hybrid dephlegmator

In the following section the analysis of the thermal performance characteristics of the first stage of the hybrid dephlegmator is presented. The geometric parameters are similar to those of the A-frame array air-cooled condenser units, but the length of the finned tubes is reduced to accommodate the horizontal tube bundle.

As stated earlier, it is assumed that the mass velocity of the air passing through the first and second stage of the hybrid dephlegmator is the same as the air mass velocity through the finned tube bundles A-frame air-cooled condenser. The air mass velocity through the finned tube bundles of the A-frame air-cooled condenser is

$$G_a = \frac{m_a}{n_b A_{fr}} = \frac{604.326}{8 \times 27.55} = 2.741951 \text{ kg/sm}^2$$

The corresponding air mass flow rate through the finned tube bundle of the first stage of the hybrid dephlegmator is

$$m_{a(1)} = G_a n_{b(1)} A_{fr(1)} = 2.741951 \times 8 \times 13.05 = 286.26 \text{ kg/s}$$

As discussed previously, the ambient air is assumed to be essentially dry. Furthermore, the effect of the fan work and the height of the heat exchanger above the ground on the inlet

temperature of the air are neglected and it is assumed that the temperature of the air entering the heat exchanger is the same as the ambient ground temperature, $T_{ai(1)} = 15.6 \text{ }^\circ\text{C}$.

The relevant energy equations are satisfied for the following values

The mean outlet air temperature after the first tube row $T_{ao(1)} = 33.623 \text{ }^\circ\text{C}$

The mean outlet air temperature after the second tube row $T_{ao(2)} = 48.367 \text{ }^\circ\text{C}$

The mean air temperature through the first row of the finned tubes is

$$T_{a(1)} = (T_{ai(1)} + T_{ao(1)}) / 2 = (15.6 + 33.623) / 2 = 24.611 \text{ }^\circ\text{C} \text{ (297.761 K)}$$

The corresponding properties for dry air may be determined from the equations given in appendix A.1

Density	$\rho_{a(1)} = 0.9896898 \text{ kg/m}^3$
Specific heat	$c_{pa(1)} = 1006.875 \text{ J/kgK}$
Dynamic viscosity	$\mu_{a(1)} = 1.836554 \times 10^{-5} \text{ kg/ms}$
Thermal conductivity	$k_{a(1)} = 0.02604786 \text{ W/mk}$
Prandtl number	$Pr_{a(1)} = 0.7099162$

The mean air temperature through the second row of tubes is

$$T_{a(2)} = (T_{ao(1)} + T_{ao(2)}) / 2 = (33.623 + 48.367) / 2 = 40.995 \text{ }^\circ\text{C} \text{ (314.145 K)}$$

The corresponding properties for dry air may be determined from the equations given in appendix A.1

Density	$\rho_{a(2)} = 0.9380747 \text{ kg/m}^3$
Specific heat	$c_{pa(2)} = 1007.552 \text{ J/kgK}$
Dynamic viscosity	$\mu_{a(2)} = 1.911463 \times 10^{-5} \text{ kg/ms}$
Thermal conductivity	$k_{a(2)} = 0.02730944 \text{ W/mk}$
Prandtl number	$Pr_{a(2)} = 0.7052132$

The rate of heat transfer to the air flowing through the first tube row is given by

$$Q_{a(1)} = m_a c_{pa(1)} (T_{ao(1)} - T_{ai(1)}) = 286.26 \times 1006.875 \times (33.623 - 15.6) = 5194638.647 \text{ W}$$

Similarly, for the second tube row

$$Q_{a(2)} = m_a c_{pa(2)} (T_{ao(2)} - T_{ao(1)}) = 286.26 \times 1007.552 \times (48.367 - 33.623) = 4252597.272 \text{ W}$$

The total heat transfer rate is

$$Q_a = Q_{a(1)} + Q_{a(2)} = 5194638.647 + 4252597.272 = 9447237.628 \text{ W}$$

The air-side characteristic flow parameter for the first tube row, $Ry_{(1)}$, taking into consideration the reduced effective frontal area due to the smaller number of tubes (bundle side walls are assumed to be shaped to avoid any by-pass of air), is

$$\begin{aligned} Ry_{(1)} &= m_a / \left[\mu_{a(1)} A_{fr} n_b n_{tb(1)} / n_{tb(2)} \right] = 286.23 / \left[1.836554 \times 10^{-5} \times 13.05 \times 8 \times 57 / 58 \right] \\ &= 151917.908 \text{ m}^{-1} \end{aligned}$$

According to the given specifications, the corresponding heat transfer parameter is

$$Ny_{(1)} = 366.007945 Ry_{(1)}^{0.433256} = 366.007945 (151917.908)^{0.433256} = 64115.946 \text{ m}^{-1}$$

and the corresponding effective heat transfer coefficient is

$$\begin{aligned} h_{ae(1)} A_{a(1)} &= k_{a(1)} Pr_{a(1)}^{0.333} n_b A_{fr} Ny_{(1)} n_{tb(1)} / n_{tb(2)} \\ &= 0.02604786 \times 0.7099162^{0.333} \times 8 \times 13.05 \times 64115.946 \times 57 / 58 \\ &= 153399.916 \text{ W/K} \end{aligned}$$

As it is assumed that the pressure losses in the steam header and ducts are negligibly small, the temperature of the steam in the system remains constant and $T_{vm} = T_v = 60^\circ \text{C}$. According to Appendix A.4, the corresponding thermophysical properties of the condensate in the first tube row are then

Density	$\rho_{c(1)} = 983.2168 \text{ kg/m}^3$
Specific heat	$c_{pc(1)} = 4184.094 \text{ J/KgK}$
Dynamic viscosity	$\mu_{c(1)} = 4.631034 \times 10^{-4} \text{ kg/ms}$
Thermal conductivity	$k_{c(1)} = 0.6531892 \text{ W/mk}$

Latent heat of evaporation $i_{fg(1)} = 2.358620 \times 10^6 \text{ J/kg}$

The mass flow rate of the steam condensed in the first tube row is

$$m_{c(1)} = Q_{a(1)} / i_{fg(1)} = 5194638.647 / 2.358620 \times 10^6 = 2.2024 \text{ kg/s}$$

Due to the relatively high steam velocity at the inlet of the tube, the shear stresses acting on the condensate film will have a strong influence on its development. However gravity control becomes more important further from the inlet and over the greater part of the tube the approximate condensation heat transfer coefficient is given by

$$h_c = 0.9245 \left[\frac{L_t k_{c(1)}^3 \rho_{c(1)}^2 g \cos(90^\circ - \theta) i_{fg(1)}}{\mu_{c(1)} m_{at(1)} c_{pa(1)} (T_{vm} - T_{ai}) \left[1 - \exp\left\{ -U_{c(1)} H_t L_t / (m_{at(1)} c_{pa(1)}) \right\} \right]} \right]^{0.333}$$

In the first tube row the inside tube area exposed to the condensing steam is

$$A_{c(1)} = n_{tb(1)} n_b A_i L_t = 57 \times 8 \times 0.21341 \times 4.5 = 437.9173 \text{ m}^2$$

By neglecting the thermal resistance of the condensate film, the approximate overall heat transfer coefficient based on the condensing surface area can be expressed as

$$U_{c(1)} H_t L_t = h_{ae(1)} A_{a(1)} / (2n_{tb(1)} n_b) = 153399.916 / (2 \times 57 \times 8) = 168.2017 \text{ W/K}$$

The corresponding air mass flow rate flowing over one side of a finned tube is

$$m_{at(1)} = m_a / (2n_{tb(1)} n_b) = 286.23 / (2 \times 57 \times 8) = 0.3138811 \text{ kg/s}$$

The mean condensation heat transfer coefficient is then

$$\begin{aligned} h_{c(1)} &= 0.9245 \left[\frac{4.5 \times 0.65318920^3 \times 983.2168^2 \times 9.8 \times \cos(90^\circ - 30^\circ) \times 2.358620 \times 10^6}{4.631034 \times 10^{-4} \times 0.3138811 \times 1006.875 \times (60 - 15.6)} \right]^{0.333} \\ &\times \left[1 - \exp\left\{ -168.2017 / (0.3138811 \times 1006.875) \right\} \right]^{-0.333} \\ &= 15886.072 \text{ W/m}^2\text{K} \end{aligned}$$

The overall heat transfer coefficient for the first tube row is given by

$$UA_{(1)} = \left[\frac{1}{(h_{ae}A_a)_{(1)}} + \frac{1}{(h_{c(1)}A_{c(1)})} \right]^{-1} = \left[\frac{1}{153399.916} + \frac{1}{15886.072 \times 437.9173} \right]^{-1}$$

$$= 150090.364 \text{ W/K}$$

It is noted that the thermal resistance of the condensate film is small compared to the overall resistance.

The effectiveness for the first row of the condenser tubes may be expressed as

$$e_{(1)} = 1 - \exp \left[-UA_{(1)} / (m_a c_{pa(1)}) \right] = 1 - \exp \left[-150090.364 / (286.23 \times 1006.875) \right]$$

$$= 0.4059166$$

and the heat transfer rate for row one is

$$Q_{a(1)} = m_a c_{pa(1)} (T_{vm(1)} - T_{ai(1)}) e_{(1)} = 286.23 \times 1006.875 \times (60 - 15.6) \times 0.4059166$$

$$= 5194638.64 \text{ W}$$

This compares well with the value previously calculated for $Q_{a(1)}$.

A similar procedure as above is followed to determine performance of the second tube row. As the steam temperature in the first and second tube rows are the same, the thermophysical properties are the same as for the first tube row.

The air-side characteristic flow parameter for the second tube row is

$$Ry_{(2)} = m_a / (\mu_{a(2)} A_{fr} n_b) = 286.23 / (1.911463 \times 10^{-5} \times 13.05 \times 8) = 143447.647 \text{ m}^{-1}$$

According to the given specifications the corresponding heat transfer parameter is

$$Ny_{(2)} = 360.588007 Ry_{(2)}^{0.470373} = 360.588007 (143447.647)^{0.470373} = 96068.417 \text{ m}^{-1}$$

and the effective heat transfer coefficient is

$$h_{ae(2)} A_{a(2)} = k_{a(2)} Pr_{a(2)}^{0.333} n_b A_{fr} Ny_{(2)} = 0.02730944 \times 0.7052132^{0.333} \times 8 \times 13.05 \times 96068.417$$

$$= 243828.641 \text{ W/K}$$

The mass flow rate of the steam condensed in the second tube row is

$$m_{c(2)} = Q_{a(2)} / i_{fg(2)} = 4252597.272 / 2.358620 \times 10^6 = 1.803003 \text{ kg/s}$$

The effective condensation heat transfer area on the inside of the tubes is

$$A_{c(2)} = A_{c(1)} n_{ib(2)} / n_{ib(1)} = 437.91732 \times 58 / 57 = 445.6 \text{ m}^2$$

and the approximate overall heat transfer coefficient based on this area is

$$U_{c(2)} H_t L_t = h_{ae(2)} A_{a(2)} / (2 n_{ib(2)} n_b) = 243828.641 / (2 \times 58 \times 8) = 262.7464 \text{ W/K}$$

The air mass flow rate flowing on the one side of a finned tube is

$$m_{at(2)} = m_a / (2 n_{ib(2)} n_b) = 286.23 / (2 \times 58 \times 8) = 0.3084694 \text{ kg/s}$$

and the condensation heat transfer coefficient is

$$\begin{aligned} h_{c(2)} &= 0.9245 \left[\frac{L_t k_{c(2)}^3 \rho_{c(2)}^2 g \cos(90^\circ - \theta) i_{fg(2)}}{\mu_{c(2)} m_{at(2)} c_{pa(2)} (T_{vm} - T_{ao(1)}) \left[1 - \exp\left\{-U_{c(2)} H_t L_t / (m_{at(2)} c_{pa(2)})\right\}\right]} \right]^{0.333} \\ &= 0.9245 \left[\frac{4.5 \times 0.6531892^3 \times 983.2168^2 \times 9.8 \times \cos(90^\circ - 30^\circ) \times 2.358620 \times 10^6}{4.631034 \times 10^{-4} \times 0.3084694 \times 1007.552 \times (60 - 33.623)} \right]^{0.333} \\ &\quad \times \left[1 - \exp\left\{-262.7464 / (0.3084694 \times 1007.552)\right\} \right]^{-0.333} \\ &= 17056.434 \text{ W/m}^2 \text{K} \end{aligned}$$

The actual overall heat transfer coefficient for the second tube row is

$$\begin{aligned} UA_{(2)} &= \left[\frac{1}{(h_{ae} A_a)_{(2)}} + \frac{1}{(h_{c(2)} A_{c(2)})} \right]^{-1} = \left[\frac{1}{243828.641} + \frac{1}{17056.43 \times 445.6} \right]^{-1} \\ &= 236120.7 \text{ W/K} \end{aligned}$$

The effectiveness for the first row of the condenser tubes may be expressed as

$$\begin{aligned} e_{(2)} &= 1 - \exp\left[-UA_{(2)} / (m_a c_{pa(2)})\right] = 1 - \exp\left[-236120.7 / (286.32 \times 1007.552)\right] \\ &= 0.5589804 \end{aligned}$$

and the heat transfer rate is given by

$$\begin{aligned} Q_{a(2)} &= m_a c_{pa(2)} (T_{vm(2)} - T_{ao(1)}) e_{(2)} = 286.32 \times 1007.552 \times (60 - 33.623) \times 0.5589804 \\ &= 4252597.272 \text{ W} \end{aligned}$$

This value of $Q_{a(2)}$ compares well to the previous value calculated for the heat transfer rate of the second tube row.

The total rate of heat rejected by the first stage of the three dephlegmators in the array is

$$\begin{aligned} Q_{(1)} &= n_s (Q_{a(1)} + Q_{a(2)}) = 3 \times (5194638.64 + 4252597.272) \\ &= 28341707.736 \text{ W} \approx 28.34 \text{ MW} \end{aligned}$$

The total amount of steam condensed in the first stage of the three hybrid dephlegmators in the array is

$$m_{c(acc \text{ hybrid})} = n_s (m_{c(1)} + m_{c(2)}) = 3 \times (2.2024 + 1.803003) = 12.0162 \text{ kg/s}$$

2.b. Second stage of the hybrid (dry/wet) dephlegmator, when operated as an evaporative condenser

The geometric parameters of the second stage of the hybrid dephlegmator as shown schematically in Figure 2.8 are:

Tube length	$L_t = 10.8 \text{ m}$
Tube outer diameter	$d_o = 0.0381 \text{ m}$
Tube inner diameter	$d_i = 0.0349 \text{ m}$
Transversal tube pitch	$P_t = 0.0762 \text{ m}$
Longitudinal tube pitch	$P_l = 0.06599 \text{ m}$
Number of tube bundles	$n_b = 2$
Number of tube rows	$n_r = 15$
Number of tubes per row	$n_{tr} = 32$
Number of tube rows at the inlet header	$n_{hr1} = 11$
Number of tube rows in the second pass	$n_{hr2} = 3$
Number of tube rows in the third pass	$n_{hr2} = 1$
Thermal conductivity of the tube wall	$k_s = 43 \text{ W/mK}$
Deluge water mass flow rate for the two bundles	$m_w = 106 \text{ kg/s}$

Geometric relations:

The minimum air flow area through one tube bank is given by

$$A_c = (n_{tr} + 1/2)(P_t - d_o)L_t = (32 + 1/2) \times (0.0762 - 0.0381) \times 10.8 = 13.3731 \text{ m}^2$$

The effective frontal area of one tube bundle is

$$A_{fr} = (n_{tr} + 1/2)P_tL_t = (32 + 1/2) \times 0.0762 \times 10.8 = 26.7462 \text{ m}^2$$

The effective air-side surface area of the tubes of one bundle

$$A_a = \pi d_o L_t n_{tr} n_r = \pi \times 0.0381 \times 10.8 \times 32 \times 15 = 620.5 \text{ m}^2$$

The tube inside cross-sectional area

$$A_{is} = \frac{\pi}{4} d_i^2 = \frac{\pi}{4} \times 0.0349^2 = 9.5662 \times 10^{-4} \text{ m}^2$$

Analysis of the second stage of the hybrid dephlegmator (two horizontal plain tube bundles)

The simplified Merkel analysis is used to evaluate the performance characteristics of two horizontal galvanized steel tube bundles when operated as an evaporative condenser. The problem is solved iteratively.

As stated earlier, it is assumed that the mass velocity of the air passing through the first and second stage of the hybrid dephlegmator is the same as the air mass velocity through the finned tube bundles A-frame air-cooled condenser. The air mass flow rate through the tube bundles of the second stage of the hybrid dephlegmator is

$$m_{av} = G_a n_{b(2)} A_{fr(2)} = 2.741951 \times 2 \times 26.7462 = 146.67 \text{ kg/s}$$

The effect of the fan work and the height of the heat exchanger above the ground on the inlet temperature of the air are neglected and it is assumed that the drybulb and wetbulb temperature of the air entering the heat exchanger is respectively, $T_{ai(1)} = 15.6 \text{ }^\circ\text{C}$ and $T_{wb} = 10 \text{ }^\circ\text{C}$.

The relevant energy equations are satisfied for the following values

The outlet air temperature

$$T_{ao} = 38.846 \text{ }^\circ\text{C}$$

The mean deluge water temperature

$$T_{wm} = 47.315 \text{ }^\circ\text{C}$$

The mass flow rate of the steam at the header inlet to the two bundles $m_s = 9.2463 \text{ kg/s}$

The enthalpy of the ambient air entering the tube bank is determined according to equation (A.3.6b), where the specific heats in this equation are evaluated at a temperature $T_{ai}/2 + 273.15 = 15.6/2 + 273.15 = 280.95 \text{ K}$ according to equation (A.1.2) and equation (A.2.2)

Specific heat of air

$$c_{pa} = 1006.441 \text{ J/kgK}$$

Specific heat of water vapor

$$c_{pv} = 1869.262 \text{ J/kgK}$$

To find the humidity ratio of the inlet air according to equation (A.3.5), determine the vapor pressure at the wetbulb temperature $T_{wb} = 10^\circ\text{C}$ according to equation (A.2.1)

$$p_{vwb} = 10^z$$

where

$$\begin{aligned} z &= 10.79586 \left[1 - 273.16 / (T_{wb} + 273.15) \right] + 5.02808 \log_{10} \left[273.16 / (T_{wb} + 273.15) \right] \\ &\quad + 1.50474 \times 10^{-4} \left[1 - 10^{-8.29692 \{ (T_{wb} + 273.15) / 273.16 - 1 \}} \right] \\ &\quad + 4.2873 \times 10^{-4} \left[10^{4.76955 \{ 1 - 273.16 / (T_{wb} + 273.15) \}} - 1 \right] + 2.786118312 \\ &= 10.79586 \left[1 - 273.16 / (283.15) \right] + 5.02808 \log_{10} \left[273.16 / (283.15) \right] \\ &\quad + 1.50474 \times 10^{-4} \left[1 - 10^{-8.29692 \{ (283.15) / 273.16 - 1 \}} \right] \\ &\quad + 4.2873 \times 10^{-4} \left[10^{4.76955 \{ 1 - 273.16 / (283.15) \}} - 1 \right] + 2.786118312 \\ &= 3.088857 \end{aligned}$$

Thus

$$p_{vwb} = 10^{3.088857} = 1227.036 \text{ N/m}^2$$

Substituting into equation (A.3.5) gives

$$\begin{aligned}
w_i &= \left[\frac{2501.6 - 2.3263T_{wb}}{2501.6 + 1.8577T_{ai} - 4.184T_{wb}} \right] \left[\frac{0.62509 p_{vwb}}{p_a - 1.005 p_{vwb}} \right] \\
&\quad - \left[\frac{1.00416(T_{ai} - T_{wb})}{2501.6 + 1.8577T_{ai} - 4.184T_{wb}} \right] \text{ kg/kg dry air} \\
&= \left[\frac{2501.6 - 2.3263(10)}{2501.6 + 1.8577(15.6) - 4.184(10)} \right] \left[\frac{0.62509(1227.036)}{84600 - 1.005(1227.036)} \right] \\
&\quad - \left[\frac{1.00416(15.6 - 10)}{2501.6 + 1.8577(15.6) - 4.184(10)} \right] \text{ kg/kg dry air} \\
&= 0.0069 \text{ kg/kg dry air}
\end{aligned}$$

Substitute these values into equation (A.3.6) and find the enthalpy of the air-vapor mixture.

$$\begin{aligned}
i_{mai} &= c_{pa} T_{ai} + w_i (i_{fgwo} + c_{pv} T_{ai}) \\
&= 1006.441(15.6) + 0.0069(2.5016 \times 10^6 + 1869.262 \times 15.6) \\
&= 33168.914 \text{ J/kg}
\end{aligned}$$

By following the same procedure as above, the enthalpy of the saturated air at the mean deluge water temperature $T_{wm} = 47.315 \text{ }^\circ\text{C}$ is found. The specific heats are evaluated at a temperature $T_{wm}/2 + 273.15 = 296.808 \text{ K}$ according to equation (A.1.2) and equation (A.2.2)

$$\begin{aligned}
\text{Specific heat of air} & \quad c_{pa} = 1006.843 \text{ J/kgK} \\
\text{Specific heat of water vapor} & \quad c_{pw} = 1882.946 \text{ J/kgK}
\end{aligned}$$

The vapor pressure is determined at the mean deluge water temperature

$$\begin{aligned}
z &= 10.79586 \left[1 - 273.16 / (T_{wm} + 273.15) \right] + 5.02808 \log_{10} \left[273.16 / (T_{wm} + 273.15) \right] \\
&\quad + 1.50474 \times 10^{-4} \left[1 - 10^{-8.29692 \{ (T_{wm} + 273.15) / 273.16 - 1 \}} \right] \\
&\quad + 4.2873 \times 10^{-4} \left[10^{4.76955 \{ 1 - 273.16 / (T_{wm} + 273.15) \}} - 1 \right] + 2.786118312 \\
&= 10.79586 \left[1 - 273.16 / (320.465) \right] + 5.02808 \log_{10} \left[273.16 / (320.465) \right] \\
&\quad + 1.50474 \times 10^{-4} \left[1 - 10^{-8.29692 \{ (320.465) / 273.16 - 1 \}} \right] \\
&\quad + 4.2873 \times 10^{-4} \left[10^{4.76955 \{ 1 - 273.16 / (320.465) \}} - 1 \right] + 2.786118312 \\
&= 4.032854
\end{aligned}$$

$$p_{vwm} = 10^z = 10^{4.032854} = 10785.846 \text{ N/m}^2$$

The corresponding humidity ratio is then

$$w_{wm} = \left[\frac{0.62509 p_{vwm}}{p_a - 1.005 p_{vwm}} \right] = \left[\frac{0.62509 \times 10785.846}{84600 - 1.005 \times 10785.846} \right] = 0.09140596 \text{ kg/kg dry air}$$

Substitute these values into equation (A.3.6) and find the enthalpy of the saturated air at the mean deluge water temperature.

$$\begin{aligned} i_{maswm} &= c_{pa} T_{wm} + w_{wm} (i_{fgwo} + c_{pv} T_{wm}) \\ &= 1006.843 \times 47.315 + 0.09140596 (2.5016 \times 10^6 + 1882.946 \times 47.315) \\ &= 284443.451 \text{ J/kg} \end{aligned}$$

The viscosity of the air evaluated at the mean air temperature, $(T_{ai} + T_{ao})/2 = 27.223^\circ\text{C}$, is $\mu_{avm} = 1.848581 \times 10^{-5} \text{ kg/ms}$ and the corresponding Reynolds number of the cooling air flowing through the tube bank is then

$$\begin{aligned} \text{Re}_{avm} &= (m_{av} \times d_o) / (n_b \times A_c \times \mu_{avm}) = (146.67 \times 0.0381) / (2 \times 13.3731 \times 1.848581 \times 10^{-5}) \\ &= 11302.581 \end{aligned}$$

If the loss of deluge water evaporated is neglected and a uniform water distribution is assumed, then the water flow rate over half a tube per unit length is

$$\begin{aligned} \Gamma_m &= m_w d_o / (2 n_b n_r P_t L_t) = 106 \times 0.0381 / (2 \times 2 \times 32 \times 0.0762 \times 10.8) \\ &= 0.03833912 \text{ kg/sm} \end{aligned}$$

The viscosity of the deluge water evaluated at the mean deluge water temperature, $T_{wm} = 47.315^\circ\text{C}$, is $\mu_{wm} = 5.699762 \times 10^{-4} \text{ kg/ms}$ and the corresponding Reynolds number of the deluge water flowing over the tube bank is then

$$\text{Re}_{wm} = 4 \Gamma_m / \mu_{wm} = 4 \times 0.03833912 / 5.699762 \times 10^{-4} = 269.0577$$

The approximate mass transfer coefficient is calculated by using a correlation given by Mizushima et al. (1967)

$$\begin{aligned} h_d &= 5.5439 \times 10^{-8} \text{Re}_{avm}^{0.9} \text{Re}_{wm}^{0.15} d_o^{-1.6} = 5.5439 \times 10^{-8} \times 11302.581^{0.9} \times 269.0577^{0.15} \times 0.0381^{-1.6} \\ &= 0.1063340 \text{ kg/sm}^2 \end{aligned}$$

The dry air mass flow rate is

$$m_a = m_{av}/(1 + w_i) = 146.67/(1 + 0.0069) = 145.67 \text{ kg/s}$$

With the above values the number of transfer units can be calculated

$$\begin{aligned} NTU_a &= n_b A_a h_a / m_a = 2 \times 620.5 \times 0.1063340 / 145.67 \\ &= 0.9058914 \end{aligned}$$

The outlet air enthalpy is

$$\begin{aligned} i_{mao} &= i_{maswm} - (i_{maswm} - i_{mai}) e^{-NTU_a} = 284443.451 - (284443.451 - 33168.914) e^{-0.9058914} \\ &= 182882.947 \text{ J/kg dry air} \end{aligned}$$

Assuming the outlet air is saturated with water vapor and with the enthalpy of the outlet air known, the corresponding air temperature can be determined from equation (A.3.6.b)

$$T_{ao} = (i_{mao} - w_{so} i_{fgwo}) / (c_{pao} + w_{so} c_{pvo})$$

where c_{pao} and c_{pvo} are evaluated at $T_{ao}/2 + 273.15 = 292.57 \text{ K}$ according to equation (A.1.2) and the saturated outlet humidity according to equation (A.2.2).

Humidity ratio	$w_{so} = 0.05584298 \text{ kg/kg dry air}$
Specific heat of dry air	$c_{pao} = 1006.713 \text{ J/kgK}$
Specific heat of water vapor	$c_{pvo} = 1879.164 \text{ J/kgK}$

With these values find

$$T_{ao} = \frac{(182882.947 - 0.05584298 \times 2.5016 \times 10^6)}{(1006.713 + 0.05584298 \times 1879.164)} = 38.846 \text{ }^\circ\text{C}$$

The rate of heat transfer to the air is then

$$\begin{aligned} Q &= m_a (i_{mao} - i_{mai}) = 145.67 \times (182882.947 - 33168.914) \\ &= 21808626.795 \text{ W} \end{aligned}$$

According to Mizushina et al. (1967), the heat transfer coefficient between the deluge water film and the tube surface can be determined using the following equation

$$h_w = 2102.9(\Gamma_m/d_o)^{0.333} = 2102.9(0.03833912/0.0381)^{0.333}$$

$$= 2107.286 \text{ W/m}^2\text{K}$$

The thermophysical properties of water condensate evaluated at $T_v = 60^\circ\text{C}$

Density	$\rho_c = 983.2168 \text{ kg/m}^3$
Specific heat	$c_{pc} = 4184.094 \text{ J/kgK}$
Dynamic viscosity	$\mu_c = 4.631034 \times 10^{-4} \text{ kg/ms}$
Thermal conductivity	$k_c = 0.6531892 \text{ W/mK}$
Latent heat of evaporation	$i_{fg(c)} = 2.358620 \times 10^6 \text{ J/kg}$
Prandtl number	$Pr_c = 2.966473$

The corresponding thermophysical properties of saturated steam evaluated at $T_v = 60^\circ\text{C}$

Density	$\rho_{vs} = 0.1302307 \text{ kg/m}^3$
Specific heat	$c_{pvs} = 1926.889 \text{ J/kgK}$
Dynamic viscosity	$\mu_{vs} = 1.108255 \times 10^{-5} \text{ kg/ms}$
Vapor pressure	$p_{vs} = 1.992512 \times 10^4 \text{ N/m}^2$
Critical pressure	$p_{cr} = 22.09 \times 10^6 \text{ N/m}^2$

For relatively low inlet vapor velocities, $Re_v < 35000$, Chato (1962) developed a correlation to determine the condensation heat transfer coefficient inside a tube, while for higher flow rates the correlation of Shah (1979) can be used. The vapor Reynolds number at the tube bundle inlet (11 tube rows) can be expressed as

$$Re_v = m_s d_i / (n_b n_{hr} n_{tr} A_{ts} \mu_{vs}) = 9.2463 \times 0.0349 / (2 \times 11 \times 32 \times 9.5662 \times 10^{-4} \times 1.108255 \times 10^{-5})$$

$$= 43235.631$$

where n_{hr} is the number of tube rows the inlet header feeds.

Shah (1979) recommends the following equation to determine the condensation heat transfer coefficient when all the steam condenses in the tube

$$Nu_c = \frac{h_c d_i}{k_c} = 0.023 Re_c^{0.8} Pr_c^{0.4} \left[0.55 + 2.09 (p_{cr}/p_v)^{0.38} \right]$$

where

$$Re_c = m_s d_i / (n_b n_{hr} n_w A_{is} \mu_c) = 9.2463 \times 0.0349 / (2 \times 11 \times 32 \times 9.5662 \times 10^{-4} \times 4.631034 \times 10^{-4}) \\ = 1034.673$$

Thus

$$h_c = \frac{0.023 k_c}{d_i} Re_c^{0.8} Pr_c^{0.4} \left[0.55 + 2.09 (p_{cr}/p_{vs})^{0.38} \right] \\ = \frac{0.023 \times 0.6531892}{0.0349} \times 1034.673^{0.8} \times 2.966473^{0.4} \times \left[0.55 + 2.09 \left(\frac{22.09 \times 10^6}{1.992512 \times 10^4} \right)^{0.38} \right] \\ = 5244.906 \text{ W/m}^2\text{K}$$

The overall heat transfer coefficient between the steam and the water film can then be expressed as

$$U_a A_a = n_b A_a \left[\frac{1}{h_w} + \frac{d_o}{d_i h_c} + \frac{d_o \ln(d_o/d_i)}{2k_s} \right]^{-1} \\ = 2 \times 620.5 \left[\frac{1}{2107.286} + \frac{0.0381}{0.0349 \times 5244.906} + \frac{0.0381 \times \ln(0.0381/0.0349)}{2 \times 43} \right]^{-1} \\ = 2 \times 620.5 \left[\frac{1}{2107.286} + \frac{1}{4804.389} + \frac{1}{25730} \right]^{-1} \\ = 1719895.145 \text{ W/K}$$

The mean temperature of the deluge water is then

$$T_{wm} = T_v - (m_a / U_a A_a) (i_{mao} - i_{mai}) \\ = 60 - (145.67 / 1719895.145) (182882.947 - 33168.914) \\ = 47.315^\circ \text{C}$$

The amount of steam condensed in the second stage of the three hybrid dephlegmators in the array is

$$m_{c(ec\ hybrid)} = n_s Q/i_{fg(c)} = 3 \times 21808626.795 / 2.358620 \times 10^6$$

$$= 27.739 \text{ kg/s}$$

and the amount of water evaporated is

$$m_{w(evap)} = m_a (w_{so} - w_i) = 145.67 (0.05584298 - 0.0069)$$

$$= 7.129098 \text{ kg/s}$$

The rate of heat rejected by the three hybrid dephlegmators is then

$$Q_{hd} = n_s (Q_{acc\ hybrid} + Q_{ec\ hybrid}) = 3 \times (9447235.912 + 21808626.795)$$

$$= 93767588.121 \text{ W} \approx 93.77 \text{ MW}$$

and the rate of heat rejected by the air-cooled condenser units as well as the hybrid dephlegmators is

$$Q = Q_{pc} + Q_{hd} = 299067300 + 93767588.121$$

$$= 392834888.121 \text{ W} \approx 392.8 \text{ MW}$$

2.c. Second stage of the hybrid dephlegmator, when operated dry as an secondary air-cooled condenser

During periods of low ambient temperature or lower demands, the second stage of the hybrid dephlegmator is operated dry as an air-cooled condenser to reduce the water usage. The thermal performance characteristics of the galvanized steel tube bundles, if operated dry as an air-cooled condenser, are analyzed using the one-dimensional analysis suggested by Zukauskas (1988). (Qengel (2003), Mills (1999) and Kakac (1997) also recommend the use of this method)

As was stated earlier, for the air-cooled condenser the inlet air is taken to be essentially dry and the ambient drybulb temperature is, $T_{a1} = 15.6^\circ\text{C}$. If the air velocity through the plain tube bundle is the same as through the finned tube bundles, the air mass flow rate is $m_{av} = 146.67 \text{ kg/s}$.

The relevant energy equations are satisfied for the following values

Outlet air temperature	$T_{ao} = 32.858^\circ\text{C}$
Condensation heat transfer coefficient	$h_c = 26089.112 \text{ W/m}^2\text{K}$

Analysis of the thermal performance of the second stage of the hybrid dephlegmator operated in dry mode

The thermophysical properties of dry air evaluated at the mean air temperature in the tube bundle, $T_{am} = (T_{ai} + T_{ao})/2 = 297.38 \text{ K}$, are:

Density	$\rho_{am} = 0.9909628 \text{ kg/s}$
Specific heat	$c_{pam} = 1006.862 \text{ J/kgK}$
Dynamic viscosity	$\mu_{am} = 1.834790 \times 10^{-5} \text{ kg/ms}$
Thermal conductivity	$k_{am} = 0.02601819 \text{ W/mK}$
Prandtl number	$\text{Pr}_{am} = 0.7100342$

The heat transfer rate to the air is

$$Q_a = m_{av} c_{pam} (T_{ao} - T_{ai}) = 146.67 \times 1006.862 \times (32.858 - 15.6) \\ = 2548628.377 \text{ W}$$

The thermophysical properties of the air at the tube wall are evaluated at the steam temperature, $T_v = 60^\circ\text{C}$, as it is assumed that the thermal resistance of the condensing steam and the tube wall is negligible.

Specific heat	$c_{pav} = 1008.641 \text{ J/kgK}$
Dynamic viscosity	$\mu_{av} = 1.996772 \times 10^{-5} \text{ kg/ms}$
Thermal conductivity	$k_{av} = 0.02874972 \text{ W/mK}$
Prandtl number	$\text{Pr}_{av} = 0.7005376$

The mean air velocity through the tube bundle is

$$v = m_{av} / (\rho_{am} n_b A_{fr}) = 146.67 / (0.9909628 \times 2 \times 26.7462) \\ = 2.766890 \text{ m/s}$$

The diagonal tube pitch is

$$P_d = \left[\left(\frac{P_t}{2} \right)^2 + P_l^2 \right]^{1/2} = 0.0762 \text{ m}$$

The maximum velocity of air, based on the smallest area of flow, through a staggered tube bundle is

$$\begin{aligned} v_{\max} &= v \times \left(\frac{P_t}{P_t - d_o} \right) = 2.766890 \times \left(\frac{0.0762}{0.0762 - 0.0381} \right) \\ &= 5.533780 \text{ m/s} \end{aligned}$$

The Reynolds number based on the maximum air velocity is

$$\begin{aligned} \text{Re}_D &= \frac{\rho_{am} v_{\max} d_o}{\mu_{am}} = \frac{0.9909628 \times 5.533780 \times 0.0381}{1.834790 \times 10^{-5}} \\ &= 11387.225 \end{aligned}$$

Zukauskas (1988) recommends the following correlation to predict the average Nusselt number

$$\begin{aligned} \text{Nu}_D &= 0.35 \text{Re}_D^{0.6} \text{Pr}_{am}^{0.38} \left(\frac{\text{Pr}_{am}}{\text{Pr}_{av}} \right)^{0.25} \left(\frac{P_t}{P_l} \right)^{0.2} \\ &= 0.35 \times 11387.225^{0.6} \times 0.7100342^{0.38} \left(\frac{0.7100342}{0.7005376} \right)^{0.25} \left(\frac{0.0762}{0.06599} \right)^{0.2} \\ &= 86.17092 \end{aligned}$$

which is valid for $10^3 < \text{Re}_D < 2 \times 10^5$.

As the tube bundles has more than 13 tube rows no tube row correction is required.

The corresponding air-side heat transfer coefficient is then

$$\begin{aligned} h_a &= \frac{\text{Nu}_D k_{am}}{d_o} = \frac{86.17092 \times 0.02601819}{0.0381} \\ &= 58.84543 \text{ W/m}^2\text{K} \end{aligned}$$

The thermophysical properties of water condensate evaluated at $T_v = 60^\circ\text{C}$ are

Density $\rho_c = 983.2168 \text{ kg/m}^3$

Specific heat $c_{pc} = 4184.094 \text{ J/kgK}$

Dynamic viscosity	$\mu_c = 4.631034 \times 10^{-4} \text{ kg/ms}$
Thermal conductivity	$k_c = 0.6531892 \text{ W/mK}$
Latent heat of evaporation	$i_{fg(c)} = 2.35862 \times 10^6 \text{ J/kg}$
Prandtl number	$Pr_c = 2.966451$

The corresponding thermophysical properties of saturated steam at $T_v = 60^\circ \text{C}$ are

Density	$\rho_{vs} = 0.1302307 \text{ kg/m}^3$
Specific heat	$c_{pvs} = 1926.889 \text{ J/kgK}$
Dynamic viscosity	$\mu_{vs} = 1.108255 \times 10^{-5} \text{ kg/ms}$
Thermal conductivity	$k_{vs} = 0.02103909 \text{ W/mK}$
Vapor pressure	$p_{vs} = 1.992512 \times 10^4 \text{ N/m}^2$
Critical pressure	$p_{cr} = 22.09 \times 10^6 \text{ N/m}^2$

The mass flow rate of the steam condensed in the bundles is

$$m_s = Q_a / i_{fg(c)} = 2548628.377 / 2.35862 \times 10^6 \\ = 1.080559 \text{ kg/s}$$

For relatively low inlet vapor velocities, $Re_v < 35000$, Chato (1962) developed a correlation to determine the condensation heat transfer coefficient inside a tube, while for higher flow rates the correlation of Shah (1979) can be used. The vapor Reynolds number at the tube bundle inlet (11 tube rows) can be expressed as

$$Re_c = m_s d_i / (n_b n_r n_{hr} A_{ts} \mu_c) = 1.080559 \times 0.0349 / (2 \times 32 \times 11 \times 9.5662 \times 10^{-4} \times 4.631034 \times 10^{-4}) \\ = 120.9158$$

The flow in the tube is therefore laminar, for which Chato (1962) recommends the following correlation for the heat transfer coefficient

$$h_c = 0.555 \left[\frac{g \rho_c (\rho_c - \rho_{vs}) k_c^3 i_{fg}'}{\mu_c (T_v - T_{wall}) d_i} \right]^{0.25}$$

where the wall temperature is

$$\begin{aligned} T_{wall} &= T_v - Q_a / (n_b A_a h_c) = 60 - 2548628.337 / (2 \times 620.4972 \times 26089.112) \\ &= 59.92101^\circ \text{C} \end{aligned}$$

and

$$\begin{aligned} i'_{fg} &= i_{fg(c)} + 0.68c_{pc} (T_v - T_{wall}) = 2.35861972 \times 10^6 + 0.68 \times 4184.094 (60 - 59.92101) \\ &= 23588844.450 \text{ J/kg} \end{aligned}$$

Thus

$$\begin{aligned} h_c &= 0.555 \left[\frac{9.8 \times 983.2168 \times (983.2168 - 0.1302307) \times 0.6531892^3 \times 23588844.450}{4.631034 \times 10^{-4} \times (60 - 59.92101) \times 0.0349} \right]^{0.25} \\ &= 26089.113 \text{ W/m}^2\text{K} \end{aligned}$$

The overall heat transfer coefficient is

$$\begin{aligned} U_a A_a &= n_b A_a \left[\frac{d_o}{d_i h_c} + \frac{d_o \ln(d_o/d_i)}{2k_s} + \frac{1}{h_a} \right]^{-1} \\ &= 2 \times 620.4972 \times \left[\frac{0.0381}{0.0349 \times 26089.113} + \frac{0.0381 \ln(0.0381/0.0349)}{2 \times 43} + \frac{1}{58.84543} \right]^{-1} \\ &= 72681.054 \text{ W/K} \end{aligned}$$

The effectiveness of the heat exchanger is

$$\begin{aligned} e_c &= 1 - e^{[-U_a A_a / (m_a c_{pam})]} = 1 - e^{[-72681.054 / (146.67 \times 1006.862)]} \\ &= 0.3886980 \end{aligned}$$

The rate of heat transfer is then

$$\begin{aligned} Q_a &= e_c m_{av} c_{pam} (T_v - T_{ai}) = 0.3886980 \times 146.67 \times 1006.862 \times (60 - 15.6) \\ &= 2548628.377 \text{ W} \end{aligned}$$

which corresponds well to the value previously calculated.

The corresponding outlet air temperature is then

$$T_{ao} = T_{ai} + Q_a / (m_a c_{pam}) = 15.6 + 2548628.377 / (146.67 \times 1006.862) \\ = 32.858^\circ \text{C}$$

3. Pressure drop over the inclined finned tube bundles and plain tube bundles of the first and second stages of the hybrid dephlegmator

The thermophysical properties of air evaluated at the mean air temperature, $T_{a1} = 31.98^\circ \text{C}$, are:

Density $\rho_{a(1)} = 0.9657896 \text{ kg/m}^3$

Dynamic viscosity $\mu_{a(1)} = 1.870404 \times 10^{-5} \text{ kg/ms}$

The air mass velocity is, $G_a = 2.741951 \text{ kg/sm}^2$

3.a. Finned tube bundle second stage of the hybrid dephlegmator

The geometric parameters of the finned tube bundles in the first stage are:

Finned tube bundle specifications:

The bundles consist of two rows of staggered plate finned flattened tubes, each row having different performance characteristics such that approximately the same amount of steam condenses in each row.

Length of finned tube	$L_t = 4.5 \text{ m}$
Inside height of the tube	$H_t = 0.097 \text{ m}$
Inside width of the tube	$W_t = 0.017 \text{ m}$
Number of tubes per bundle (first row)	$n_{tb(1)} = 57$
Number of tubes per bundle (second row)	$n_{tb(2)} = 58$
Number of bundles	$n_b = 8$
Effective frontal area of one bundle (second row)	$A_{fr} = 13.05 \text{ m}^2$
Apex angle of the A-frame	$2\theta = 60^\circ$
Ratio of minimum to free stream flow area through finned tube bundle	$\sigma = 0.48$
Ratio of minimum to free stream flow area at the inlet to the finned tube bundle	$\sigma_{21} = 0.875$

The loss coefficient across the entire bundle under normal isothermal flow conditions is given as

$$K_{he} = 4177.08481Ry^{-0.4392686}$$

Pressure loss over the fin tube bundles

The air mass flow rate through the fin tube bundles is

$$\begin{aligned} m_a &= G_a A_{fr} n_b \\ &= 2.741951 \times 13.05 \times 8 \\ &= 286.2587 \text{ kg/s} \end{aligned}$$

The velocity of the air entering the finned tube bundle

$$\begin{aligned} v_a &= G_a / \rho_a \\ &= 2.741951 / 0.9657896 \\ &= 2.839077 \text{ m/s} \end{aligned}$$

The characteristic flow number, based on the minimum frontal area, is calculated as follows:

$$\begin{aligned} Ry &= m_a / (n_b A_{fr} \mu_a n_{tb(1)} / n_{tb(2)}) \\ &= 286.2587 / (8 \times 13.05 \times 1.870404 \times 10^{-5} \times 57 / 58) \\ &= 149168.624 \text{ m}^{-1} \end{aligned}$$

Thus the heat exchanger loss coefficient is

$$\begin{aligned} K_{he} &= 4177.08481(149168.624)^{-0.4392686} \\ &= 22.29663 \end{aligned}$$

The contraction coefficient is

$$\begin{aligned} \sigma_{ci} &= 0.6144517 + 0.04566493\sigma_{21} - 0.336651\sigma_{21}^2 + 0.4082743\sigma_{21}^3 \\ &\quad + 2.672041\sigma_{21}^4 - 5.963169\sigma_{21}^5 + 3.558944\sigma_{21}^6 \\ &= 0.6144517 + 0.04566493(0.875) - 0.336651(0.875)^2 + 0.4082743(0.875)^3 \\ &\quad + 2.672041(0.875)^4 - 5.963169(0.875)^5 + 3.558944(0.875)^6 \\ &= 0.7751481 \end{aligned}$$

and the entrance contraction loss coefficient is

$$\begin{aligned}
K_{ci} &= \left[\frac{1}{\sigma_{21}} \left(\frac{1}{\sigma_{ci}} - 1 \right) \right]^2 \\
&= \left[\frac{1}{0.875} \left(\frac{1}{0.7751481} - 1 \right) \right]^2 \\
&= 0.1099025
\end{aligned}$$

The effective mean inlet flow angle is

$$\begin{aligned}
\theta_m &= 0.0019\theta^2 + 0.9133\theta - 3.1558 \\
&= 0.0019(30)^2 + 0.9133(30) - 3.1558 \\
&= 25.95320^\circ
\end{aligned}$$

The downstream loss coefficient, K_d , consists of the turning and the jetting losses as well as the kinetic energy loss to the atmosphere. The fin jetting loss is

$$\begin{aligned}
K_{dj} &= \left[\left\{ -2.89188 \left(\frac{L_w}{L_t} \right) + 2.93291 \left(\frac{L_w}{L_t} \right)^2 \right\} \left(\frac{L_t}{L_s} \right) \left(\frac{L_b}{L_s} \right) \left(\frac{28}{\theta} \right)^{0.4} \right. \\
&\quad \left. + \left\{ \exp(2.36987 + 5.8601 \times 10^{-2} \theta - 3.3797 \times 10^{-3} \theta^2) \left(\frac{L_s}{L_b} \right) \right\}^{0.5} \left(\frac{L_t}{L_r} \right) \right]^2 \\
&= \left[\left\{ -2.89188 \left(\frac{0.2}{4.5} \right) + 2.93291 \left(\frac{0.2}{4.5} \right)^2 \right\} \times \{ \sin 30^\circ - 1.25/(2 \times 4.5) + 0.2/4.5 \}^{-1} \right. \\
&\quad \times \left[1 - 0.5 \times 1.25 / \{ 4.5 (\sin 30 + 0.2/9.5) \} \right]^{-1} \times (28/30)^{0.4} \\
&\quad \left. + \left\{ \exp(2.36987 + 5.8601 \times 10^{-2} \times 30 - 3.3797 \times 10^{-3} \times 30^2) \right\} \right. \\
&\quad \left. \times \left(1 - 0.5 \times 1.25 / (4.5 (\sin 30 + 0.2/4.5)) \right) \right]^{0.5} \times \left[1 + 0.2 / (4.5 \times \sin 30) \right]^{-1} \right]^2 \\
&= 0.9392075
\end{aligned}$$

and the outlet loss coefficient is

$$\begin{aligned}
K_o &= \left[\left\{ -2.89188 \left(\frac{L_w}{L_t} \right) + 2.93291 \left(\frac{L_w}{L_t} \right)^2 \right\} \left(\frac{L_s}{L_b} \right)^3 \right. \\
&\quad \left. + 1.9874 - 3.02783 \left(\frac{d_s}{2L_b} \right) + 2.0187 \left(\frac{d_s}{2L_b} \right)^2 \right] \left(\frac{L_t}{L_s} \right)^2 \\
&= \left[\left\{ -2.89188 \left(\frac{0.2}{4.5} \right) + 2.93291 \left(\frac{0.2}{4.5} \right)^2 \right\} \times \left[1 - 0.5 \times 1.25 / \{ 4.5 (\sin 30 + 2/4.5) \} \right]^3 \right. \\
&\quad \left. + 1.9874 - 3.02783 \{ 0.5 \times 1.25 / 4.5 (\sin 30 + 0.2/4.5) \} \right. \\
&\quad \left. + 2.0187 \{ 0.5 \times 1.25 / 4.5 (\sin 30 + 0.2/4.5) \}^2 \right] \\
&\quad \times \{ \sin 30 - 1.25 / (2 \times 4.5) + 2 \times 4.5 \}^{-2} \\
&= 7.877391
\end{aligned}$$

Thus

$$K_d = 0.9392075 + 7.877391 = 8.816598$$

For iso-thermal flow, the total loss coefficient at the outlet of the finned tube bundle is

$$\begin{aligned}
K_{\theta t} &= K_{he} + \left(\frac{1}{\sin \theta_m} - 1 \right) \left[\left(\frac{1}{\sin \theta_m} - 1 \right) + 2 K_{ci}^{0.5} \right] + (K_{dj} + K_o) \\
&= 22.29663 + \left(\frac{1}{\sin (25.95320^\circ)} - 1 \right) \left[\left(\frac{1}{\sin (25.95320^\circ)} - 1 \right) + 2 \times 0.1099025^{0.5} \right] + 8.816598 \\
&= 33.61645
\end{aligned}$$

The pressure drop over the A-frame condenser unit is thus

$$\begin{aligned}
\Delta p &= \frac{K_{\theta t} (m_a / A_{fr})^2}{2 \rho_m} \\
&= \frac{33.61645 (286.2587 / 13.05)^2}{2 (0.9657896)} \\
&= 130.8455 \text{ N/m}^2
\end{aligned}$$

3.b. Pressure drop over the deluged galvanized steel tube bundle

The geometric parameters of the horizontal plain tube evaporative condenser are:

Tube length	$L_t = 10.8$ m
Tube outer diameter	$d_o = 0.0381$ m
Tube inner diameter	$d_i = 0.0349$ m
Transversal tube pitch	$P_t = 0.0762$ m
Longitudinal tube pitch	$P_l = 0.06599$ m
Number of tube bundles	$n_b = 2$
Number of tube rows	$n_r = 15$
Number of tubes per row	$n_{tr} = 32$
Spray zone height	$L_{sz} = 0.6$ m
Deluge water mass flow rate over both tube bundles	$m_w = 107$ kg/s

The air mass flow rate is

$$\begin{aligned}m_{av} &= G_a A_{fr} n_b \\ &= 2.741951 \times 26.7462 \times 2 \\ &= 146.6735 \text{ kg/s}\end{aligned}$$

The velocity of the air entering the plain tube bundle

$$\begin{aligned}v_a &= G_a / \rho_a \\ &= 2.741951 / 0.9657896 \\ &= 2.839077 \text{ m/s}\end{aligned}$$

The approximate water flow rate over half a tube per unit length

$$\begin{aligned}\Gamma_m &= m_w d_o / (2 A_{fr} n_b) \\ &= 107 \times 0.0381 / (2 \times 26.7462 \times 2) \\ &= 0.03810541 \text{ kg/sm}\end{aligned}$$

According to Nitsu (1969) the estimated pressure drop over the wetted tube bundle is

$$\Delta p_a = 4.9 n_r P_l \left(m_{av} / (n_b A_c) \right)^{1.85} (\Gamma_m / d_o)^{0.285}$$

if $2 \leq m_{av} / A_c \leq 6$ and $1.3 \leq \Gamma_m / d_o \leq 3.5$.

where

$$m_{av} / (n_b A_c) = 146.6735 / (2 \times 13.3731) = 5.483902 \text{ kg/sm}^2$$

$$\Gamma_m / d_o = 0.03810541 / 0.0381 = 1.000142 \text{ kg/sm}^2$$

The pressure drop over the horizontal plain tube bundle is then

$$\begin{aligned} \Delta p_a &= 4.9 \times 15 \times 0.05699 (5.483902)^{1.85} (1.000142)^{0.285} \\ &= 113.0053 \text{ N/m}^2 \end{aligned}$$

The water mass velocities based on the frontal area of the fill is

$$G_w = m_w / (n_b A_{fr}) = 107 / (2 \times 26.7462) = 2.000284 \text{ kg/sm}^2$$

The pressure drop over the water collecting troughs is (Kröger, 2008)

$$\begin{aligned} \Delta p_{tr} &= 0.6954 G_w^{0.2471} G_a^{2.3365} + 0.00526 G_w^{3.9812} G_a^{0.3947} \\ &= 0.6954 (2.000284)^{0.2471} (2.741951)^{2.3365} + 0.00526 (2.000284)^{3.9812} (2.741951)^{0.3947} \\ &= 8.836627 \text{ N/m}^2 \end{aligned}$$

Cale (1982) suggested the loss coefficient for the spray zone be expressed as

$$\begin{aligned} K_{sz} &\approx L_{sp} [0.4 (G_w / G_a) + 1] \\ &= 0.6 \times [0.4 (2.000284 / 2.741951) + 1] \\ &= 0.7750827 \end{aligned}$$

The drop coefficient for the drift eliminators can be expressed as (Kröger, 2004)

$$K_{de} = 27.4892 R_y^{-0.14247}$$

where

$$\begin{aligned} R_y &= m_a / (n_b \mu A_{fr}) = 146.6735 / (2 \times 1.870404 \times 26.7472) \\ &= 146596.751 \end{aligned}$$

Thus

$$K_{de} = 27.4892(146596.751)^{-0.14247} = 2.469341$$

The pressure drop in the spray zone and over the drift eliminators is

$$\begin{aligned}\Delta p_{de} + \Delta p_{sz} &= (K_{de} + K_{sz}) \left[m_a / (n_b A_{fr}) \right] / (2\rho_a) \\ &= (2.469341 + 0.7750827) \left[146.6735 / (2 \times 26.7462) \right] / (2 \times 0.9657896) \\ &= 4.605584 \text{ N/m}^2\end{aligned}$$

Pressure drop due to a loss in kinetic energy at the exit of the bundle is

$$\begin{aligned}\Delta p_{ke} &= \frac{1}{2} \rho v^2 \\ &= \frac{1}{2} \times 0.9657896 \times 2.839077^2 \\ &= 3.892305 \text{ N/m}^2\end{aligned}$$

The total pressure drop over the wet plain tube bundle is then

$$\begin{aligned}\Delta p_{ec} &= \Delta p_a + \Delta p_{ir} + \Delta p_{sz} + \Delta p_{de} + \Delta p_{ke} \\ &= 113.0053 + 8.836627 + 4.605584 + 3.892305 \\ &= 130.3399 \text{ N/m}^2\end{aligned}$$

This pressure drop is essentially the same as that across the finned tube bundle or first stage of the dephlegmator (130.8455 N/m²)

4. Adiabatic cooling

If the ambient air entering an A-frame air-cooled condenser is adiabatically cooled by introducing a fine spray or mist into the air, a higher heat rejection rate can be achieved. To find the humidity ratio of the ambient air according to equation (A.3.5), the vapor pressure at the wetbulb temperature is determined according to equation (A.2.1)

$$p_{vwb} = 10^z$$

where

$$\begin{aligned}
z &= 10.79586 \left[1 - 273.16 / (T_{wb} + 273.15) \right] + 5.02808 \log_{10} \left[273.16 / (T_{wb} + 273.15) \right] \\
&\quad + 1.50474 \times 10^{-4} \left[1 - 10^{-8.29692 \{ (T_{wb} + 273.15) / 273.16 - 1 \}} \right] \\
&\quad + 4.2873 \times 10^{-4} \left[10^{4.76955 \{ 1 - 273.16 / (T_{wb} + 273.15) \}} - 1 \right] + 2.786118312 \\
&= 10.79586 \left[1 - 273.16 / (283.15) \right] + 5.02808 \log_{10} \left[273.16 / (283.15) \right] \\
&\quad + 1.50474 \times 10^{-4} \left[1 - 10^{-8.29692 \{ (283.15) / 273.16 - 1 \}} \right] \\
&\quad + 4.2873 \times 10^{-4} \left[10^{4.76955 \{ 1 - 273.16 / (283.15) \}} - 1 \right] + 2.786118312 \\
&= 3.088857
\end{aligned}$$

thus

$$p_{vwb} = 10^{3.088857} = 1227.036 \text{ N/m}^2$$

Substituting into equation (A.3.5) gives

$$\begin{aligned}
w_i &= \left[\frac{2501.6 - 2.3263T_{wb}}{2501.6 + 1.8577T_{ai} - 4.184T_{wb}} \right] \left[\frac{0.62509 p_{vwb}}{p_a - 1.005 p_{vwb}} \right] \\
&\quad - \left[\frac{1.00416(T_{ai} - T_{wb})}{2501.6 + 1.8577T_{ai} - 4.184T_{wb}} \right] \text{ kg/kg dry air} \\
&= \left[\frac{2501.6 - 2.3263(10)}{2501.6 + 1.8577(15.6) - 4.184(10)} \right] \left[\frac{0.62509(1227.036)}{84600 - 1.005(1227.036)} \right] \\
&\quad - \left[\frac{1.00416(15.6 - 10)}{2501.6 + 1.8577(15.6) - 4.184(10)} \right] \text{ kg/kg dry air} \\
&= 0.0069 \text{ kg/kg dry air}
\end{aligned}$$

It is assumed that during adiabatic cooling the constant wetbulb temperature line on the psychrometric chart is followed and the air leaving the spray zone, entering the condenser units, is saturated with water vapor. If the air is cooled up to a point where it is saturated with water vapor, then $T_a = T_{wb} = 10^\circ\text{C}$ and according to equation (A.3.5) the saturated humidity ratio is

$$\begin{aligned}
w_{so} &= \frac{0.62509 p_{vwb}}{p_a - 1.005 p_{vwb}} \text{ kg/kg dry air} \\
&= \left[\frac{0.62509(1227.036)}{84600 - 1.005(1227.036)} \right] \\
&= 0.0092 \text{ kg/kg dry air}
\end{aligned}$$

Taking the dry-bulb temperature as $T_a = 10^\circ\text{C}$ and following the same procedure as given in Section 1, the heat rejected by one of the finned tube A-frame air-cooled condenser units is, $Q = 328 \text{ MW}$ and the air mass flow rate through one of the units is, $m_a = 619.5 \text{ kg/s}$.

The total mass flow rate of the water evaporated in all the condenser units during the adiabatic cooling of the ambient air is

$$\begin{aligned}
m_{w(\text{evap})} &= n_s n_c m_a (w_{so} - w_i) \\
&= 3 \times 6 \times 619.5 (0.0092 - 0.0069) \\
&= 25.6473 \text{ kg/s}
\end{aligned}$$

5. Comparison between the heat transfer coefficients

The correlations of various heat transfer coefficients are compared with each other. The conditions given in Section 1 and Section 2 are used.

5.a. Condensation heat transfer coefficient in a tube

The vapor Reynolds number at the tube bundle inlet can be expressed as

$$\begin{aligned}
\text{Re}_v &= m_s d_i / (n_b n_{hr} n_{tr} A_{ts} \mu_{vs}) = 9.2463 \times 0.0349 / (2 \times 11 \times 32 \times 9.5662 \times 10^{-4} \times 1.108255 \times 10^{-5}) \\
&= 43235.631
\end{aligned}$$

For relative low inlet vapor Reynolds numbers, $\text{Re}_v < 35000$, Chato (1962) recommends the following correlation for calculating the condensation heat transfer coefficient

$$h_c = 0.555 \left[\frac{9.8 \rho_c (\rho_c - \rho_{vs}) k_c^3 i_{fg}'}{\mu_c (T_v - T_{wall}) d_i} \right]^{0.25}$$

where the wall temperature is

$$T_{wall} = T_v - Q / (n_b A_a h_c) = 60 - 21808626.795 / (2 \times 620.5 \times 5244.906)$$

$$= 56.649^\circ \text{C}$$

and i'_{fg} is

$$i'_{fg} = i_{fg(c)} + 0.68c_{pc} (T_v - T_{wall})$$

$$= 2.35861972 \times 10^6 + 0.68 \times 4184.094 (60 - 56.649)$$

$$= 2.368154 \times 10^6 \text{ J/kg}$$

Thus

$$h_c = 0.555 \left[\frac{9.8 \times 983.2168 \times (983.2168 - 0.1302307) \times 0.6531892^3 \times 2.368154 \times 10^6}{4.631034 \times 10^{-4} \times (60 - 56.649) \times 0.0349} \right]^{0.25}$$

$$= 10156.582 \text{ W/m}^2\text{K}$$

For higher vapor flow rates, Shah (1979) recommends the following equation to determine the condensation heat transfer coefficient

$$Nu_c = \frac{h_c d_i}{k_c} = 0.023 \text{Re}_c^{0.8} \text{Pr}_c^{0.4} \left[0.55 + 2.09 (p_{cr} / p_v)^{0.38} \right]$$

where

$$\text{Re}_c = m_s d_i / (n_b n_{hr} n_w A_{is} \mu_c) = 9.2463 \times 0.0349 / (2 \times 11 \times 32 \times 9.5662 \times 10^{-4} \times 4.631034 \times 10^{-4})$$

$$= 1034.673$$

Thus

$$h_c = \frac{0.023 k_c}{d_i} \text{Re}_c^{0.8} \text{Pr}_c^{0.4} \left[0.55 + 2.09 (p_{cr} / p_{vs})^{0.38} \right]$$

$$= \frac{0.023 \times 0.6531892}{0.0349} \times 1034.673^{0.8} \times 2.966473^{0.4} \times \left[0.55 + 2.09 \left(\frac{22.09 \times 10^6}{1.992512 \times 10^4} \right)^{0.38} \right]$$

$$= 5244.906 \text{ W/m}^2\text{K}$$

5.b. Deluge water film heat transfer coefficient

According to Mizushina et al. (1967), the heat transfer coefficient between the deluge water film and the tube surface can be determined using the following equation

$$\begin{aligned}h_w &= 2102.9(\Gamma_m/d_o)^{0.333} = 2102.9(0.03833912/0.0381)^{0.333} \\ &= 2107.286 \text{ W/m}^2\text{K}\end{aligned}$$

Parker and Treybal (1961) recommend the following correlation

$$\begin{aligned}h_w &= 704(1.3936 + 0.02214T_{wm})(\Gamma_m/d_o)^{0.333} \\ &= 704(1.3936 + 0.02214 \times 47.315)(0.03833912/0.0381)^{0.333} \\ &= 1722.157 \text{ W/m}^2\text{K}\end{aligned}$$

and Nitsu et al. (1969) suggest the following correlation

$$\begin{aligned}h_w &= 990(\Gamma_m/d_o)^{0.46} \\ &= 990(0.03833912/0.0381)^{0.46} \\ &= 992.8533 \text{ W/m}^2\text{K}\end{aligned}$$

5.c. Water-air interface mass transfer coefficient

The approximate mass transfer coefficient is calculated by using correlation given by Mizushina et al. (1967)

$$\begin{aligned}h_d &= 5.5439 \times 10^{-8} \text{Re}_{avm}^{0.9} \text{Re}_{wm}^{0.15} d_o^{-1.6} = 5.5439 \times 10^{-8} \times 11302.581^{0.9} \times 269.0577^{0.15} \times 0.0381^{-1.6} \\ &= 0.1063340 \text{ kg/sm}^2\end{aligned}$$

Parker and Treybal (1961) recommend the following correlation

$$\begin{aligned}h_d &= 0.04935(m_{avi}/(n_b A_c))^{0.905} \\ &= 0.04935(146.67/(2 \times 13.3731))^{0.905} \\ &= 0.2302 \text{ kg/sm}^2\end{aligned}$$

and Nitsu et al. (1969) suggest the following correlation

$$\begin{aligned}h_d &= 0.076(m_{avi}/A_c)^{0.8} \\ &= 0.076(146.67/(2 \times 13.3731))^{0.8} \\ &= 0.2965 \text{ kg/sm}^2\end{aligned}$$